

**IMAGE RESOLUTION ENHANCEMENT USING IMPROVED EDGE  
DIRECTED INTERPOLATION ALGORITHM**

**MD SHAMIM HOSSAIN**

**FACULTY OF COMPUTER SCIENCE AND INFORMATION  
TECHNOLOGY  
UNIVERSITY OF MALAYA  
KUALA LUMPUR**

**2018**

**IMAGE RESOLUTION ENHANCEMENT USING  
IMPROVED EDGE DIRECTED INTERPOLATION  
ALGORITHM**

**MD SHAMIM HOSSAIN**

**DISSERTATION SUBMITTED IN PARTIAL  
FULFILMENT OF THE REQUIREMENTS FOR THE  
DEGREE OF MASTER OF COMPUTER SCIENCE**

**FACULTY OF COMPUTER SCIENCE AND  
INFORMATION TECHNOLOGY  
UNIVERSITY OF MALAYA  
KUALA LUMPUR**

**2018**

**UNIVERSITY OF MALAYA**  
**ORIGINAL LITERARY WORK DECLARATION**

Name of Candidate: Md Shamim Hossain

Matric No: WGA150045

Name of Degree: Master of Computer Science (Mix Mode)

Title of Project Paper/Research Report/Dissertation/Thesis (“this Work”):

**Image Resolution Enhancement Using Improved Edge Directed  
Interpolation Algorithm**

Field of Study: Computer Science – Image Processing

I do solemnly and sincerely declare that:

- (1) I am the sole author/writer of this Work;
- (2) This Work is original;
- (3) Any use of any work in which copyright exists was done by way of fair dealing and for permitted purposes and any excerpt or extract from, or reference to or reproduction of any copyright work has been disclosed expressly and sufficiently and the title of the Work and its authorship have been acknowledged in this Work;
- (4) I do not have any actual knowledge nor do I ought reasonably to know that the making of this work constitutes an infringement of any copyright work;
- (5) I hereby assign all and every right in the copyright to this Work to the University of Malaya (“UM”), who henceforth shall be owner of the copyright in this Work and that any reproduction or use in any form or by any means whatsoever is prohibited without the written consent of UM having been first had and obtained;
- (6) I am fully aware that if in the course of making this Work I have infringed any copyright whether intentionally or otherwise, I may be subject to legal action or any other action as may be determined by UM.

Candidate’s Signature

Date:

Subscribed and solemnly declared before,

Witness’s Signature

Date:

Name:

Designation:

# [IMAGE RESOLUTION ENHANCEMENT USING IMPROVED EDGE DIRECTED INTERPOLATION ALGORITHM]

## ABSTRACT

Image resolution enhancement is a process to convert the low-resolution image into high-resolution image. This method is applied in many image processing field. One of the commonly used techniques for image resolution enhancement is interpolation. The results of pixel interpolation can vary significantly depending on the interpolation algorithm. Moreover, the conventional interpolation methods are not efficient to assign accurate interpolation value to the high-resolution edge pixels. Therefore, in this study, we propose an improved edge directed interpolation algorithm, which is able to preserve the sharpness of edges. The proposed method is divided into three main steps: edge pixel filtering; bi-cubic interpolation, and edge directed interpolation. The edge pixels and non-edge pixels are separated by the adaptive edge filtering method. After that bi-cubic interpolation is applied for non-edge pixels. The Lagrange interpolation polynomial is used for bi-cubic interpolation and the average weight of sixteen neighbour pixels are calculated for each high-resolution non-edge pixel. Finally, an improved edge directed interpolation is applied on the edge pixels. The proposed method is tested on the several standard grayscale images and compared with the existing methods. According to the evaluation results, the proposed method provides the highest performance of the subjective and objective quality than the standing edge directed interpolation methods.

**Keywords:** Image resolution, edge-directed, interpolation, edge pixels

# [PENINGKATAN RESOLUSI GAMBAR MENGGUNAKAN BERTAMBAH BAIK TEPI DIARAHKAN ALGORITMA INTERPOLASI]

## ABSTRAK

Peningkatan resolusi imej adalah proses untuk menukar imej resolusi rendah ke imej resolusi tinggi. Kaedah ini digunakan dalam banyak bidang pemprosesan imej. Salah satu teknik yang biasa digunakan untuk peningkatan resolusi imej ialah Interpolation. Hasil dari interpolasi pixel dapat bervariasi secara signifikan bergantung pada algoritma interpolasi. Selain itu, kaedah interpolasi konvensional tidak berkesan untuk memberikan nilai interpolasi yang tepat kepada piksel tepi resolusi tinggi. Oleh itu, dalam kajian ini, kami mencadangkan algoritma interpolasi yang diarahkan ke tepi yang lebih baik, yang dapat mengekalkan ketajaman tepi. Kaedah yang dicadangkan dibahagikan kepada tiga langkah utama: penapisan pixel tepi; interpolasi bi-cubic, dan interpolasi diarahkan ke tepi. Pixel tepi dan piksel tanpa tepi dipisahkan oleh kaedah penapisan yang sesuai. Selepas itu interpolasi bi-cubic digunakan untuk piksel tanpa tepi. Polinomial interpolasi Lagrange digunakan untuk interpolasi bi-cubic dan berat purata piksel jiran enam belas dikira untuk setiap piksel tanpa tepi resolusi tinggi. Akhirnya, interpolasi diarahkan ke arah yang lebih baik digunakan pada tepi piksel. Kaedah yang dicadangkan diuji pada beberapa imej skala kelabu standard dan dibandingkan dengan kaedah sedia ada. Menurut hasil penilaian, kaedah yang dicadangkan memberikan prestasi tertinggi terhadap kualiti subjektif dan obyektif daripada kaedah penunjuk arah yang ditentukan.

**Kata kunci:** Resolusi imej, tepi yang diarahkan, sisipan, piksel kelebihan

## ACKNOWLEDGEMENTS

I am grateful to my Almighty for his grace. I would like to thanks to my supervisor Dr. Hamid Abdullah Jalab Altulea for his kind support. Without his proper guideline it would have been impossible to accomplish this dissertation successfully. His continuous advice, friendly communication and evaluation help to finish this dissertation on time.

I am grateful to the Faculty of Computer Science & Information Technology, University of Malaya. The course curriculum has encouraged me in the research field. Nice campus environment and good lab facility give me a chance to continue this research smoothly. I am thankful to all faculty members for their friendly and helpful mind. I am showing my respect to my AI lab in charge Dr. Ram Gopal Raj for his helping hand to solve different problems and special thanks to my all lab mates and friends.

Finally, I would like to thanks my parents. Specially, I am glad to my father who has encouraged me to continue my higher study and without his support I would not be able to study in the University of Malaya.

## TABLE OF CONTENTS

Abstract .....	iii
Abstrak .....	iv
Acknowledgement .....	v
Table of Contents .....	vi
List of Figures .....	x
List of Tables .....	xiv
List of Symbols and Abbreviations .....	xv
<b>CHAPTER 1: INTRODUCTION .....</b>	<b>1</b>
1.1 Introduction .....	1
1.2 Motivation .....	2
1.3 Problem Statement .....	3
1.4 Research Questions .....	4
1.5 Research Objectives .....	5
1.6 Research Contributions .....	5
1.7 Dissertation Structure .....	6
<b>CHAPTER 2: LITERATURE REVIEW .....</b>	<b>8</b>
2.1 Introduction .....	8
2.2 Reconstruction Based Image Resolution Enhancement .....	9
2.3 Learning Based Image Resolution Enhancement .....	10
2.3.1 Hallucination Based Method .....	11
2.4 Interpolation Based Image Resolution Enhancement .....	12
2.4.1 Non-Edge Directed Interpolation Method .....	13
2.4.1.1 The Cubic convolution Method .....	13

2.4.1.2	The Second Order Derivative Method .....	16
2.4.1.3	The Curvature Based Method .....	17
2.4.1.4	The Covariance Based Method .....	18
2.4.2	Edge Directed Interpolation Methods .....	19
2.4.2.1	Edge Directed Method .....	22
2.4.2.2	Markov Random Field Edge Directed Method .....	26
2.4.2.3	Non-local Edge Directed Method .....	27
2.4.2.4	Window Selection Edge Directed Method .....	28
2.4.2.5	Multidirectional Edge Directed Method .....	31
2.4.2.6	Pixel Mapping Edge Directed Method .....	32
2.4.2.7	Fast Edge Directed Method .....	34
2.5	Summary .....	38
 <b>CHAPTER 3: METHODOLOGY</b> .....		<b>39</b>
3.1	Introduction .....	39
3.2	Down Sample Image .....	40
3.3	Edge Pixels and Non-Edge Pixels Determination .....	41
3.3.1	Canny Edge Detection .....	41
3.4	Bi-cubic Interpolation for Non-Edge Pixels .....	46
3.4.1	Lagrange Interpolation Polynomial .....	47
3.5	Proposed Improved Edge Directed Interpolation Method .....	50
3.5.1	High Resolution Edge Direction .....	50
3.5.2	Improved Edge Direction Interpolation .....	54
3.5.2.1	Improved Edge Directed Interpolation On Vertical Direction .....	55
3.5.2.2	Improved Edge Directed Interpolation On Horizontal Direction .....	57
3.5.2.3	Improved Edge Directed Interpolation On 45° angle Direction .....	59

3.5.2.4	Improved Edge Directed Interpolation On 135° angle Direction	60
3.6	Summary	62
<b>CHAPTER 4: EXPERIMENTAL RESULTS</b>		<b>63</b>
4.1	Introduction	63
4.2	Software and Platform	63
4.3	Experimental Images	63
4.4	Experiment Design	64
4.5	Existing Methods	65
4.6	Experiment Results	65
4.7	Quantitative Test	67
4.7.1	Means Square Error	67
4.7.2	Root Means Square Error	69
4.7.3	Signal to Noise Ratio	70
4.7.4	Peak Signal to Noise Ratio	71
4.7.5	Structural Similarity Index Measurement	73
4.7.6	Computational Complexity	74
4.8	Qualitative Assessment	75
4.8.1	Comparison with Nearest Neighbour Interpolation	76
4.8.2	Comparison with Bilinear Interpolation	77
4.8.3	Comparison with Bi-cubic Interpolation	78
4.8.4	Comparison with DCCI	79
4.8.5	Comparison with ICBI	80
4.8.6	Comparison with iNEDI	81
4.9	Summary	84

<b>CHAPTER 5: CONCLUSION AND FUTURE WORK</b> .....	85
5.1 Introduction .....	85
5.2 Fulfilment of the Research Objectives .....	85
5.3 Contribution .....	86
5.4 Future Work .....	86
5.5 Summary .....	87
<b>REFERENCES</b> .....	88

University of Malaya

## LIST OF FIGURES

Figure 1.1:	The example of edge directed interpolation; The value of LR pixel $S_1$ is directly assign to the HR edge pixel $Q$ ; Since, the LR pixel value $S_1$ is close to the HR edge pixel value $Q$ .....	3
Figure 1.2:	The example of image resolution enhancement from LR image to HR image.....	4
Figure 1.3:	The example of HR image cross section.....	4
Figure 2.1:	The taxonomy of image resolution enhancement. ....	8
Figure 2.2:	The example of reconstruction interpolation; (a) Upper row is the original images and bottom row is the output images; (b) Original images are passed through the low pass and high pass filters.....	10
Figure 2.3:	The example of CCI interpolation; (a) The gradient of the diagonal directions are calculated. The black circles are defined as LR pixels. Grey and white circles are defined as the unknown HR pixels; (b) & (c) The vertical and horizontal gradients are estimated.....	15
Figure 2.4:	The example of second order derivative interpolation; (a) The first step four diagonal pixels are taken for interpolation; (b) The second step four nearest neighbour pixels are taken for interpolation.....	16
Figure 2.5:	The example of iterative based interpolation on 12 nearest neighbour pixels and determine the interpolation value based on second order derivative.....	17
Figure 2.6:	The example of the process of estimating $Y_{2i+1,2j+1}$ from $Y_{2i,2j}$ ....	19
Figure 2.7:	The example of the framework of edge directed interpolation.....	21
Figure 2.8:	The example of fast edge directed interpolation; The surrounding pixel selection and the structural relation between HR pixels and LR pixels.....	21
Figure 2.9:	The example of the NEDI process; (a) The geometric duality for NEDI from the image scale $Y_{2i,2j}$ to $Y_{2i+1,2j+1}$ ; (b) The rotation of lattice is in $\pi / 4$ position.....	22
Figure 2.10:	The example of eight types of elliptic windows.....	23

Figure 2.11:	The example of estimating diagonal weight $w$ of the nearest neighbour pixels.....	25
Figure 2.12:	The example of Markov random field EDI method; (a) The neighbour pixels structure; (b) Sixteen directions are consider on the $7 \times 7$ pixel matrix.....	26
Figure 2.13:	The framework of edge preserving method.....	27
Figure 2.14:	The example of interpolation steps and window block of the window selection method.....	29
Figure 2.15:	The example of window blocks; (a) The high resolution window block; (c)-(e) The covariance are calculated.....	29
Figure 2.16:	The example of window extension and the nearby pixels range of the standing window.....	30
Figure 2.17:	The example of multidirectional interpolation of $Y_{2i+1,2j+1}$ edge pixel.....	31
Figure 2.18:	The example of LR pixels are copied and placed in the HR grid....	32
Figure 2.19:	The example of cubic spline interpolation in horizontal and vertical direction.....	33
Figure 2.20:	The example of unknown HR pixel; (a), (b) and (c) The arrangement of LR neighbour pixels.....	35
Figure 2.21:	The example of edge pixel is surrounded by the different arrangement of nearest neighbour pixels; (a) The interpolation of $Y_{2i,2j+1}$ edge pixel; (b) The interpolation of $Y_{2i+1,2j}$ edge pixel; (c) The interpolation of $Y_{2i+1,2j+1}$ edge pixel.....	37
Figure 3.1:	The flow chart of the proposed algorithm.....	39
Figure 3.2:	The example of down sample image conversion.....	40
Figure 3.3:	The example of Canny edge detection (a) the input grey scale image; the automatic threshold selection (b) when $\alpha = 8$ ; (c) when $\alpha = 4$ ; (d) when $\alpha = 2$ .....	46
Figure 3.4:	The example of bi-cubic interpolation for non-edge pixel.....	47
Figure 3.5:	The example of possible combination of LR, HR non-edge and HR edge pixels. non-edge pixel is also used as nearest neighbor pixel for improved edge directed interpolation.....	49

Figure 3.6:	The example of neighbor LR and HR pixels around the HR edge pixel.....	50
Figure 3.7:	The example of features of HR edge pixel and the type of edge directions, (a) vertical edge direction; (b) horizontal edge direction; (c) 45° angle edge direction; (d) 135° angle edge direction.....	52
Figure 3.8:	The example of arrangement of LR and HR pixels for improved edge directed interpolation.....	54
Figure 3.9:	The example of blank HR edge pixel $Q$ and the selection of improved EDI is continued through vertical edge direction when (a) $W < 0.5$ ; (b) and (c) $W \geq 0.5$ .....	56
Figure 3.10:	The example of blank HR edge pixel $Q$ and the selection of improved EDI is continued through horizontal HR edge direction when (a) $W < 0.5$ ; (b) and (c) $W \geq 0.5$ .....	58
Figure 3.11:	The example of blank HR edge pixel $Q$ and the selection of improved EDI is continued through 45° angle edge direction when (a) $H < 0.5$ and $W < 0.5$ ; (b) and (c) $H \geq 0.5$ and $W \geq 0.5$ .....	60
Figure 3.12:	The example of blank HR edge pixel $Q$ and the selection of improved EDI is continued through 135° angle edge direction when (a) $H < 0.5$ and $W < 0.5$ ; (b) and (c) $H \geq 0.5$ and $W \geq 0.5$ .....	61
Figure 4.1:	The sample of test images.....	64
Figure 4.2:	The example of cross section of image after applied the edge directed interpolation method.....	66
Figure 4.3:	The example of cross section of image after applied the proposed improved edge directed interpolation method.....	66
Figure 4.4:	The graph line of the MSE results.....	68
Figure 4.5:	The graph line of the RMSE results.....	69
Figure 4.6:	The graph line of the SNR results.....	70
Figure 4.7:	The graph line of the PSNR results.....	72
Figure 4.8:	The graph line of the SSIM results.....	73
Figure 4.9:	The graph line of the computational complexity results.....	75

Figure 4.10:	The visual comparison between Nearest Neighbor interpolation and proposed improved EDI method.....	76
Figure 4.11:	The visual comparison between Bilinear interpolation and proposed EDI method.....	77
Figure 4.12:	The visual comparison between Bi-cubic interpolation and proposed EDI method.....	79
Figure 4.13:	The visual comparison between DCCI interpolation and proposed EDI method.....	80
Figure 4.14:	The visual comparison between ICBI interpolation and proposed EDI method.....	81
Figure 4.15:	The visual comparison between iNEDI interpolation and proposed EDI method.....	82
Figure 4.16:	The overall visual comparison of (a) Nearest Neighbour; (b) Bilinear; (c) Bi-cubic; (d) DCCI; (e) ICBI; (f) iNEDI; (g) Proposed improved EDI method.....	83

## LIST OF TABLES

Table 2.1:	The comparison between reviewed edge directed interpolation methods .....	38
Table 4.1:	MSE results of the selected images .....	68
Table 4.2:	RMSE results of the selected images.....	69
Table 4.3:	SNR $dB$ results of the selected images.....	70
Table 4.4:	PSNR ( $dB$ ) results of the selected images.....	72
Table 4.5:	SSIM results of the selected images.....	73
Table 4.6:	Processing time of the proposed and other interpolation methods (s).....	75

University of Malaya

## LIST OF SYMBOLS AND ABBREVIATIONS

BCI	: Bi-Cubic Interpolation
CC	: Cubic Convolution
CCD	: Charge Coupled Device
DCC	: Directional Cubic Convolution
DCCI	: Directional Cubic Convolution Interpolation
DT-CWT	: Duel Tree Complex Wave Length Transform
DWT	: Discrete Wavelet Transformation
EDI	: Edge Directed Interpolation
FEDI	: Further Improved Edge Directed Interpolation
FO-PDE	: Fourth Order Partial Differential Equation
HDTV	: High Definition Television
HF	: High Frequency
HH	: High-High
HL	: High-Low
HR	: High Resolution
IEDI	: Improved Edge Directed Interpolation
IFEDI	: Improved Fast Edge Directed Interpolation
ICBI	: Iterative Curvature Based Interpolation
LH	: Low-High
LL	: Low-Low
LoG	: Logarithm
LR	: Low Resolution
MER	: Means Square Error
NEDI	: New Edge Directed Interpolation
NNI	: Nearest Neighbour Interpolation

PDE : Partial Differential Equation  
PSNR : Peak Signal To Noise Ratio  
RMSE : Root Means Square Error  
SDTV : Standard Definition Television  
SNR : Signal To Noise Ratio  
SSIM : Structural Similarity Index Measurement

University of Malaya

## CHAPTER 1: INTRODUCTION

### 1.1 Introduction

The image resolution enhancement can be described as the process of producing of large scale image from the low scale images. The basically image resolution enhancement is the arithmetic mean of the neighbouring low resolution pixels surrounded to the high resolution pixel. Therefore, image resolution enhancement requires the knowledge of millions pixels of low resolution (LR) image. The image would be as like as natural image after the enhanced in large scale (Yun et al., 2011). The image upscaling recently becomes the important topics in computer vision field with respect to the use of wide variety of practical applications in both video and image processing. Image enlargement is necessary in different types of electronic devices for better view and understanding such as digital TV, printer, graphics render, forensic, surveillance, media players and medical imaging devices etc. (Tian, Wen, Zhou, & Chen, 2012). However, it is critical to improve the quality of images edges because edges perceptually carry salient features of the image (Tai et al., 2010). Smooth edges provide better visual quality of images. Human visual system is sensitive and easily detect the luminance variations corresponding to chrominance values, that is why sometimes the reconstruction images are too sharp in the edges regions and look unnatural. Moreover, when the resolution enhancement factor increases then the performance of the resolution enhancement algorithms fall down (Hosogai & Tanaka, 2014). Therefore, edges preserving interpolation algorithm becomes essential and the primary focus of the researchers and the conversion from the LR images to high resolution (HR) images (Wu, Li, & Jeon, 2017).

## 1.2 Motivation

The methods which are commonly used to produce the HR images from the low resolution LR images are known as interpolation methods. The HR pixels values comes directly from the known LR pixels values. So the interpolation values are an approximate value and does not fulfil the optimum results (Park & Jeong, 2017). Therefore, the problems still remain such as high frequency blur, noticeable aliasing, over-smoothing and artifacts through the edge regions. Among all the problems edges sharpness and visual artifacts are critical problems in image reconstruction. The problems are mainly related with image edges. The estimation of poor edges pixels of images drops the image quality (Jagadeesh & Pragatheeswaran, 2011). Moreover, to mitigate the problems several edges directed interpolation algorithms are existed. Some of these algorithms use predefine geometrical model to construct the interpolation images. While other algorithms estimate the value of unknown pixels from the low resolution images (M. Li & Nguyen, 2008). Several classical methods which are used in image resolution enhancement for example, Pixel Replication, interpolation algorithms such as Nearest Neighbour Interpolation, Bilinear Interpolation, Cubic Spline and Cubic Interpolation exist (Yu, Zhang, Wu, Hu, & Xie, 2013). These methods are efficient with the low frequency regions or homogenous regions and not in the edges or high frequency regions where image intensity is changed in abruptly. The low frequency regions are responsible to build the shape of HR images. Therefore, still now improvement and further research is desirable in this field. Based on the algorithm performance edges directed interpolation methods provide much better results than the others methods. The primary benefits of the edges directed interpolation algorithms are cost effective (Giachetti & Asuni, 2011). An accurate interpolation algorithm can be able to construct HR enhanced images with better visual quality. So, improvement is necessary in image resolution enhancement process.

### 1.3 Problem Statement

The most of the regions of an image are covered by the numerous edges, and the accurate interpolation value for HR blank edge pixels from the LR neighbouring pixels considers as big challenge when the problem is are highly related to the edge directions (Park & Jeong, 2017).

The interpolation value of the HR edge pixel is directly replaced by the nearest neighbouring LR pixel which is close to the LR edge pixel shown in Figure 1.1. Therefore, HR edge pixels are not interpolated properly by the value of nearest neighbour LR pixels which degrades the quality of edges as well as the image quality. As a result, inaccurate interpolation and aliases problems are arisen because the large distortion on the edge regions shown in Figure 1.3 and unable to provide the fine details in the HR edge regions (Kao, Lai, & Tseng, 2015). The conventional interpolation methods are not efficient to assign accurate interpolation value to the HR edge pixels.

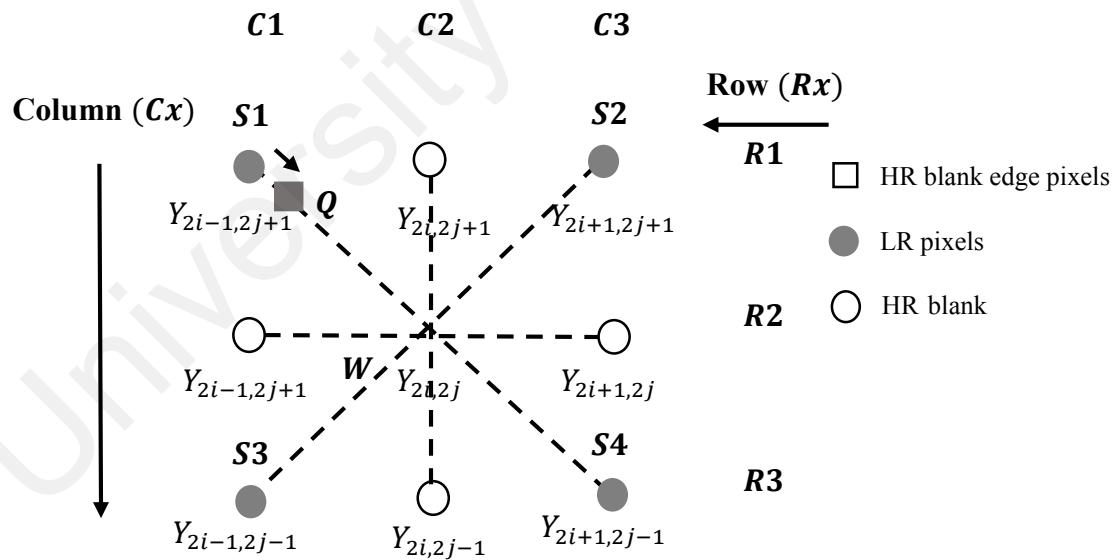


**Figure 1.1: The example of edge directed interpolation**  
**The value of LR pixel S1 is directly assign to the HR edge pixel Q; Since, the LR pixel value S1 is close to the HR edge pixel value Q**

The visual quality of the enhanced image is depended on the appropriate interpolation algorithm. Therefore, it is required to apply a proper edge directed interpolation method to reconstruct the HR image from the LR image.

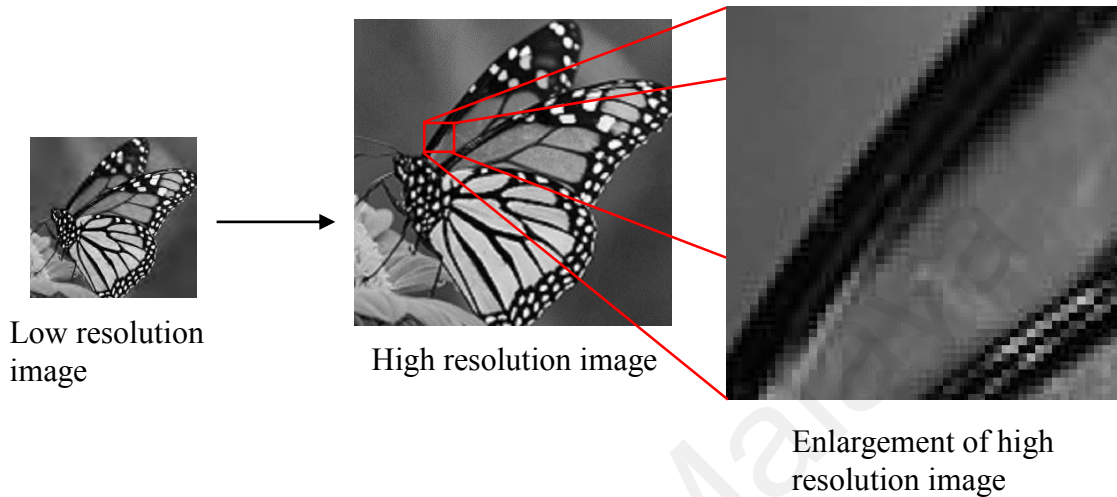


**Figure 1.2: The example of image resolution enhancement from LR image to HR image**

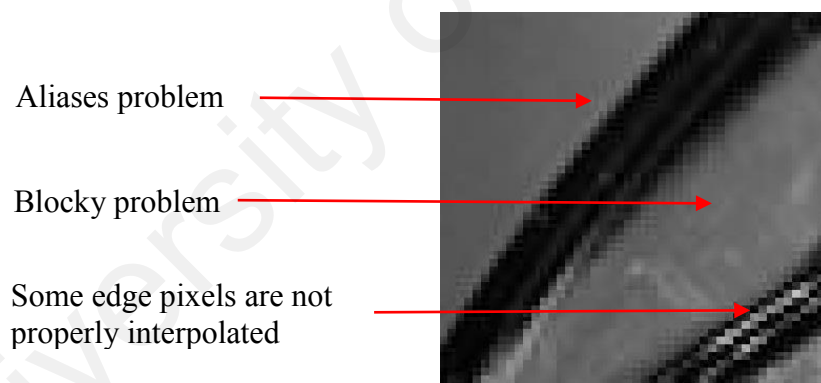


**Figure 1.3: The example of HR image cross section**

#### 1.4 Research Questions

Artifacts problem becomes severe when the image is enlarged with high scales because of the traditional interpolation method does not work properly to preserve the edge sharpness, information are loss along the edge regions and difficult to measure the values of unknown HR pixels (Yu, Zhang, et al., 2013).

In order to overcome the problems that has been identified, there are some research questions which need to be considered:

1. What is the interpolation processes for HR edge pixels?
2. How can HR edge pixels would get the proper and accurate value from LR pixels?
3. What are the best procedures to prevent the miss-interpolation and aliases problem for improving the edge quality?

The above basic questions are unaddressed in the review of literature study. The proposed method would be able to deal with the above questions.

### **1.5 Research Objectives**

The main objective of the image interpolation is to reconstruct sharp edges and texture of the HR image. Therefore, the primary condition to improve the image visual quality and decrease the image deterioration (Ousguine, Essannouni, Essannouni, & Aboutajdine, 2014). To meet the mentioned aim, the following objectives should be achieved:

1. To investigate different methods for image resolution enhancement.
2. To proposed an improved edge directed interpolation algorithm for HR edges pixels no matter whether the position of HR edges pixels is.
3. To test the proposed method using standard image sets.
4. To compare the result with other interpolation algorithms.

### **1.6 Research Contributions**

An improved sedge directed interpolation algorithm is proposed which improves the (Kao et al., 2015) method as well as the standing methods. The proposed method is able to interpolate HR edges directed pixels in any position. So the interpolation values of

edges pixels are more accurate than the other interpolation works. The proposed method considers four arrangements of the edge pixels such as horizontal, vertical and two diagonals from the LR edge pixels. The value of HR blank edge pixels is estimated from four weighted neighbouring LR edge pixels. The interpolation co-efficient for each HR neighbouring pixel is obtained from the corresponding LR pixels with Wiener filter method. This improved edge directed interpolation algorithm is reduced the artifices. Moreover, it ensures the accurate interpolation value for each HR edge pixels in fine edges regions with neighboring pixels.

In summary, the proposed method preserved the image edges well and can maintain the quality of image after image enhancement. The experimental results show that, proposed method outperforms the conventional edge directed interpolation in terms of qualitative and quantitative image quality.

## 1.7 Dissertation Structure

The dissertation is organized in to six chapters and short overview about all chapters are given bellows:

- **Chapter 1:** This chapter presents the introduction of interpolation algorithms and gives the brief discussion about motivation, research questions, research objectives and research contribution of this work.
- **Chapter 2:** Complete literature review are presented in this section mentioning the classical interpolation algorithm for image resolution enhancement as well as edge directed interpolation methods. Comparative reviews are given among different EDI algorithms. Strength and weakness are discussed about different EDI image enhancement methods.

- **Chapter 3:** In this chapter the whole methodology of this work is included with flow diagram. In each step graphical representation are included for better understanding.
- **Chapter 4:** The results of the proposed method as well as the results of existing EDI interpolation methods are calculated and described in this chapter based on the standard images data. After that, compare the results of proposed with the results of other existing EDI methods.
- **Chapter 5:** In this chapter the summary of the proposed work is given by mentioning the contribution of the proposed method and draws a conclusion by point out the further research work of the proposed method.

University of Malaya

## CHAPTER 2: LITERATURE REVIEW

### 2.1 Introduction

In this chapter, a comprehensive discussion is presented about various image resolution enhancement methods which are described by the various researchers. At the beginning of this chapter an overview of image resolution enhancement method is given. The rest of this chapter is briefly explained about the findings and different techniques of the image enhancement methods. Generally, image enlargement process is categorized in to three groups such as reconstruction based image resolution enhancement, learning based image resolution enhancement and interpolation based image resolution enhancement (L. Wang, Xiang, Meng, Wu, & Pan, 2013). However, the interpolation based image resolution enhancement is classified in to two sub-groups:

- I. Non-edge directed interpolation
- II. Edge directed interpolation

The graphical representation is as shown in Figure 2.1 as follow:

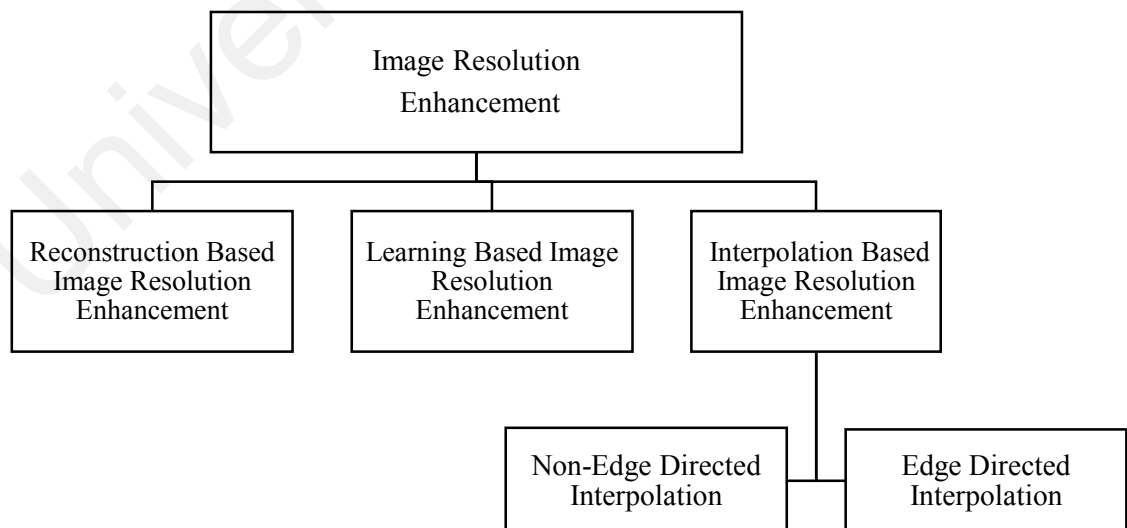


**Figure 2.1: The taxonomy of image resolution enhancement**

## 2.2 Reconstruction Based Image Resolution Enhancement

The reconstruction based image resolution enhancement method is used to build the relation between LR image and HR image. This method is effective and easy method which is used in many applications (Lin & Shum, 2004). The HR image is constructed based on the prior knowledge of framework. The HR image is the up sampling version of the LR image. The value of LR pixels are adjacent to the value of HR pixels and statistical edge features are used between LR image and HR image. The performance and quality of the enhanced HR image is depended on the kernel size and the capability of the given image (Shan, Li, Jia, & Tang, 2008).

The common problem of this method is the sharp edges which become blur after applying reconstruction algorithm but excellent results are produced in the smooth regions, except in the edge regions (Sun, Xu, & Shum, 2011). The blocking and artifacts along the line or diagonal edge are produced by this reconstruction method as shown in the Figure 2.2 (a). The diagonal edges are not only blur but also a staircase problem is visible. The blocking and staircase problem are raised by the vertical and horizontal kernel resampling area and unable to reconstruct or follow the diagonal edges. This reconstruction based method unable to produce the high frequency regions as shown in the Figure 2.2 (b). The input image is passed through the high pass and low pass filters and the results are shown that the higher distortion in the high pass filter rather than low pass filter (Van Ouwerkerk, 2006).

Gradient profile based edge reconstruction interpolation is proposed by (Tai et al., 2010). In this method HR edge are reconstructed from the LR image with learning based structure. In this approach, the edge regions are reconstructed and then gradient profile of the LR edge pixels are used as a prior knowledge and then transfer this gradient profile to the HR pixels but sometimes this gradient profile is mismatched with the HR pixels. As a result, image looks unnatural after employing reconstruction

algorithm. Generally, edge features are used for the prior knowledge. In some algorithm, nonlocal self-similarity is also considered for the prior knowledge (He & Siu, 2011).

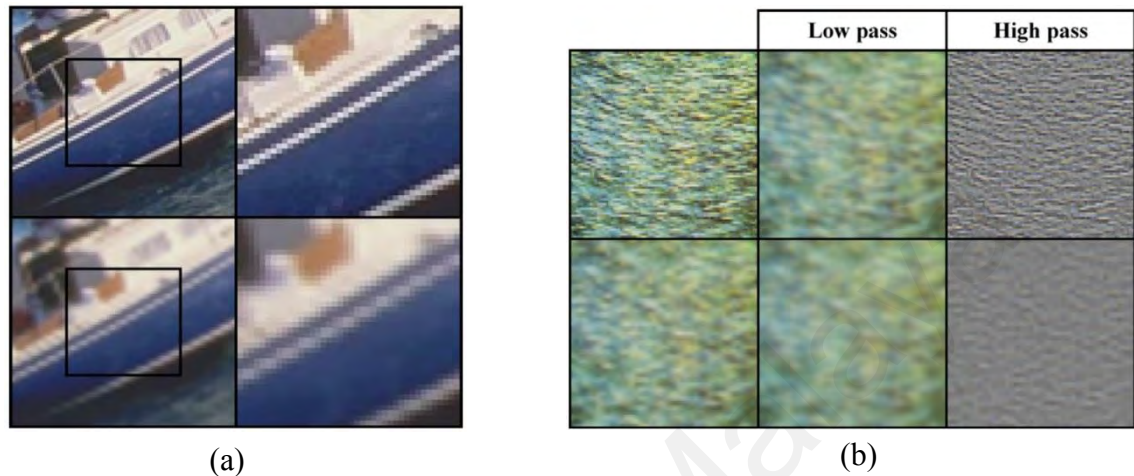


**Figure 2.2: The example of reconstruction interpolation**

(a) Upper row is the original images and bottom row is the output images; (b) Original images are passed through the low pass and high pass filters

### 2.3 Learning Based Image Resolution Enhancement

In the learning based method, the high frequency details of images are trained with the large amount of LR images. This process is highly depended on the images database and the test images. The image patches such as corners, ridges and edges are learned from the LR images then applied on HR frame to recover the HR image. The drawback of this method is that, the quality of HR image is depended on the prior knowledge of learning patches and the sufficient amount of training sets are required for this method which is time consuming (Kim & Kwon, 2008). The quality of edges is considerably degraded when the corresponding edges do not match with the training data set.

The self-example based learning method which is first proposed by (Freedman & Fattal, 2011) where the whole input LR image is not used instead, the patches are extracted from the extremely localized area of the input image. To find the appropriate example

patches, the local self-similarity is applied around the similar relative coordinates of the input image. As a result, the search time of the image patches are significantly reduced without degrading the HR image quality. Therefore, multiple small scaling factors are performed to achieve the enlarge image scale. Though it provides better results but computational complexity is high for calculating similarity matrix. Other problem of this approach is that the prior information may or may not valid for the approximate scaling factors (Giachetti & Asuni, 2011).

A neighbour embedding learning based algorithm for image resolution enhancement is presented by the (Gao, Zhang, Tao, & Li, 2012). In this method, the joint learning with coupled constraint is used to enlarge image. The K-nearest neighbour features are found for linear embedding to learn the image patch rather than the features of LR image alone. The pre-processing is applied to construct the K-nearest patches and this pre-process is linked the features of LR image with the corresponding HR image. The joint learning process based on projection matrices are used to learn the LR patches. The neighbour embedding algorithm is used to calculate optimal weights of the learned features and combine linearly higher frequency patches to synthesize high resolution image patches. Finally, back projection is used to maximize the prior knowledge and the construction constraint so that HR image would be near to LR image.

### **2.3.1 Hallucination Based Method**

Image hallucination method is proposed by (Xiong, Sun, & Wu, 2009) where the high frequency information is recovered by learning the co-occurrence examples with two resolutions levels. In this method, mapping accuracy is improved by the examples of LR image regarding to the mapped features such as primitives and derivatives. A pre-filtering process is used to enhance the features of LR image and the lost information in the high frequency regions are restored with non-blind de-blurring. The features of the

HR image are learned in hallucination with the energy conservation of LR features. Consequently, the dimensionality difference among the features of LR and HR images are decreased which are improved by the features mapping procedure. The high quality output result is produced for the enhancement of image features.

Context constrained hallucination image enhancement is presented by (Sun, Zhu, & Tappen, 2010). In this method, the examples the of HR image are learned from the textural related training segments. The pixels of HR image are hallucinated from the training set through texture similarity. Then a continuous energy function is applied to transform HR image from LR image. This method is able to provide sharp edges with minimum artifacts along textures and edge regions. The new patches are selected based on the textures appearance. These textures segments are used to introduce the high frequency regions in the HR image. The context constrain hallucination are implemented through the uniform segmentation of texture area of the LR image. The segmented patches are chosen based on the textural similarity to up sample the HR image. Then top similarity segment patches are searched on the training database and provided the corresponding HR textural contexts. Once the best matching patches are found on the LR training database then these patches are extracted to build the HR image.

#### **2.4 Interpolation Based Image Resolution Enhancement**

The basic structure of the interpolation methods are simple liner filtering and polynomial interpolation. The values of the HR pixels are obtained by the approximate values of the nearest neighbour LR pixels. The accuracy of the interpolation value is depended on the position of the HR pixels and selection process of the neighbour LR pixels. The values of the derived HR pixels are near to the values of LR pixels. The

existing interpolation methods are categorized into two groups. One group which does not consider the edge directions and another group which does consider the edge directions.

#### **2.4.1 Non-Edge Directed Interpolation Method**

Typical methods such as bilinear, cubic spline, bi-cubic, pixel replication interpolations are known as non-edge directed interpolation methods. The non-edge directed interpolation algorithms are used for their simplicity (M. Li & Nguyen, 2008). Nearest neighbour, kernel based, bilinear and bi-cubic interpolation methods are commonly used for processing the homogeneous regions in image. These algorithms are efficient in non-edge regions. But they fail to provide better results in edge regions by producing blur, halo and artifacts across the edge regions (Kao et al., 2015; Yu, Zhu, Wu, & Xie, 2013). The information of image structure is lost with the typical interpolation process.

##### **2.4.1.1 The Cubic Convolution Method**

The cubic convolution interpolation (CCI) method provides better results among the classical interpolation, for example linear and bilinear interpolation. But CCI interpolation does not preserve the better interpolation quality on the edge regions of the HR image (Meijering & Unser, 2003).

Gradient cubic convolution interpolation (GCCCI) method is introduced by (D. Zhou, Shen, & Dong, 2012) to enlarge an image. In this method, the pixels of blank HR edges are identified by calculating the gradient of vertical, horizontal, 135° diagonal direction and 45° diagonal direction and then interpolation is performed. But the common problem is the inaccurate interpolation in texture regions. To mitigate this problem only the pixels of strong gradient magnitude are considered for the GCCCI method and weak edges are interpolated by CCI. But the pixels of weak edges are also carry the strong

attributes of the HR image. So this method is not capable to provide the effective quality of HR image.

The equation of CCI interpolation is given below:

$$u(s) = \begin{cases} (a+2)|s|^3 - (a+3)|s|^2 + 1 & 0 \leq |s| < 1 \\ a|s|^3 + 5a|s|^2 + 8a|s| - 4a & 1 \leq |s| < 2 \\ 0 & 2 \leq |s| \end{cases} \quad (2.1)$$

Where,  $a = -\frac{1}{2}$  and  $s = \frac{1}{2}$  are known as the optimal constants for every two interpolations processes. The value of the pixel gradient is used to predict the horizontal, vertical,  $45^\circ$  diagonal and  $135^\circ$  diagonal directions as shown in Figure 2.3. After that, the pixel strength on the  $45^\circ$  diagonal and  $135^\circ$  diagonal direction are calculated based on the value of the pixel gradient. According to the  $7 \times 7$  neighbour matrix where the values of the pixels are known as shown in Figure 2.3 (a).

The gradient values of the central point  $(i, j)$  are calculated as follows:

$$G_1 = \sum_{m=3, \pm 1} \sum_{n=3, \pm 1} |I(i+m, j-n) - I(i+m-2, j-n+2)|$$

$$\text{For } 45^\circ \text{ diagonal edge pixels} \quad (2.2)$$

$$G_1 = \sum_{m=3, \pm 1} \sum_{n=3, \pm 1} |I(i+m, j+n) - I(i+m-2, j+n-2)|$$

$$\text{For } 135^\circ \text{ diagonal edge pixels} \quad (2.3)$$

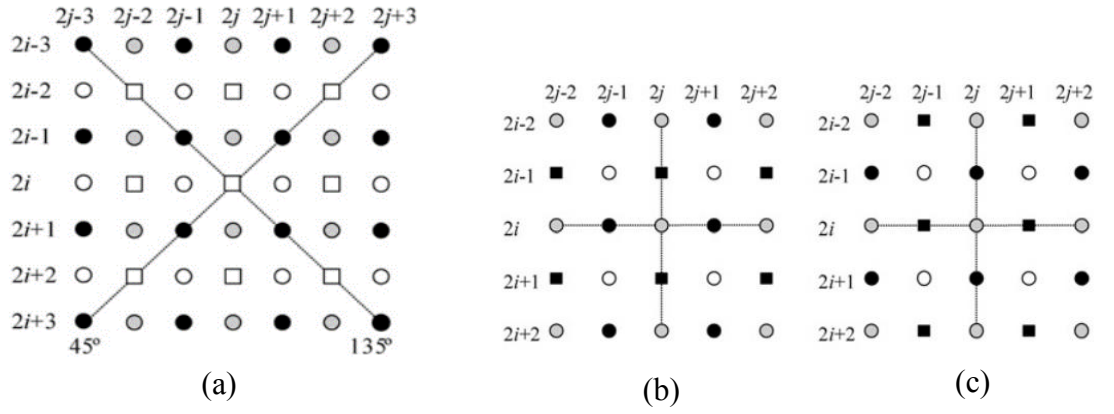


**Figure 2.3: The example of CCI interpolation**

(a) The gradient of the diagonal directions is calculated. The black circles are defined as LR pixels. Grey and white circles are defined as the unknown HR pixels; (b) & (c) The vertical and horizontal gradients are estimated

To measure the strength of pixels along the vertical and horizontal directions the gradient values are estimated as shown in Figure 2.3 (b) and 2.3 (c). In  $5 \times 5$  neighbour pixels matrix the gradient values at the central point  $(i, j)$  are calculated as follows:

$$G_1 = \sum_{m=3, \pm 1} \sum_{n=3, \pm 1} |I(i+m, j-n) - I(i+m, j-n-2)| + \sum_{n=0, \pm 2} |I(i-1, j+n) - I(i+1, j+n)|$$

*For horizontal pixels* (2.4)

$$G_2 = \sum_{m=3, \pm 1} \sum_{n=3, \pm 1} |I(i-m, j+n) - I(i-m+2, j+n)| + \sum_{n=0, \pm 2} |I(i-1, j+n) - I(i+1, j+n)|$$

*For vertical pixels* (2.5)

The direction of the pixel at location  $(x, y)$  is estimated based on the two orthogonal gradients  $G_1$  and  $G_2$ . Since the gradient value is small so the ratio of the orthogonal gradient is taken.

Cubic spline interpolation method are presented by (Ousguine et al., 2014). In this method after computing the position of blank HR pixels, the intensity of blank HR pixels are estimated with cubic spline interpolation where the values of four nearest

neighbour pixels are taken (Park & Jeong, 2017). The equation of cubic spline interpolation is given below:

$$\beta^3(x) = \begin{cases} \frac{2}{3} - \frac{1}{2}|x|^2(2-|x|) & 0 \leq |x| < 1 \\ \frac{1}{6}(2-|x|)^3 & 1 \leq |x| < 2 \\ 0 & 2 \leq |x| \end{cases} \quad (2.6)$$

Where,  $\beta$  is known as the spline function with degree  $n=3$  and  $x$  is known as the intensity of the LR pixel.

#### 2.4.1.2 The Second Order Derivative Method

The second order derivative interpolation method is proposed by (Asuni & Giachetti, 2008). In this method, the images are enlarged approximately copying from original images by the factor scale two. The original pixels are indexed with  $(i,j)$  and placed in an enhanced grid with indexed  $(2i,2j)$ . Then, fill up the hole of the grid recursively by analysing the local pixels. The average weight of the pixels of four diagonals pixels are taken to fill the hole.

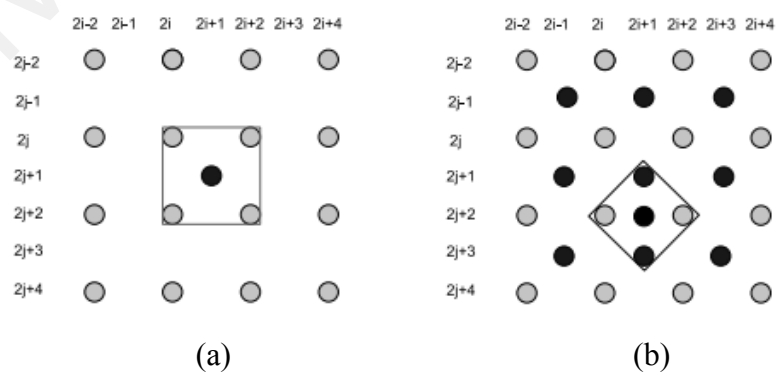


**Figure 2.4: The example of second order derivative interpolation**

(a) The first step four diagonal pixels are taken for interpolation; (b) The second step four nearest neighbour pixels are taken for interpolation

Then four nearest pixels are taken to interpolate in vertical and horizontal directions are shown in Figure 2.4 (a) and Figure 2.4 (b). In this method, computational complexity is increased for recursive process.

### 2.4.1.3 Curvature Based Method

Curvature based interpolation method is presented by (Giachetti & Asuni, 2008; Vairavaraja & Gunasekaran, 2013). In this method, the second order derivatives are calculated along the two diagonal directions. Then the interpolation is performed with the opposite neighbour pixels according to that direction where the value of derivative is minimum. The interpolation is as shown in Figure 2.5. The twelve neighbour pixels are considered along two diagonal orders. Then, the approximate value of second order derivative is calculated along the vertical and horizontal directions.

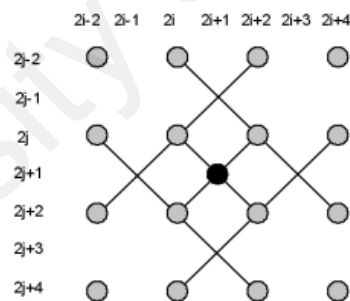


**Figure 2.5: The example of iterative based interpolation on 12 nearest neighbour pixels and determine the interpolation value based on second order derivative**

Here, only the value of second order derivative which is larger than the fixed value is avoided. The interpolation is continued only through the direction of minimum grey scale difference. The iterative process is continued until current iterative value is lower than the constant threshold value or has been reached the number of maximum iterations.

The non-linear fourth order partial differential equation (FO-PDE) (Warbhe & Gomes, 2016). In this method, bi-cubic interpolation is combined with FO-PDE. The PDE is used for de-noising the image and decrease the artifacts. PDE is applied after interpolation on the HR image. In this method, LR image is up scaled with the factor scale 2 or 4 corresponding to the dimensions of rows and columns. Then, blank HR pixels are interpolated with the bi-cubic interpolation. After applied the bi-cubic interpolation, the output HR image is taken as input for the FO- PDE. The FO-PDE is used for removing the noise of bi-cubic interpolated image  $Y(x, y)$  and reconstruct the output image  $I(x, y)$  FO-PDE is applied iteratively until to get a stable output.

The equation of non-linear FO-PDE is calculated as follow:

$$I^{k+1} = I^k - \Delta t \left[ E_{xx} \left( \frac{E_{xx} I^k}{|E^2 I^k|} \right) + E_{yx}^- \left( \frac{E_{xy}^+ I^k}{|E^2 I^k|} \right) + E_{xy}^+ \left( \frac{E_{yx}^+ I^k}{|E^2 I^k|} \right) + E_{yy} \left( \frac{E_{yy} I^k}{|E^2 I^k|} \right) \right] - \Delta t \lambda (I^k - Y)$$

$(k = 0, 1, 2, 3, \dots, n)$

(2.7)

Where, k is known as the number of iteration, time step is define by  $\Delta t$ ,  $I^k$  is defined the enlarged output image after iteration. Though, the better visual quality is provided with bi-cubic interpolation but the time complexity is high. However, the staircase and blurring problems are existed in the edge regions.

#### 2.4.1.4 Covariance Based Method

The covariance based interpolation is proposed by (Bo Wang, 2013). The several neighbour pixels of LR image are considered to estimate the covariance of HR image. This method is fast to compute but drops the visual quality. Covariance are estimated with the linear interpolation equations is as follow:

$$\hat{Y}_{2i+1, 2j+1} = \sum_{k=0}^1 \sum_{l=0}^1 \alpha_{2k+l} Y_{2(i+k), 2(j+l)}$$

(2.8)

$$\alpha = R^{-1}r \quad (2.9)$$

Where,  $\vec{r} = [r_k], (0 \leq k \leq 3)$  and  $R = [R_{kl}], (0 \leq k, l \leq 3)$  these are known as the covariance of HR pixels.

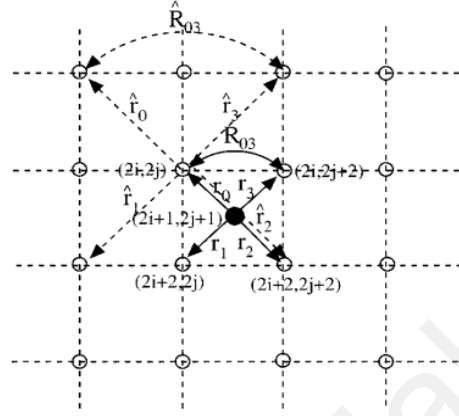


**Figure 2.6: The example of the process of estimating  $Y_{2i+1, 2j+1}$  from  $Y_{2i, 2j}$**

In this process  $r_0$  is calculated by  $E[Y_{2i, 2j}Y_{2i+1, 2j-1}]$  and the value of unknown pixel  $Y_{2i+1, 2j+1}$  is determined as shown in Figure 2.6. The covariance of LR pixels  $R_{kl}$  and  $r_k$  are estimated with the traditional covariance method known as local window and the equations are given as below:

$$\hat{R} = \frac{1}{M^2} C^T C, \hat{r} = \frac{1}{M^2} C^T \vec{y} \quad (2.10)$$

Where,  $\vec{y} = [y_1 \dots y_k \dots y_{M^2}]^T$  is defined as a data vector having the local window of  $M \times M$  pixels and data matrix is defined as  $C$  with size  $4 \times M^2$  whose  $k$ th column is four neighbor pixels of  $y_k$  on the diagonal direction.

#### 2.4.2 Edge Directed Interpolation Method

Edges are easily attracted by the human visual system. Therefore, to preserve the edge quality, it is important to apply an adaptive edge directed interpolation for edge regions.

The main idea of the edge directed methods are to maintain the sharp edges after image upscaling and directly related to the edges reconstruction. Therefore, it is required to estimate the edges orientation. Since, the edges of the image are blurred, aliases, blocky and noisy. So, the performance of the edges directed interpolation algorithm is depended on the accurate estimation of edges directions of the LR images (Tam, Kok, & Siu, 2010). Considering the necessity of the interpolation through edges directions, several methods are mentioned. Some edge directed interpolation algorithms have been proposed to detect the edge regions and improve the HR image visual quality after enlargement. In these methods, the edges are preserved after enlarged the LR image while untouched the smooth regions. But the primary limitation is that, the high frequency regions are not able to reconstructed. As a result, the image becomes unnatural in the high frequency regions (Kao et al., 2015). The successful extraction of the edges information is a challenged for this technique specially for low contrast image and often artifacts are raised.

The first edge directed interpolation (EDI) method is proposed by (Allebach & Wong, 1996). This method is divided into two phases. The first phase is known as rendering phase. In this phase, the HR edge map is generated by the rectangular center on surround off the filter. Then piecewise linear interpolation is applied on the output filtered image. The interpolation along the edges regions are prevented by the bilinear interpolation where edges are determined during the HR edge map. The second phase is known as correction phase. In this phase, the mesh values are modified for the disparity between LR image and HR rendered image. The whole process is as shown in Figure 2.7 and recursively repeated but the artifacts and efficiency are the major issue for this method.

Filter based edge directed interpolation method is introduced by the (Q. Wang & Ward, 2001). In this method the edges are detected with Sobel filter.

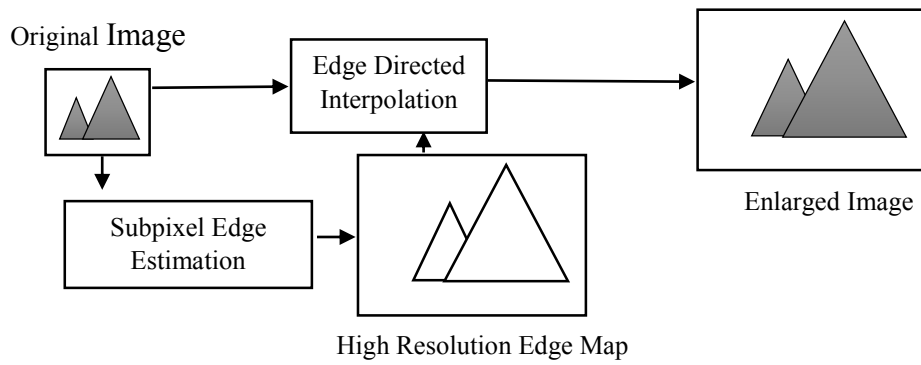


**Figure 2.7: The example of the framework of edge directed interpolation**

In filter based edge directed interpolation method where image pixels are separated into homogenous and edge regions depend on the pre-defined threshold value (Chen, Huang, & Lee, 2005). After that, LR edge pixels are mapped with the expanded grid of HR pixels as shown in Figure 2.8. Each LR edge pixel is considered as a parent pixel of the mapped HR pixels. The pixels around the LR edge pixels are considered as child pixels. Then mean intensity value is taken.

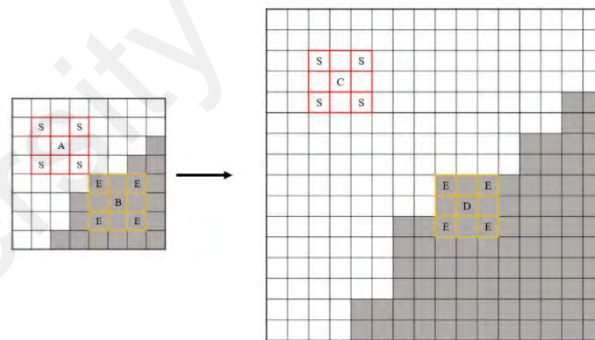


**Figure 2.8: The example of fast edge directed interpolation**  
**The surrounding pixel selection and the structural relation between HR pixels and LR pixels**

After employing the HR pixel mapping, the function of edge sharpening is used as follow:

$$f(x) = \frac{x^2}{2x^2 - 2x + 1} \quad 0 \leq x \leq 1 \quad (2.11)$$

Where,  $x$  is defined as the pixel intensity.

### 2.4.2.1 Edge Directed Method

New edge directed interpolation (NEDI) method is the most promising algorithm proposed by (X. Li & Orchard, 2001). The basic idea of the NEDI is based on pixel covariance and fourth order linear interpolation are used to fill the enlarged lattice where four nearest neighbor pixels are used for the interpolation through diagonal direction. The pixel covariance of HR image is estimated with the geometric duality. The local window corresponding to the pixel covariance of the LR image is as shown in the Figure 2.9. The pixel covariance of HR image is defined as  $R_{kl}, r_k$  and the pixel covariance of LR image is defined as  $\hat{R}_{kl}, \hat{r}_k$  shown in Figure 2.9 (a). The orientation of edges  $Y_{i,j}(i+j = odd)$  and  $Y_{i,j}(i+j = even)$  are considered to estimate the geometric duality where the scaling factor is  $2^{1/2}$  and the rotation factor is  $\pi/4$  as shown in Figure 2.9 (b).

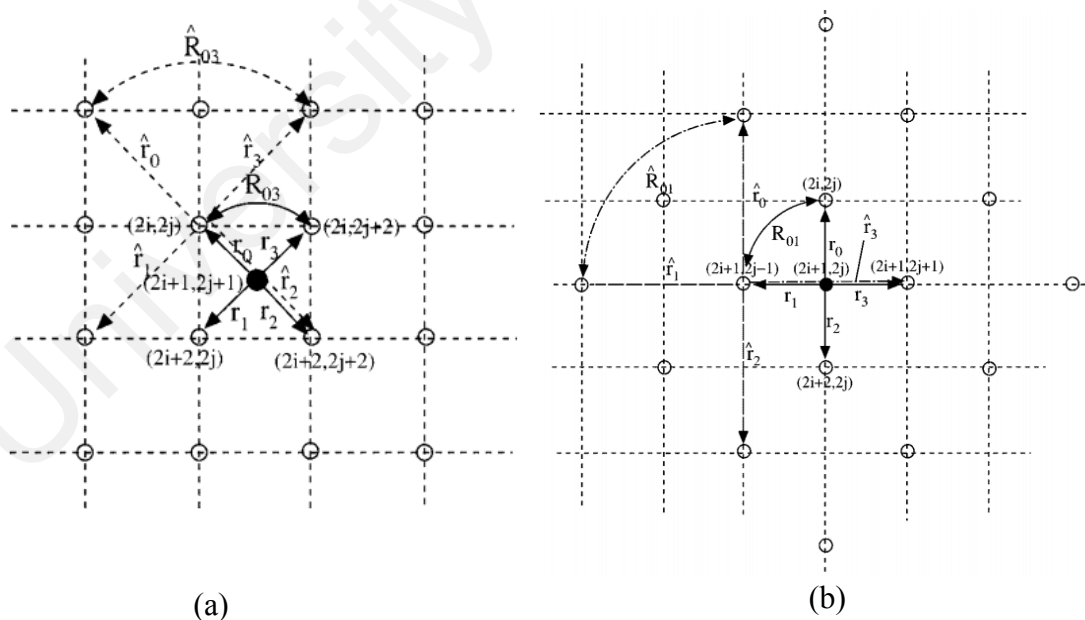


**Figure 2.9: The example of the NEDI process**

(a) The geometric duality for NEDI from the image scale  $Y_{2i,2j}$  to  $Y_{2i+1,2j+1}$  ; (b) The rotation of lattice is in  $\pi / 4$  position

The pixel covariance of LR image is measured. Then, the interpolation value is obtained from the matrix operation based on the edge types. The classical interpolation methods are compared with this covariance based method. The image visual quality is improved dramatically and preserved the edge sharpness. But the main problem is that, the operational cycle of this method is too long. Also, global brightness and error propagation problem are existed. Also, the size of interpolation kernel is large (Tam et al., 2010). However, only four neighbor pixels are considered in the diagonal edge regions. As a result, few of the unknown HR pixels are not interpolated from the LR original pixels. Therefore, the visual quality of the interpolated image is degraded along the edge regions. It is assuming that significant correlation is existed between HR and LR image which is not sufficient for approximation and the artifacts problem is introduced in the high-frequency area (Yu, Zhu, et al., 2013). Moreover, in NEDI method, the covariance mismatch are raised in low frequency and high-frequency regions because of proper window selection.

An improved window selection method is proposed by (Wong & Siu, 2010a). In this method, the appropriate and best elliptic window are selected as shown in Figure 2.10. The minimum means square error (MER) is estimated based on the edge direction with these elliptic windows.

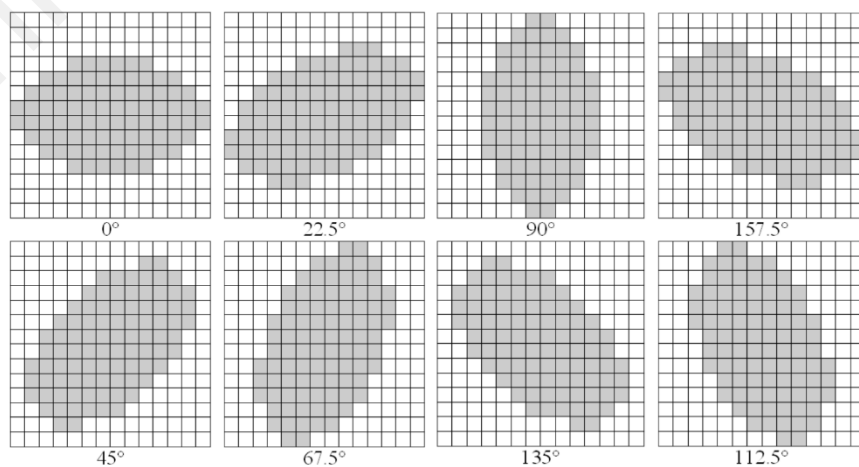


**Figure 2.10: The example of eight types of elliptic windows**

The eight different filters are used to determine the eight types of directions. They are  $0^\circ$ ,  $22.5^\circ$ ,  $45^\circ$ ,  $67.5^\circ$ ,  $90^\circ$ ,  $112.5^\circ$ ,  $135^\circ$ , and  $157.5^\circ$ . Adaptive elliptic windows are applied on the corresponding edge pixels based on the edge direction. The elliptic window is defined as follow:

$$E_\theta : \frac{(x \cos(\theta) - y \sin(\theta))^2}{a} + \frac{(x \sin(\theta) - y \cos(\theta))^2}{b^2} = 1 \quad (2.12)$$

Where,  $\theta = 0^\circ$ ,  $22.5^\circ$ ,  $45^\circ$ ,  $67.5^\circ$ ,  $90^\circ$ ,  $112.5^\circ$ ,  $135^\circ$  and  $157.5^\circ$ .  $a=3$  and  $b=7$  for wiener filter to get the sufficient sample points. The eight directions of elliptic windows are determined by  $14 \times 14$  matrix where sample points and direction are presented by grey color as shown in Figure 2.10. Though, this method is able to overcome the pixel mismatch problem but ringing and artifacts effects are still existed.

Improved new edge directed interpolation (iNEDI) method is introduced with the multiple window shapes (H. Zhou et al., 2016). In (iNEDI), the direction of edge pixel is determined. Then multiple window shape is used based on the edge characteristics, directions, and geometric regularity. The window shape is changed from circular to an ellipse for the lengthy axis through the edge directions. This window selection process is better than the constant covariance constraint. To reduce the error propagation problem of NEDI method which is sensitive for edges estimation. An effective trick is applied by adding a constant with the grey levels so that all values are far from the zero. The improvement is done by subtracting the mean value of the four nearest neighbor pixels from the inserted value in  $C$  as follows:

$$C\bar{\alpha} = \bar{y} \quad (2.13)$$

$$C = \begin{pmatrix} I_{h1-1,k1-1}, I_{h1-1,k1-1}, I_{h1-1,k1-1}, I_{h1-1,k1-1} \\ I_{h2-1,k2-1}, I_{h2-1,k2-1}, I_{h2-1,k2-1}, I_{h2-1,k2-1} \\ \dots \\ I_{hN-1,kN-1}, I_{hN-1,kN-1}, I_{hN-1,kN-1}, I_{hN-1,kN-1} \end{pmatrix} \quad (2.14)$$

Where,  $h, k \in W(2i + 1, 2j + 1)$ ,  $\bar{y} = (I_{h_1, k_1}, I_{h_2, k_2}, I_{h_3, k_3}, \dots, I_{h_N, k_N})^T$  and  $W(2i + 1, 2j + 1)$  is defined as the average value of the center pixel of the square window as shown in the Figure 2.11. The coordinate of  $n$ -th pixel point inside the circular window is defined as  $(h_n, k_n)$ . The coefficient  $\alpha_i$  is obtained by solving the least square algorithm.

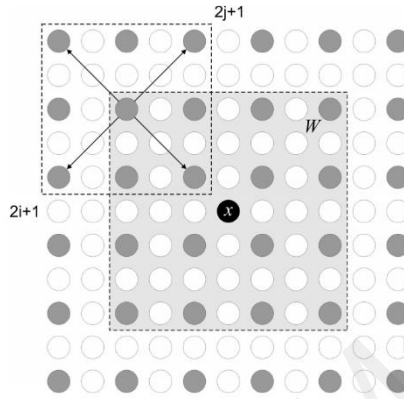


**Figure 2.11: The example of estimating diagonal weight  $W$  of the nearest neighbour pixels**

The non-edge pixels are interpolated with bilinear interpolation for easy and simple calculation. The edge direction is estimated based on the covariance process and the  $\theta$  is calculated as follow:

$$\theta_{I(x,y)} = \tan^{-1} \left( \frac{\partial I / \partial y}{\partial I / \partial x} \right) \quad (2.15)$$

Where,  $\partial I / \partial y = I(x, y + 1) - I(x, y)$  and  $\partial I / \partial x = I(x + 1, y) - I(x, y)$  for image  $I(x, y)$

After estimating the direction of the edge, the range of pre-set threshold  $T_\theta$  is determined. If the angle of edge orientation is fallen within the threshold rang then the elliptic window is selected for edge pixel interpolation otherwise circular window is taken. But the time complexity is increased significantly for the window selection process and noticeable artifacts are visible at edge regions.

### 2.4.2.2 Markov Random Field Edge Directed Method

Markov random field EDI method is proposed by (M. Li & Nguyen, 2008). In this method the direction of the edge is not measured explicitly rather than the direction of edge is determined with implicit information. In this method the continuity of the edge direction is preserved with the range of rational number from 0 to 1 instead of labelling the pixel either it is non-edge or edge pixel. The strong edge directional continuity is indicated with the higher value and the weak edge directional continuity is specified with the lower value. In this method sixteen directional edges are considered as shown in Figure 2.12. The values of the directional pixels are presented in a vector. The magnitude of the vector is represented the distance between centre pixel and the neighbour pixels corresponding to the edge direction. The continuity of edge direction is determined with the variation of local data frames which is the statistical property of the pixel intensity. So the directional information of edge is obtained from the relative continuity of edge strength in all directions and this directional information is used to calculate the spatial constraint of geometric regularity which is responsible for the sharpness of pixel across the edge regions. The ringing problem and computational complexity are reduced in this process. Though the direction of edge is accurately identified by the implicit information of the pixels but the edge continuity is not able to

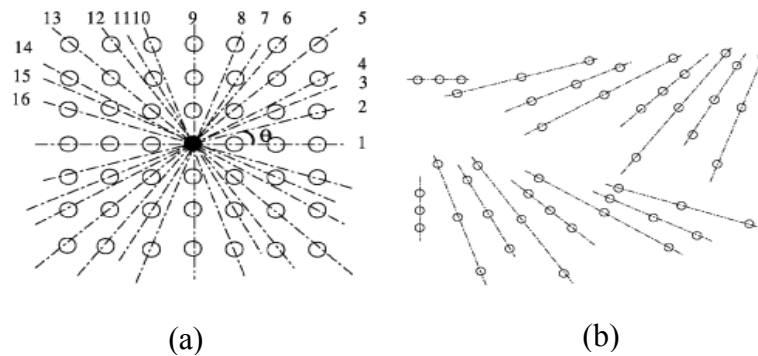


**Figure 2.12: The example of Markov random field EDI method**  
(a) The neighbour pixels structure; (b) Sixteen directions are consider on the  $7 \times 7$  pixel matrix

determine the edge width. This method is not robust for outlier because of the ordinary least square method. In the noisy image, the performance of this method is severely hampered.

### 2.4.2.3 Non-local Edge Directed Method

Non-local edge directed interpolation (NLEDI) is introduced by (Zhang, Ma, Zhang, Zhang, & Gao, 2009) where the coefficient of optimal interpolation is calculated with the least square weight. After that, NLEDI are obtained with the geometric duality of LR pixels. The stable interpolation solution is obtained from the difference of geometric configuration. But the different values of blank HR edge pixel are produced from the different structures of the LR edge pixel.

Segmentation based edge directed interpolation method is proposed by (Tai et al., 2010). In this method, the image is up-scaled with both the mean shift segmentation and bilateral filtering. In the upscaled image, the edges are divided into two groups, one is hard edge and another is soft edge constraints. The shock filter is applied to enhance the strong edge regions and intermediate enhanced HR image is produced. Since the strong edges of intermediate result are enhanced so artifacts and ringing problem are suppressed. The soft edges constrain are enforced with bilateral filtering for preserving the edges. Finally, the reconstruction constraint is applied on the HR image and final results are obtained by the back projection. The overall process is shown in the Figure 2.13.

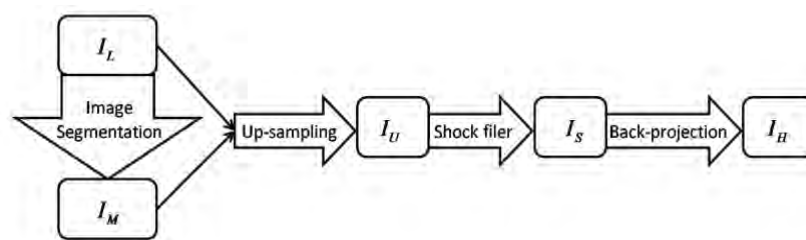


**Figure 2.13: The framework of edge preserving method**

Moreover, the noticeable ringing problem is raised for the combination of complex shock filter and back projection process.

#### 2.4.2.4 Window Selection Edge Directed Method

Window selection edge directed interpolation is proposed by (Wong & Siu, 2010b) to enhance the performance and to mitigate the error propagation problem of edge directed interpolation. The multiple LR windows are considered as shown in Figure 2.14. to solve the covariance mismatch problem which is appeared in EDI methods. The covariance is obtained from the window blocks as shown in Figure 2.15. The existence of an edge is ensured by the higher value of covariance. In the local block, if the covariance of the pixels is greater than the pre-defined threshold value then the unknown pixel is defined as an edge pixel otherwise non-edge pixel. Bilinear interpolation is applied at the smooth regions. The fourth order linear interpolation is applied for HR edge pixels and the unknown HR edge pixel ( $Y_{2i,2j+1}$ ) is estimated as follow:

$$(Y_{2i,2j+1}) = \sum_{l=0}^2 \alpha_l Y_{2(i+l-1),2j} + \sum_{l=0}^1 \alpha_{3+l} Y_{2(i+l)-1,2j+1} + \sum_{l=0}^2 \alpha_{5+l} Y_{2(i+l-1),2j+2} \quad (2.16)$$

Where,  $\alpha_l$  is defined as the coefficient of linear predictor. The false value of edge pixels is reduced with this directional window selection method and the sharpness of HR image edges is improved with the full use of relative information of LR image.

Since, fourth order linear interpolation is applied to calculate the unknown value of HR edge pixels, so the computational complexity is relatively high and the image quality is depended on the chosen parameter.

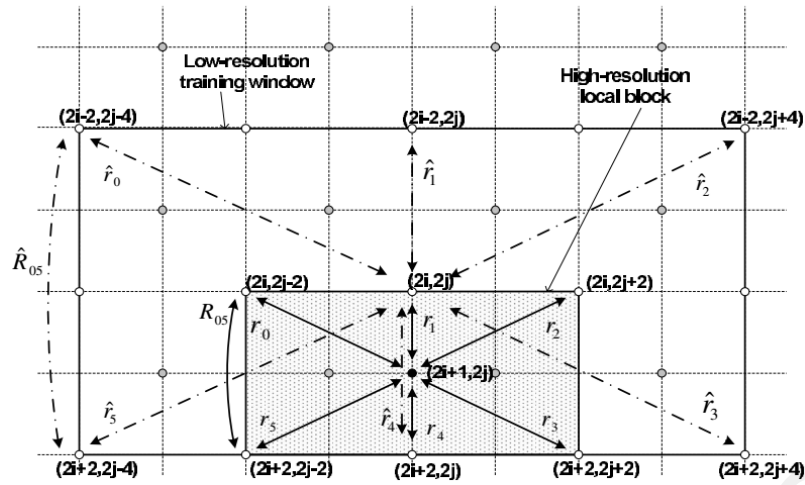


Figure 2.14: The example of interpolation steps and window block of the window selection method

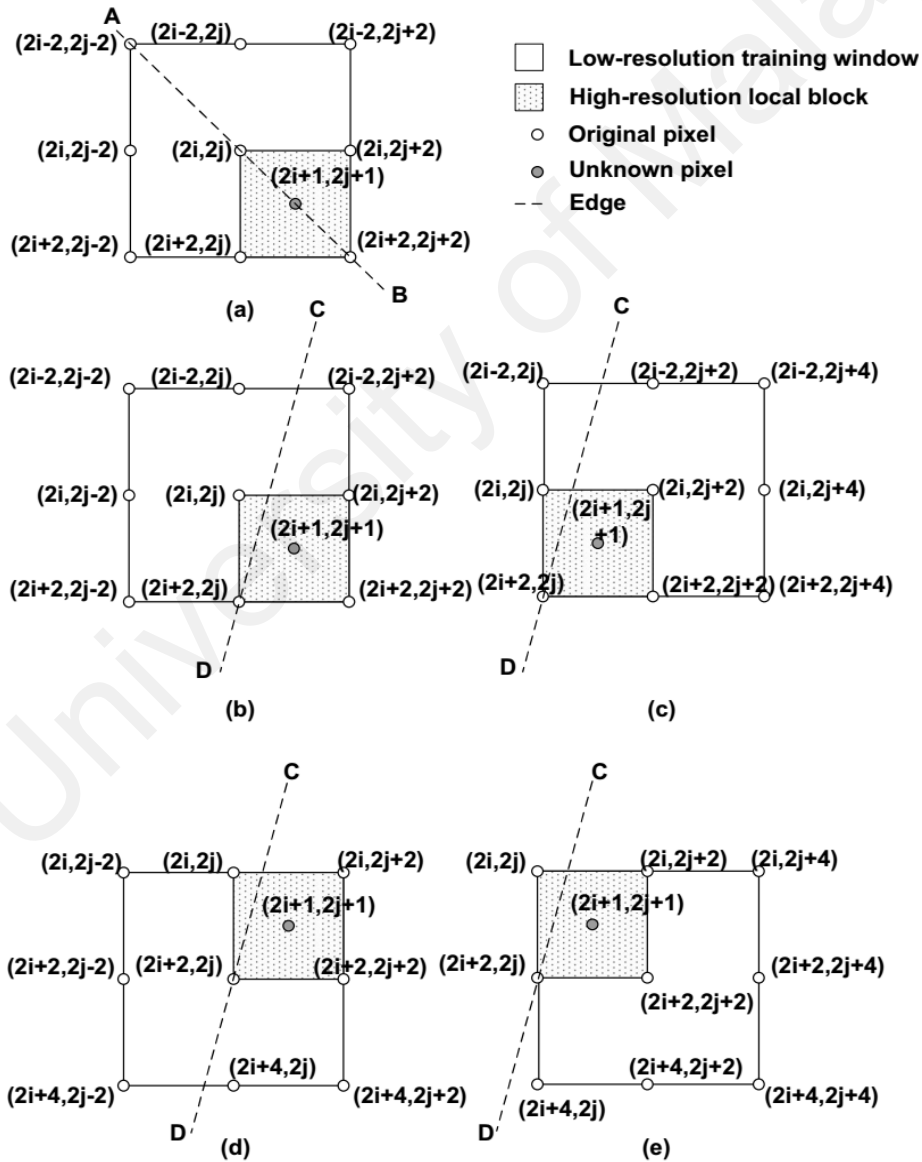
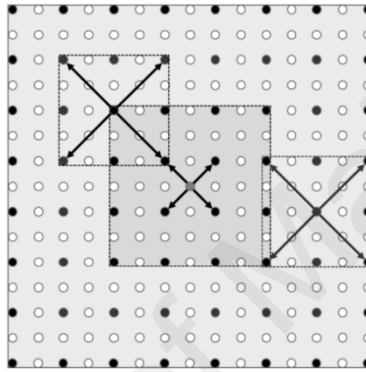


Figure 2.15: The example of window blocks

(a) The high resolution window block; (c)-(e) The covariance are calculated

The window extension edge directed interpolation method is introduced by (Wee et al., 2017). The geometric duality is used for window selection. Inside the window the pixels are limited and the similarity of pixel structure between LR and HR pixels are different based on the pixel characteristics. As a result, distortion is happened at the edge regions. The nearby pixels for window extension of the current window are shown in the Figure 2.16. This process is applied repeatedly to find all the surrounding pixels of the present window.



**Figure 2.16: The example of window extension and the nearby pixels range of the standing window**

When the pixel arrangement of the current window is irregular then geometric duality among LR and HR pixels is reduced. As a result, unusual reference pixels are made up. The interpolation error is estimated as follow:

$$I = \begin{cases} \max(N) & \text{if } I > (N) \\ \min(N) & \text{if } I < (N) \end{cases} \quad (2.17)$$

$$N_k \in \{the\ neighbor\ 4\ pixels\ of\ I\ to\ be\ interpolated\}$$

If the interpolated value of HR pixel is larger than the surrounding 4-pixel values, then this interpolated value is replaced with the near most value among the 4 neighbor pixels. The irregularity pixel arrangement inside the present window is reduced by the clipping process.

### 2.4.2.5 Multidirectional Edge Directed Method

Multidirectional edge directed interpolation method is introduced by (Yun et al., 2011) where the algorithm is divided into three parts for reducing the computational complexity. Edge is mapped by the canny filter to upscale from LR image to HR image. So the homogenous regions are separated from the edge regions. Then long edge areas are interpolated with edge directed interpolation where twelve LR neighbor pixels in vertical, horizontal and two diagonal directions are considered for interpolation as shown in Figure 2.17. The interpolation for  $Y_{2i+1,2j+1}$  edge pixel is given below:

$$Y_{2i+1,2j+1} = \sum_{k=0}^3 \sum_{l=0}^3 \alpha_{4k+l} Y_{2(i+k-1),2(j+l-1)} \quad (2.18)$$

Where,  $\alpha_i$  is known as interpolation coefficient and  $\alpha_{0,3,12,15} = 0$ . Short edge areas are interpolated with multidirectional edge directed interpolation method and smooth areas are interpolated with linear interpolation. But there is no smooth transition in the junction of short and long edge regions. As a result, artifacts and blocky problems are appeared on that regions. This method is not able to provide the optimal result.

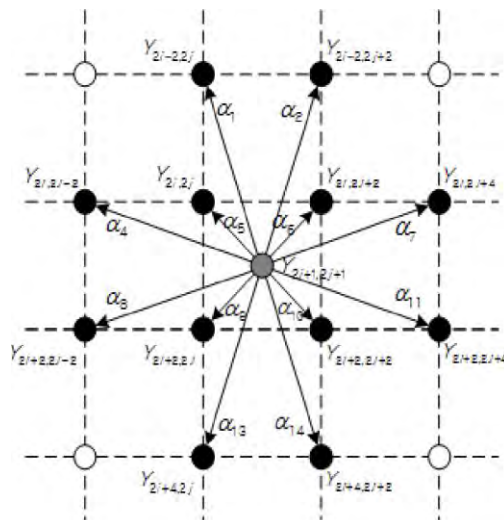
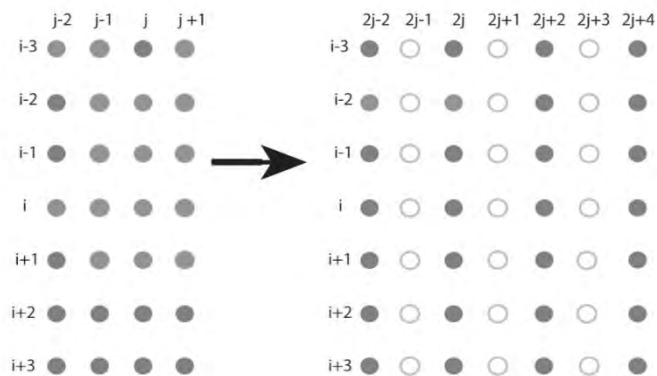


Figure 2.17: The example of multidirectional interpolation of  $Y_{2i+1,2j+1}$  edge

### 2.4.2.6 Pixel Mapping Edge Directed Method

The edge map EDI method is directly used to interpolated the edges orientation based on the gradient operators. This method able to eliminate the staircase and blurring problem but edge map has some limitation. The inherent problem exists in the edge map process and the image structure is not completely adaptive with the gradient operator (Q. Zhou, Chen, Liu, & Tang, 2011).

The grid method for the image enhancement is proposed by (Giachetti & Asuni, 2011). The corresponding edge features, natural texture and enlarged image without artifacts are preserved with this method. According to this method, the original image is enlarged in double size then the holes of the enlarged grid are filled with neighbor pixels as shown in Figure 2.18. The process of filling holes is done by the two steps. The linear interpolation is performed where the image brightness of second order derivative is lower. After that iterative approach is employed to refine the value of each hole for update and find the optimum value. In this process, the strong discontinuity of image intensity is maintained and the local variance is minimized. The constraint which is used for this method to preserve the continuity of second order derivatives is simple and effective for removing artifacts and the limitations are removed by changing the constant covariance (Hosogai & Tanaka, 2014).



**Figure 2.18: The example of LR pixels are copied and placed in the HR grid**

Improved grid edge mapping analysis and optimal interpolation for edge and non-edge regions are presented by the (Park & Jeong, 2017). In this method, all LR pixels are separated into high-frequency regions and low-frequency regions. The edge map of HR pixels is built with Sobel filter. Then pixel intensities are calculated. The pixel would be an edge pixel if the pixel intensity is greater than the average intensity of the neighbor pixels. Edge pixels are divided into four directions ( horizontal, vertical, 45° diagonal and 135° diagonal ) using threshold value. Bilinear interpolation is performed in the non-edge regions and in the edge regions, four surrounding pixels are used to build an edge map.

The reference pixels in vertical and horizontal directions are used to interpolate the edge pixels. If the reference pixels are not present, then interpolation is accomplished after estimating the values of reference pixels with cubic spline interpolation as shown in Figure 2.19.

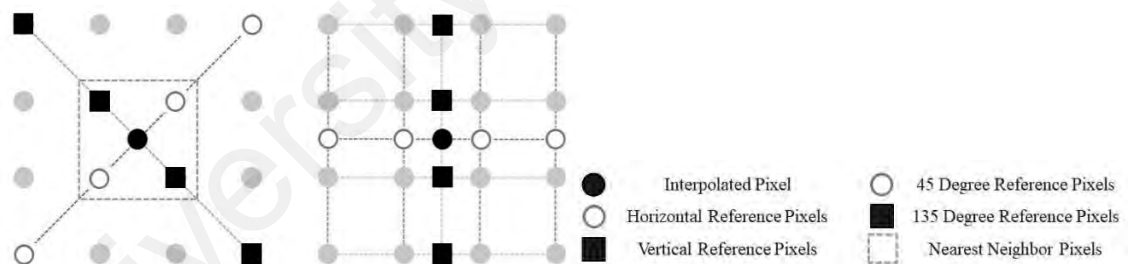


**Figure 2.19: The example of cubic spline interpolation in horizontal and vertical direction**

However, the computational complexity of this algorithm is low but could not reduce the artifacts due to edge mapping. There is no smooth transition between the non-edge region and edge regions. As a result, the staircase problem are visible in the edge area.

### 2.4.2.7 Fast Edge Directed Method

A fast edge directed interpolation (IFEDI) method is proposed by (Bo Wang, 2013). In this algorithm image pixels are partitioned in the edge pixels and non-edge regions by using the pre-set threshold value based on the characteristics of local structure (Tian et al., 2012; Q. Wang & Ward, 2001; H. Zhou et al., 2016). The edge pixels and non-edge pixels are determined based on the local covariance. The unknown pixels would be the edge pixels if the covariance of LR pixels is above the fixed threshold value. The threshold value is determined with experimentally (Tian et al., 2012). In this algorithm, the local covariance is estimated from the nearest neighbor pixels to determine the HR unknown pixels to be edge pixels or non-edge pixels as shown in Figure 2.20. The three possible types of unknown HR pixel positions  $Y(2i,2j)$ ,  $Y(2i,2j-1)$ , and  $Y(2i-1,2j)$  are presented accordingly. The possible unknown HR pixel  $Y(2i,2j)$  and nearest four neighbor pixels are taken as shown in Figure 2.20 (a). The process to determine the non-edge pixel and edge pixel are described based on the pixel intensity value.

The values of neighbour pixels are  $Y(2i-1,2j+1)$ ,  $Y(2i+1,2j-1)$  and  $Y(2i+1,2j+1)$  respectively. If the covariance of vertical, horizontal, 45° diagonal and 135° diagonal neighbor pixels are smaller than the per defined threshold value then the unknown HR pixel  $Y(2i,2j)$  is identified as non-edge pixels. Otherwise, the unknown pixel  $Y(2i,2j)$  is determined as edge pixels. The unknown HR pixels  $Y(2i-1,2j)$ ,  $Y(2i,2j-1)$  and their closest neighbor pixels are presented in Figure 2.20 (b) and 2.20 (c). The separation process for non-edge and edge pixels is as same as the process for  $Y(2i,2j)$  in Figure 2.20 (a). The process for calculating the difference of LR neighbor pixels is given as follows (Tian et al., 2012):

$$\begin{aligned}\Delta y_{45^\circ} &= |Y(2i-1,2j-1) - Y(2i+1,2j+1)| \\ \Delta y_{135^\circ} &= |Y(2i-1,2j+1) - Y(2i+1,2j-1)|\end{aligned}\tag{2.16}$$

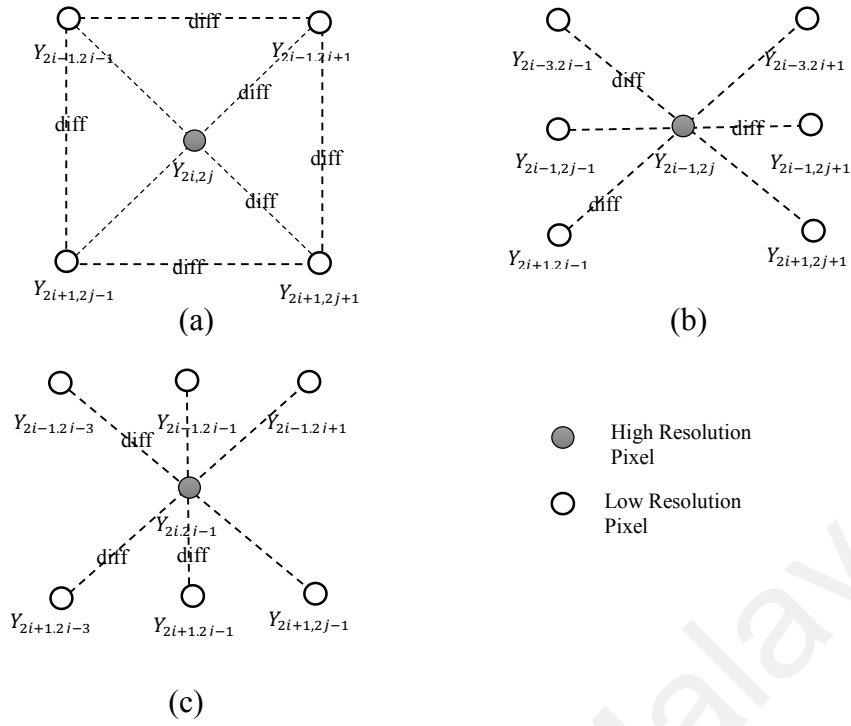


**Figure 2.20: The example of unknown HR pixel**  
 (a), (b) and (c) The arrangement of LR neighbour pixels

The minimum value is estimated between  $\Delta y_{45}$  and  $\Delta y_{135}$  if  $\Delta y_m > T$ , then  $Y(2i,2j)$  is an edge pixel.

$$\begin{aligned} \Delta y &= |Y(2i-1,2j-1) - Y(2j-1,2j+1)| \\ \Delta y &= |Y(2i-1,2j-1) - Y(2j-1,2j+1)| \end{aligned} \quad (2.19)$$

Where,  $\Delta y$  is compared with the  $T$  to find the edge and non-edge pixels. After that, bilinear interpolation equation for the non-edge pixel is given as follows (Park & Jeong, 2017):

At first, the linear interpolation is calculated in the x-direction

$$\begin{aligned} f(x, y_1) &= \frac{x_2 - x}{x_2 - x_1} f(Q_{11}) + \frac{x - x_1}{x_2 - x_1} f(Q_{21}) \\ f(x, y_2) &= \frac{x_2 - x}{x_2 - x_1} f(Q_{12}) + \frac{x - x_1}{x_2 - x_1} f(Q_{22}) \end{aligned} \quad (2.20)$$

Where, the pixel values of four points,

$$Q_{11} = (x_1, y_1), Q_{12} = (x_1, y_2), Q_{21} = (x_2, y_1), Q_{22} = (x_2, y_2) \quad (2.21)$$

Then, these new interpolation values are used to interpolate in the y-direction

$$f(x, y) = \frac{y_2 - y}{y_2 - y_1} f(x, y_1) + \frac{y - y_1}{y_2 - y_1} f(x, y_2) \quad (2.22)$$

Where,  $f(x, y)$  is known as the blank HR non-edge pixel.

Edge structure based edge directed interpolation method is proposed by (Yu, Zhang, et al., 2013). In this method, the edge information is extracted automatically with the edge detector. Canny edge detection technique is used to separate the homogeneous and non-homogeneous pixels and adaptive interpolation is applied for edge pixels. In this method, each pair of non-edge pixels are considered and if the pixel difference between them is smallest then highest correlation exist. The edge pixel is interpolated along that direction which have the minimum pixel difference. In this method, only four edges directions are considered. They are vertical, horizontal, 45° angle and 135° angle directions as shown in the Figure 2.21 (Yu, Zhu, et al., 2013).

The minimum distance estimation is given as follow (Tian et al., 2012):

$$\begin{aligned} diff_1 &= |Y_{2i+1,2j+1} - Y_{2i-1,2j+1}|, diff_2 = |Y_{2i+1,2j+2} - Y_{2i-1,2j}| \\ diff_3 &= |Y_{2i,2j+2} - Y_{2i-1,2j+1}|, diff_4 = |Y_{2i-1,2j+2} - Y_{2i+1,2j}| \\ diff_{\min} &= \min\{diff_k\} (1 \leq k \leq 4) \end{aligned} \quad (2.23)$$

After determined the orientation of edge pixels, the mathematical interpolation rules are applied as follow (Tian et al., 2012):

$$Y_{2i,2j+1} = (Y_{2i+1,2j+1} + Y_{2i-1,2j+1}) / 2 ; \text{ if } diff_2 \text{ is the } diff_{\min} \quad (2.24)$$

The pre-set threshold value is used to estimate edge pixels and non-edge pixels. The image is varied in different circumstances. As a result, image upscaling accuracy is degraded because of the intensity and characteristics of LR pixels. Noticeable ringing and blurry are seen at the edges domain.

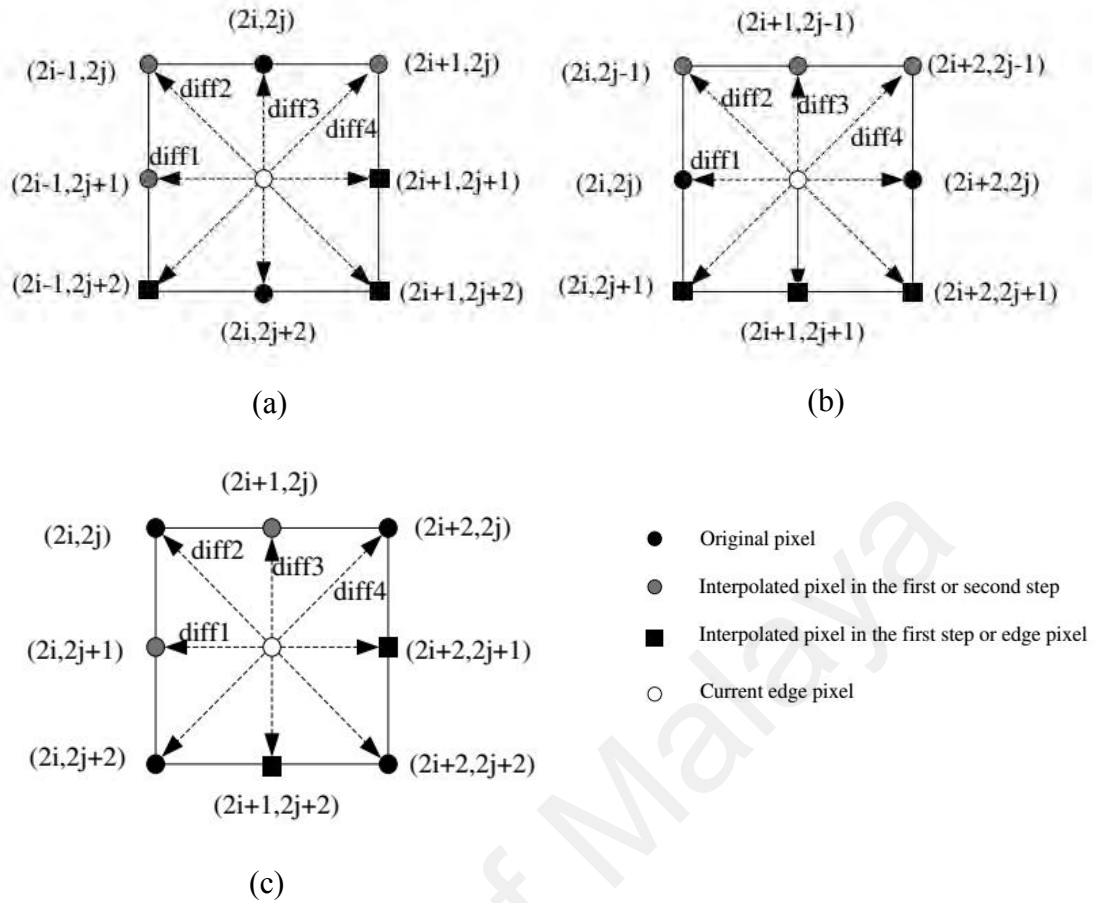


**Figure 2.21: The example of edge pixel is surrounded by the different arrangement of nearest neighbour pixels**

- (a) The interpolation of  $Y_{2i,2j+1}$  edge pixel;
- (b) The interpolation of  $Y_{2i+1,2j}$  edge pixel;
- (c) The interpolation of  $Y_{2i+1,2j+1}$  edge pixel

Among the edge directed interpolation methods, a comparison table has been provided to illustrate the performance evaluation as shown in Table 2.1.

**Table 2.1: The comparison between reviewed edge directed interpolation**

Properties Methods	Neighbour Pixels	Ringing	Artifacts	Blur	Interpolation Result
<b>Markov Random Field Edge Directed Method (M. Li &amp; Nguyen, 2008)</b>	49 pixels	✓	✗	✗	Non-efficient
<b>Non-local Edge Directed Method (Tai, Liu, Brown, &amp; Lin, 2010)</b>	9 pixels	✗	✓	✗	Non-efficient
<b>Multidirectional Edge Directed Method (Yun, Bae, &amp; Kim, 2011)</b>	12 pixels	✓	✗	✓	Partially efficient
<b>Fast Edge Directed Method (Bo Wang, 2013)</b>	4 pixels	✓	✓	✗	Partially Efficient
<b>Edge Directed Method (H. Zhou, Yan, Zhang, Zheng, &amp; Yu, 2016)</b>	4 pixels	✗	✗	✓	Non-efficient
<b>Window Selection Edge Directed Method (Wee, Park, &amp; Jeong, 2017)</b>	4 pixels	✓	✗	✓	Partially efficient
<b>Pixel Mapping Edge Directed Method (Park &amp; Jeong, 2017)</b>	16 pixels	✓	✓	✗	Partially efficient

## 2.6 Summary

A clear view of the different image resolution enhancement methods and techniques are presented in this chapter which is applied for the image resolution enhancement. According to the literature review, an interpolation method is divided into two sub-methods i.e. non-edge directed interpolation and edge-direction interpolation. Non-edge direction interpolation methods are briefly explained. On the other hand, edge-direction interpolation which is the primary focus of this study are grouped into different categories and described elaborately. The limitation of each method is analyzed and explained with the deep insight. Finally, the proposed method is described in the next chapter to fulfill the objective of this study.

## CHAPTER 3: METHODOLOGY

### 3.1 Introduction

In this chapter, the procedure of the proposed improved edge directed interpolation (EDI) method for image resolution enhancement is explained briefly. Aliasing, blurring, and artifacts, are the major problems for image resolution enhancement. Particularly the edge regions are responsible for these problems. In the proposed method, improved EDI approach is introduced by dividing the image regions into two parts. The overall conceptual process of the proposed method is as shown in Figure 3.1. Adaptive edge filtering method is used to separate the edge pixels and non-edge pixels.

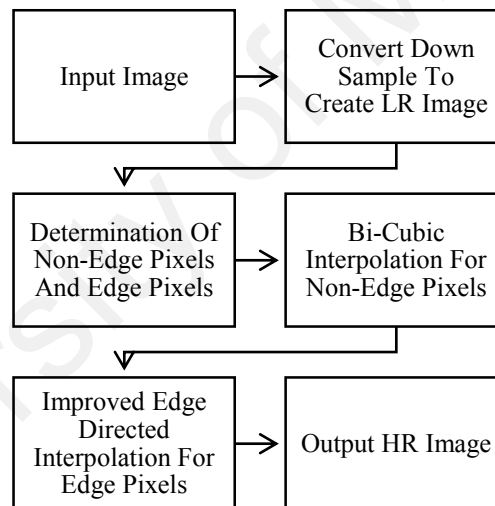


**Figure 3.1: The flow chart of the proposed algorithm**

The Canny edge detection is used to detect all the possible edge regions. After that, Bi-cubic interpolation is employed for non-edge pixels. The Lagrange interpolation polynomial is used for Bi-cubic interpolation and the average weight of sixteen neighbour LR pixels are calculated for each HR non-edge pixel. Finally, the proposed improved (EDI) is used for edge pixels. The computational complexity is reduced by applying separate interpolation method for image resolution enhancement. The

proposed improved EDI method ensures that the pixels of the HR edge are properly interpolated with the nearest neighbour LR pixels and provided the accurate interpolation value.

### 3.2 Down Sample Image

Grey scale image is taken as input for this work. The minimum and maximum intensity range from 0 to 255 which is carried only the black and white information as shown in Figure 3.2. We assume that, HR output image  $X$  of the size  $2m \times 2n$  is directly derived from the LR input image  $Y$  of the size  $m \times n$  without any loss. For example, the pixel  $Y(2i,2j)$  is the zoomed format of pixel  $Y(i,j)$ . Initially, the down sampled LR image is up-sampled by placing the blank HR pixels inside the LR image.

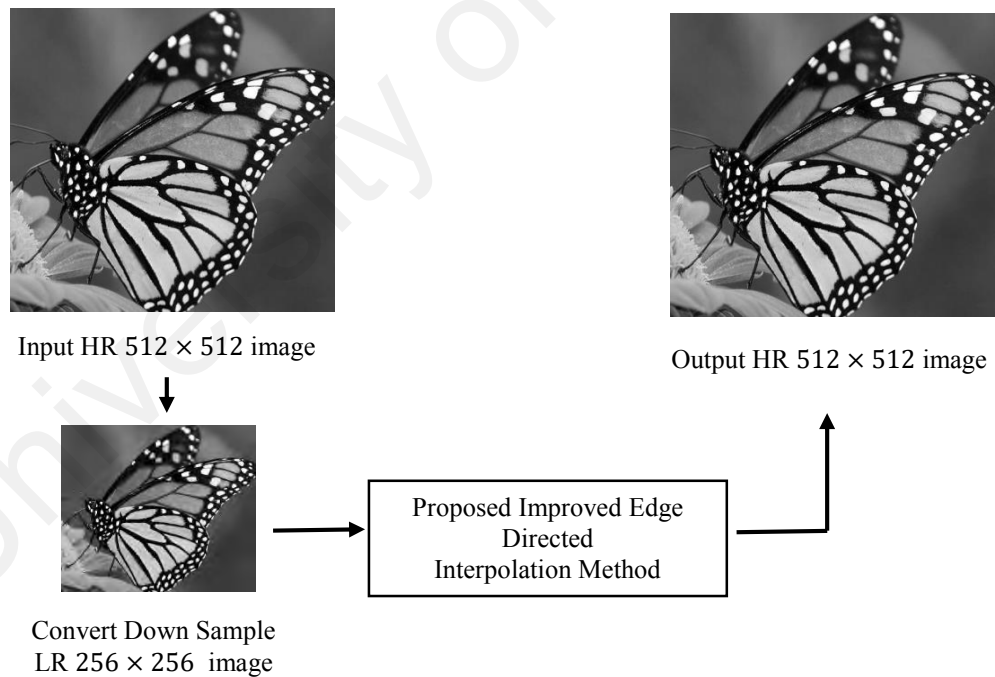


**Figure 3.2: The example of down sample image conversion**

### **3.3 Edge Pixels and Non-Edge Pixels Determination**

The LR image region is divided into two separate regions one is HR edge regions and another is HR non-edge or homogenous regions. The Canny edge detection is used for this purpose. The computational complexity is reduced for the classification of HR edge and non-edge pixels and the visual quality of the enhanced HR image is improved. The information of every HR edge pixel is stored and this information is used for further proposed improved EDI processing (Yu, Zhu, et al., 2013).

#### **3.3.1 Canny Edge Detection**

The accuracy of the proposed improved EDI method is depended on the detection of the HR edge and non-edge regions. In the Canny edge detection process, the HR edge information is automatically extracted from the HR image and the structure of the HR edge is preserved. The Canny edge detection is the standard edge detection method. This edge detection process is accurate, robust and effective as compared to the former edge detection processes. An edge detector is considered as a good edge detector if the three criteria are satisfied as follows (L. Liu, Liang, Zheng, He, & Huang, 2018):

- The detection probability of the edge pixel is increased and minimized the detection probability of the non-edge pixel.
- The detected edge pixel is nearby to the centre of the edge regions.
- The width of the detected edge is as possible as minimum.

The threshold value selection is important for Canny edge detection algorithm. Inaccurate edges are detected without the appropriate threshold value. If the threshold value is high, then the edges are become discontinuous and interrupt. Even if the threshold value is low, then the noise is increased. In the classic canny edge detection method, the threshold value is a constant with in a range and unable to select the threshold value independently based on the image characteristics. The repeatedly test

are performed to find the appropriate threshold value for the image. As a result, light and other factors easily affects the detection result (Meng, Zhang, Yin, & Ma, 2017). In the Canny edge detection, an adaptive threshold selection algorithm is used to select threshold. The appropriate threshold value is automatically selected based on the image characteristics.

A Canny edge detection algorithm is required in the proposed improved EDI method. At first, the LoG filter is applied on the image to detect the regions where the intensity of the pixels is changed rapidly and the image is decomposed in to two images. In the first image, the information of the image is contained and the value of this image is equal to or greater than the LoG value. The second image is discard because of noise information are contained. After applying the LoG filter, the gradient direction and magnitude are calculated. A modified kernel is used for smoothing the first image. The image is smoothed with the following kernel (Stosic & Rutesic, 2018):

$$\begin{pmatrix} 1 & 0 & 1 \\ 1 & \alpha & 1 \\ 1 & 0 & 1 \end{pmatrix} \quad (3.1)$$

Where,  $\alpha = 2, 4 \text{ or } 8$ . The more details edge information are detected if the value of  $\alpha$  is increased. Although more details edge information is not necessary for the edge detection. The number of iteration K is considered to determine the optimal threshold for the image. The K is estimated based on the correlation coefficient. The correlation coefficient is determined when the correlation value of the noise and the smooth image are minimum. The correlation coefficient is given as follow (T.-S. Liu, Liu, & Pan, 2014):

$$\rho_{u_0-u_t, u_t} = \frac{\text{cov}(u_0 - u_t, u_t)}{\sqrt{\text{var}(u_0 - u_t)}\sqrt{\text{var}(u_t)}} \quad (3.2)$$

Where,  $u_0$  is determine as LR image;  $u_t$  is defined as the filtered image;  $t$  is defined as the iteration processing time;  $u_0 - u_t$  is determined as the noise of the image. After that the gradient magnitude is adjusted based on the gradient direction. The equation is given as follow (Stosic & Rutesic, 2018):

$$\text{magnitude}(m, n, \theta) = \max(\cos \theta G_m, \sin \theta G_n) \quad (3.3)$$

The gradient of the kernel is also adjusted. In the conventional canny edge detection, the gradient direction and magnitude are measured based on the  $2 \times 2$  neighbour pixels. As a result, false edges are detected easily. So the modified kernel is used for measuring gradient direction and magnitude within the  $x \times y$  neighbour pixels are given as follow (T.-S. Liu et al., 2014):

$$G_m^k(m, n) = \frac{1}{2} [f^k(m+1, n) - f^k(m-1, n)] \quad (3.4)$$

$$G_n^k(m, n) = \frac{1}{2} [f^k(m, n+1) - f^k(m, n-1)] \quad (3.5)$$

The weight of the filter is estimated as follow:

$$w^k(m, n) = \exp\left[-\frac{[G_m^k(m, n)]^2 + [G_n^k(m, n)]^2}{2h^2}\right] \quad (3.6)$$

The average of weight of the  $f^k(m, n)$

$$f^{k+1}(m, n) = \frac{\sum_{i=-1}^1 \sum_{j=-1}^1 f^k(m+i, n+j) w^k(m+i, n+j)}{\sum_{i=-1}^1 \sum_{j=-1}^1 w^k(m+i, n+j)} \quad (3.7)$$

In the traditional method, non-maximum suppression is used to determine the width of the edge. However, the probability of the false edges detection is increased (Stosic &

Rutesic, 2018). In this Canny edge detection method, the width of the edge is defined by the combination of the two images where the first image is produced by applying the modified kernel and the second image is produced by applying the kernels where the modified values of gradient direction and magnitude are used.

Suppose,  $M$  is the total number of pixels of the image and the range of the grey scale level is from  $0$  to  $L$  of the image. After that, the image pixels are classified in to two sets based on the grey scale value  $t$ . Among the two groups  $A$  is defined as the background regions whose grey scale range from  $0$  to  $t$ . On other hand,  $B$  is defined as the object regions whose grey scale range from  $t$  to  $L$ . However, the histogram grey scale level is calculated according to the probability  $p_i$ . The probability equation is given as follow (T.-S. Liu et al., 2014):

$$p_i = \frac{n_i}{M}, \quad i = 0, 1, 2, 3, \dots, L-1 \quad (3.8)$$

$$\sum_{i=0}^{L-1} p_i = 1, \quad \sum_{i=0}^{L-1} n_i = M \quad (3.9)$$

If the probability of the background regions and object regions are defined as  $p_A$  and  $p_B$  respectively then the probability occurrence is given as follows (T.-S. Liu et al., 2014):

$$P_A = \sum_{i=0}^t p_i, \quad P_B = \sum_{i=t+1}^L p_i \quad (3.10)$$

The maximum cluster variance between  $A$  and  $B$  regions are estimated. The cluster variance is defined with  $\sigma$ .

The corresponding equations are given as follow (T.-S. Liu et al., 2014):

$$u_T = \sum_{i=0}^K ip_i \quad (3.11)$$

$$u_A = \sum_{i=0}^t \frac{ip_i}{p_A}, \quad u_B = \sum_{i=t+1}^K \frac{ip_i}{p_B} \quad (3.12)$$

$$u_T = p_A u_A + p_B u_B \quad (3.13)$$

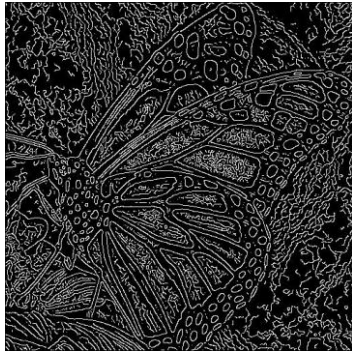
$$\sigma = p_A (u_T - u_A)^2 + p_B (u_T - u_B)^2 \quad (3.14)$$

Where, the average grey scale of the LR image is defined as  $u_T$ . The average grey scale of the A and B regions are defined as  $u_A$  and  $u_B$  respectively.

The value of the optimum thresholds  $t_1$  and  $t_2$  are obtained according to the highest value of the cluster variance between A and B regions of the image and the edge regions are connected (T.-S. Liu et al., 2014). The all possible edges are detected by the adaptive and optimum threshold value which is automatically selected and the false edges detection are reduced as shown in Figure 3.3.



(a)



```
threshold =
0.0039  0.0062
```

(b)



```
threshold =
0.0039  0.0124
```

(c)



```
threshold =
0.0042  0.0186
```

(d)

**Figure 3.3: The example of Canny edge detection**

(a) The input grey scale image; the automatic threshold selection (b) When,  $\alpha = 8$ ; (c) When,  $\alpha = 4$ ; (d) when  $\alpha = 2$

### 3.4 Bi-cubic Interpolation for Non-Edge Pixels

Bi-cubic interpolation is the extension of the Bilinear interpolation and this algorithm is the standard interpolation algorithm in the interpolation field. The primary advantage of the Bi-cubic interpolation is the stability. The performance of this interpolation is much better than the Bilinear interpolation algorithm (Ousguine et al., 2014).

At first, the linear interpolation is calculated through the horizontal direction using four neighbor pixels. After that, again linear interpolation is calculated through the vertical direction using the new interpolation values to find the blank HR non-edge pixel value. This new interpolation values are taken from the previous linear interpolation through the horizontal direction.

The unknown HR non-edge pixel  $p_j(x)$  is estimated by the Bi-cubic interpolation process with the intensity values of sixteen neighbor LR pixels as shown in Figure 3.4 (Park & Jeong, 2017).

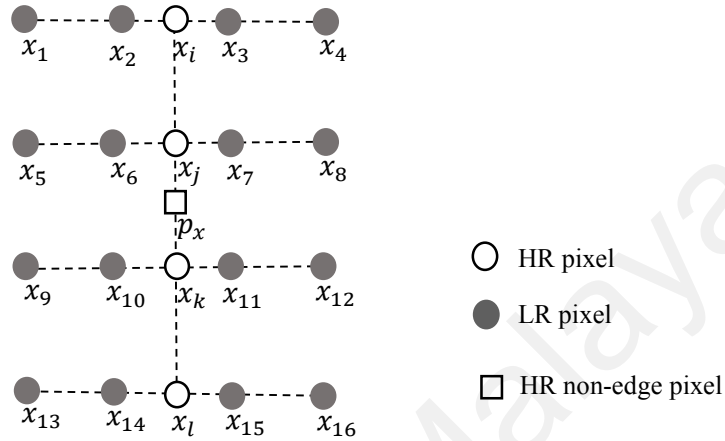


**Figure 3.4: The example of bi-cubic interpolation for non-edge pixel**

### 3.4.1 Lagrange Interpolation Polynomial

The Lagrange interpolation polynomial is convenient to use for interpolation of image pixels and convenient to write program. The large amount of pixels is able to be calculated with this function and the time complexity of the interpolation process is efficient. Moreover, the high quality of the interpolated HR image is preserved. The polynomial function for the determination of the HR non-edge pixel  $p_j(x)$  is given as follows (Jana, 2018). The Lagrange interpolation polynomial is the polynomial  $p(x)$  of degree  $\leq (n - 1)$  that is passed through the  $n$  points.

$$(x_1, y_1) = f(x_1), (x_2, y_2) = f(x_2), \dots, (x_n, y_n) = f(x_n) \quad (3.15)$$

$$p(x) = \sum_{j=1}^n p_j(x) \quad (3.16)$$

Where,

$$p_j(x) = y_j \prod_{\substack{k=1 \\ k \neq j}}^n \frac{x_i - x_k}{x_j - x_k} \quad (3.17)$$

Written explicitly,

$$\begin{aligned} & \frac{(x_i - x_2)(x_i - x_3) \dots (x_i - x_n)}{(x_1 - x_2)(x_1 - x_3) \dots (x_1 - x_n)} y_1 + \frac{(x_i - x_1)(x_i - x_3) \dots (x_i - x_n)}{(x_2 - x_1)(x_2 - x_3) \dots (x_2 - x_n)} y_2 \\ & + \dots + \frac{(x - x_1)(x - x_2) \dots (x - x_{n-1})}{(x_n - x_1)(x_n - x_2) \dots (x_n - x_{n-1})} y_n \end{aligned} \quad (3.18)$$

Here,  $y_n$  is defined as the distance between two rows which is constant;  $x_n$  is defined as the value of the pixel intensity. The process steps of the HR non-edge pixel interpolation are given as follows (Kao et al., 2015):

- **Step 1:**

At first the weighted value of four pixels  $x_1, x_2, x_3$  and  $x_4$  are calculated with the Lagrange interpolation polynomial function to determine the  $x_i$  pixel value through horizontal direction as shown in Figure 3.4.

- **Step 2:**

Repeat the step 1 to find the interpolation value of the four pixels  $x_i, x_j, x_k$  and  $x_l$  as shown in Figure 3.4.

- **Step 3:**

The blank HR non-edge pixel value  $p_j(x)$  is calculated using the new derived four weighted values  $x_i, x_j, x_k$  and  $x_l$  with the above stated Lagrange interpolation polynomial function through vertical direction as shown in Figure 3.4.

In Bi-cubic interpolation, the sixteen nearest neighbor LR pixels are considered for interpolation to determine the blank HR non-edge pixel value. According to the visual

observation as well as the mathematical results of structural similarity index (SSIM), the homogenous regions are clear and quality is higher than the existing methods.

The Bi-cubic interpolation is employed to find the value of HR non-edge pixels. After that, this known HR non-edge pixel value may or may not use as the nearest neighbor pixel to the HR edge pixel for applying the proposed improved EDI method. The four possible arrangements of the known HR non-edge pixel and unknown HR edge pixel are as shown in Figure 3.5.

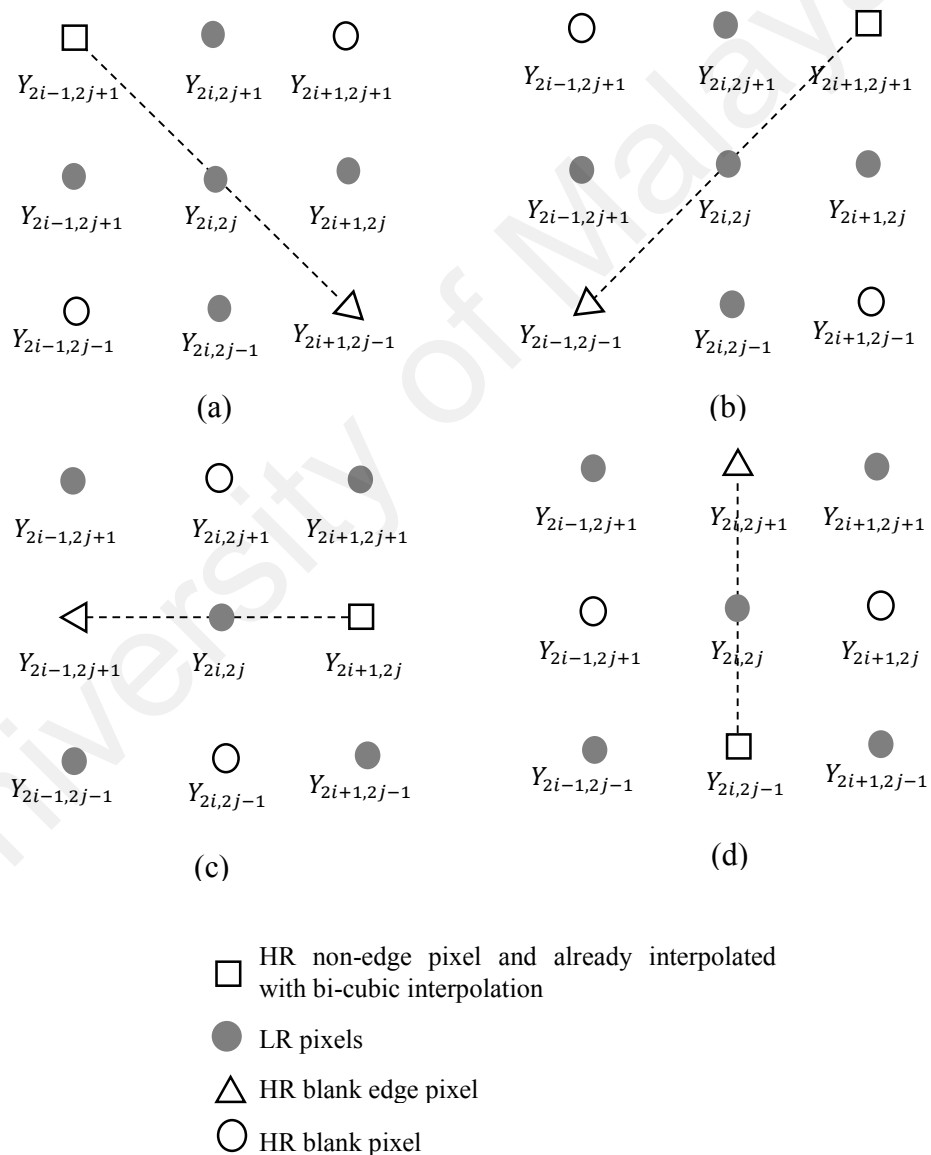


**Figure 3.5: The example of possible combination of LR, HR non-edge and HR edge pixels. Non-edge pixel is also used as nearest neighbor pixel for improved edge directed interpolation**

Therefore, after applying the Bi-cubic interpolation method on the HR non-edge pixel, it is ensured that the appropriate interpolation value is estimated for the HR edge pixel with the proposed improved EDI method.

### 3.5 Proposed Improved Edge-Directed Interpolation Method

The accurate interpolation value for the HR edge pixels is estimated with the proposed improved edge directed interpolation (EDI) method where the nearest neighbor non-edge and edge pixels are considered. After classifying the HR non-edge and edge pixels, if the pixel is an edge pixel, then improved EDI method is applied otherwise for the non-edge pixel the Bi-cubic interpolation is applied.

#### 3.5.1 High-Resolution Edge Direction

At first, it is essential to analyze the arrangement of nearest neighbor LR pixels around the HR pixel whether there is an edge existed. After analyzing the HR edge pixel and their features, it is required to determine the direction of the edge on which the improved EDI is performed. The HR edge direction is estimated from the LR pixels. The fast and simple way to determine the edge direction by the difference of LR pixels which are nearest neighbor pixels of HR edge pixel as shown in Figure 3.6.

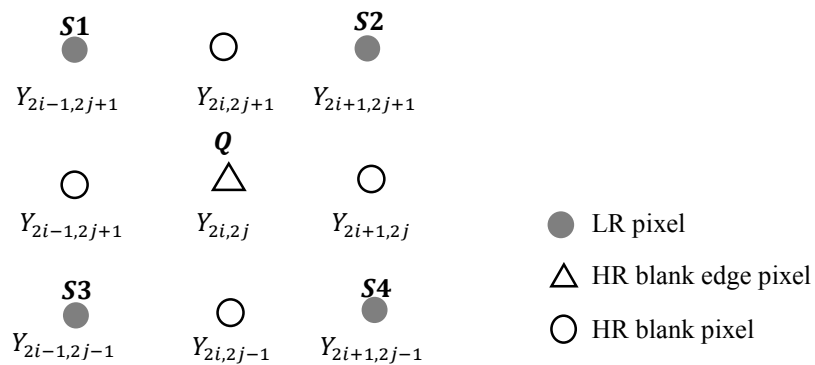


Figure 3.6: The example of neighbor LR and HR pixels around the HR edge pixel

The highest correlation is existed between two neighbor LR pixels if the intensity difference between the pair of nearest neighbor LR pixels is minimum among the other pair differences of the LR pixels. The efficiency of the improved EDI method depends on the number of direction. If the number of direction is increased, then the sharpness of HR edge is also increased. The more relative HR edge directions are determined by the more nearest neighbor LR pixels. But the cost and complexity of the algorithm are increased for considering the more HR edge directions (Kao et al., 2015). According to the experimental results and observation, the highest efficiency and better quality of HR edge are provided for considering the four HR edge directions. They are vertical, horizontal and two diagonal directions. The estimation process of HR edge direction is described through the three steps as follows (Tian et al., 2012):

- **Step 1:** The six difference of the nearest neighbor LR pixels is estimated around the HR edge pixel. Let,  $Y_{2i,2j}$  is the HR edge pixel and the weight of this pixels is  $Q$ . Similarly, the corresponding weights of the nearest neighbor LR pixels  $Y_{2i-1,2j+1}, Y_{2i+1,2j+1}, Y_{2i-1,2j-1}$  and  $Y_{2i+1,2j-1}$  are  $S1, S2, S3$  and  $S4$  as shown in Figure 3.7. The weights of six directional difference are calculated as follows (X. Wang, Chen, & Bao, 2012):

$$\begin{aligned} Diff1 = |S1 - S2|, Diff2 = |S1 - S3|, Diff3 = |S1 - S4|, Diff4 = |S2 - S3|, \\ Diff5 = |S2 - S4|, Diff6 = |S3 - S4| \end{aligned} \quad (3.19)$$

- **Step 2:** In this step, after calculating the  $Diff1, Diff2, Diff3, Diff4, Diff5, Diff6$ , the value of the minimum difference is determined among them. This minimum value is used to determine the edge direction in the next step.
- **Step 3:** The edge directions are classified into four directions: Horizontal edge, Vertical edge,  $45^\circ$  angle diagonal edge and  $135^\circ$  angle diagonal edge as shown in Figure 3.7.

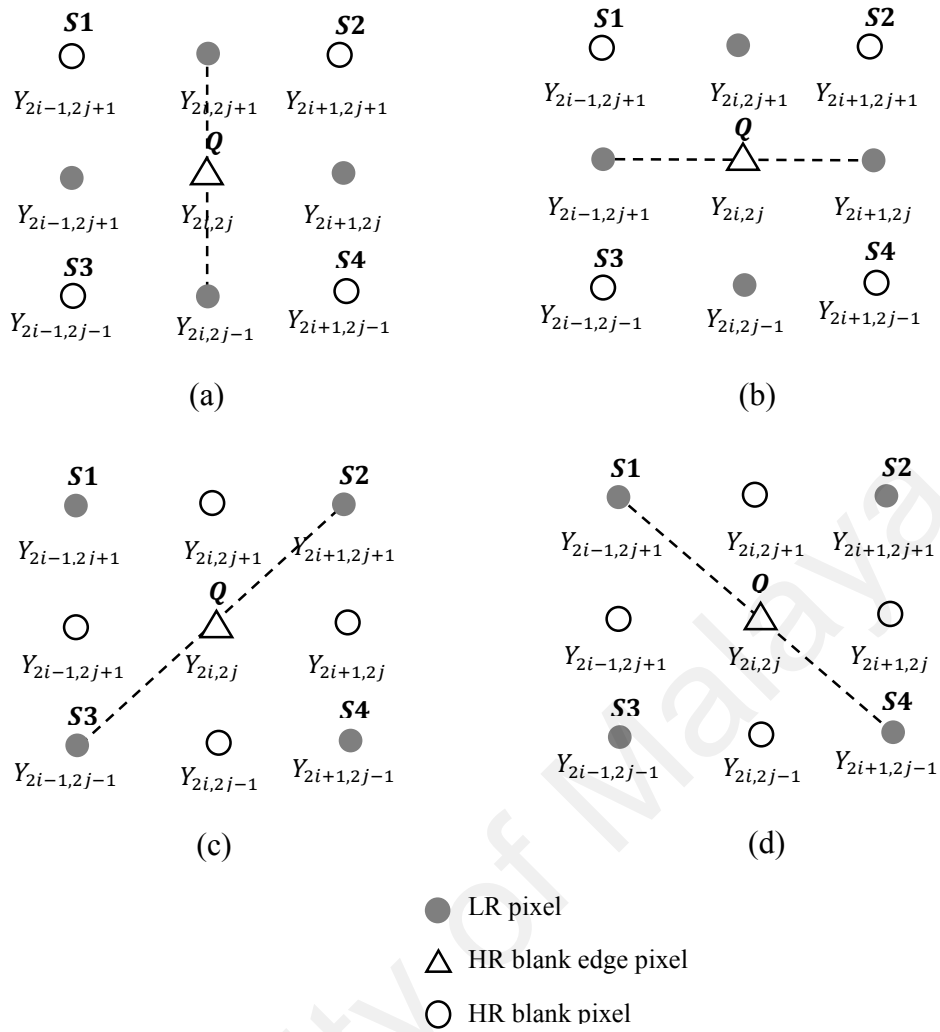


**Figure 3.7: The example of features of HR edge pixel and the type of edge directions**

- (a) Vertical edge direction; (b) Horizontal edge direction; (c) 45° angle edge direction; (d) 135° angle edge direction

After that, the HR edges features and direction are described based on the minimum intensity difference of the nearest neighbor LR pixels and the direction are categorized according to the conditions as follows:

- **Type 1: Vertical Edge Direction:**

The vertical HR edge direction is existed if the two following conditions are satisfied as shown in Figure 3.7 (a).

The conditions are given as follows (D. Zhou et al., 2012):

$$\min \text{Diff} 1 = \text{if } \text{Diff} 2, \text{Diff} 3, \text{ and } \text{Diff} 4 \text{ are less than } \text{Diff} 1 \quad (3.20)$$

$$\min \text{Diff} 6 = \text{if } \text{Diff} 5, \text{Diff} 3, \text{ and } \text{Diff} 4 \text{ are less than } \text{Diff} 6 \quad (3.21)$$

- **Type 2: Horizontal Edge Direction:**

The horizontal HR edge direction is existed if the following two conditions are satisfied as shown in Figure 3.7 (b).

The conditions are given as follows (D. Zhou et al., 2012):

$$\min \text{Diff} 2 = \text{if } \text{Diff} 1, \text{Diff} 3, \text{ and } \text{Diff} 4 \text{ are less than } \text{Diff} 2 \quad (3.22)$$

$$\min \text{Diff} 5 = \text{if } \text{Diff} 6, \text{Diff} 3, \text{ and } \text{Diff} 4 \text{ are less than } \text{Diff} 5 \quad (3.23)$$

- **Type 3: 45° Angle Diagonal Edge Direction:**

The 45° angle diagonal HR edge direction is existed If the following condition is satisfied as shown in Figure 3.7 (c).

The condition is given as follow (D. Zhou et al., 2012):

$$\min \text{Diff} 4 = \text{if } \text{Diff} 1, \text{Diff} 3, \text{ and } \text{Diff} 6 \text{ are less than } \text{Diff} 4 \quad (3.24)$$

- **Type 4: 135° Angle Diagonal Edge Direction:**

The 135° angle diagonal HR edge direction is existed if the following condition is satisfied as shown in Figure 3.7 (d).

The condition is as follow (D. Zhou et al., 2012):

$$\min \text{Diff} 3 = \text{if } \text{Diff} 1, \text{Diff} 4, \text{ and } \text{Diff} 6 \text{ are less than } \text{Diff} 3 \quad (3.25)$$

Finally, if any one condition as stated in the above is not satisfied then HR edge direction is not existed. In the above method, only four nearest neighbor pixels around the HR edge pixel are considered to determine the direction of the HR edge. As a result, the computational complexity is relatively less. However, the HR edge detection

process is accurate. The sharpness of the edge regions is maintained and satisfied quality of HR edge is provided with this approach.

### 3.5.2 Improved Edge Direction Interpolation

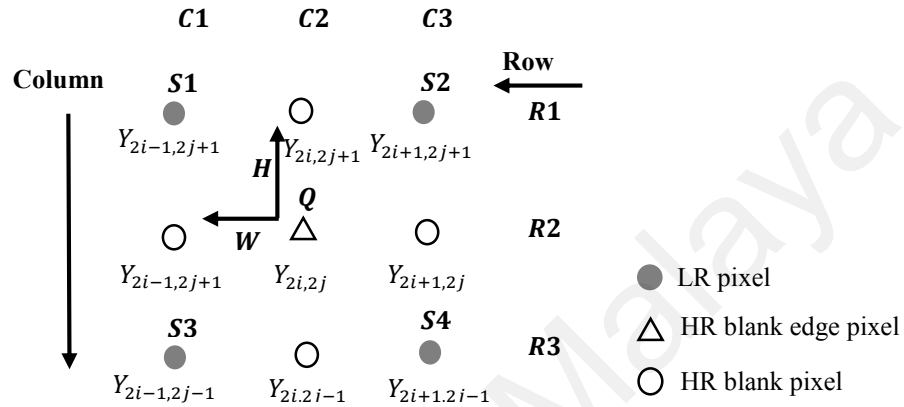


**Figure 3.8: The example of arrangement of LR and HR pixels for improved edge directed interpolation**

If an edge is detected around the blank HR edge pixel, then the appropriate HR edge direction is chosen with the minimum intensity difference method and the proposed improved EDI method is employed. For example,  $C1, C2,$  and  $C3$  are the columns and  $R1, R2,$  and  $R3$  are the rows as shown in Figure 3.8. The distance between  $C1$  to  $C2$  and  $C2$  to  $C3$  are the unit distance. Similarly, the distance between  $R1$  to  $R2$  and  $R2$  to  $R3$  are also the unit distance. Let's the distance between pixel position from  $(C2, R2)$  to  $(C2, R1)$  is unit distance  $H$  and known as the vertical component as shown in Figure 3.8. Similarly, the distance between pixel position from  $(C2, R2)$  to  $(C1, R2)$  is also unit distance  $W$  and known as the horizontal component as shown in Figure 3.8. In the super-resolution pixels, the distance between two pixels is not uniform (Mareboyana & Le Moigne, 2018). This improved EDI method also works effectively with the irregular distance between two LR pixels which is the great advantage of this

proposed method. The weighted values of the four corner LR pixels which are the nearest neighbor of the HR edge pixel are defined  $S_1, S_2$ , and  $S_3$  as shown in Figure 3.8. Let's the weighted value of the blank HR edge pixel is  $Q$  as shown in Figure 3.8.

After detecting the HR edge direction, the appropriate pair of LR pixels is selected around the HR edge pixel for applying improved EDI method. The appropriate pair of LR pixels is selected based on the HR edge pixel position. Otherwise, improved EDI method is continued towards the wrong direction because of the selection of wrong LR pixel pair. As a result, the HR edge quality is degraded. The three possible positions of HR edge pixel are considered in the proposed improved EDI method.

### 3.5.2.1 Improved Edge-Directed Interpolation On Vertical Direction

After determined the vertical HR edge direction with the minimum intensity difference method, the three possible positions of HR edge pixel are considered as shown in Figure 3.9. The appropriate pair of LR pixels are selected for improved EDI method according to the three conditions as follows (Kao et al., 2015):

- If the condition is  $W < 0.5$ , then blank HR edge pixel  $Q$  position would be left the side of the middle point as presented by the bolt black dot line as shown in Figure 3. (a). So,  $S_1$  and  $S_3$  LR pixel values are used to interpolate blank HR edge pixel through vertical HR edge direction. The HR edge pixel value  $Q$  is calculated as follow:

$$Q = (1 - H)S_1 + HS_3 \quad (3.26)$$

Where,  $H$  is defined as the unit distance and known as the vertical component.

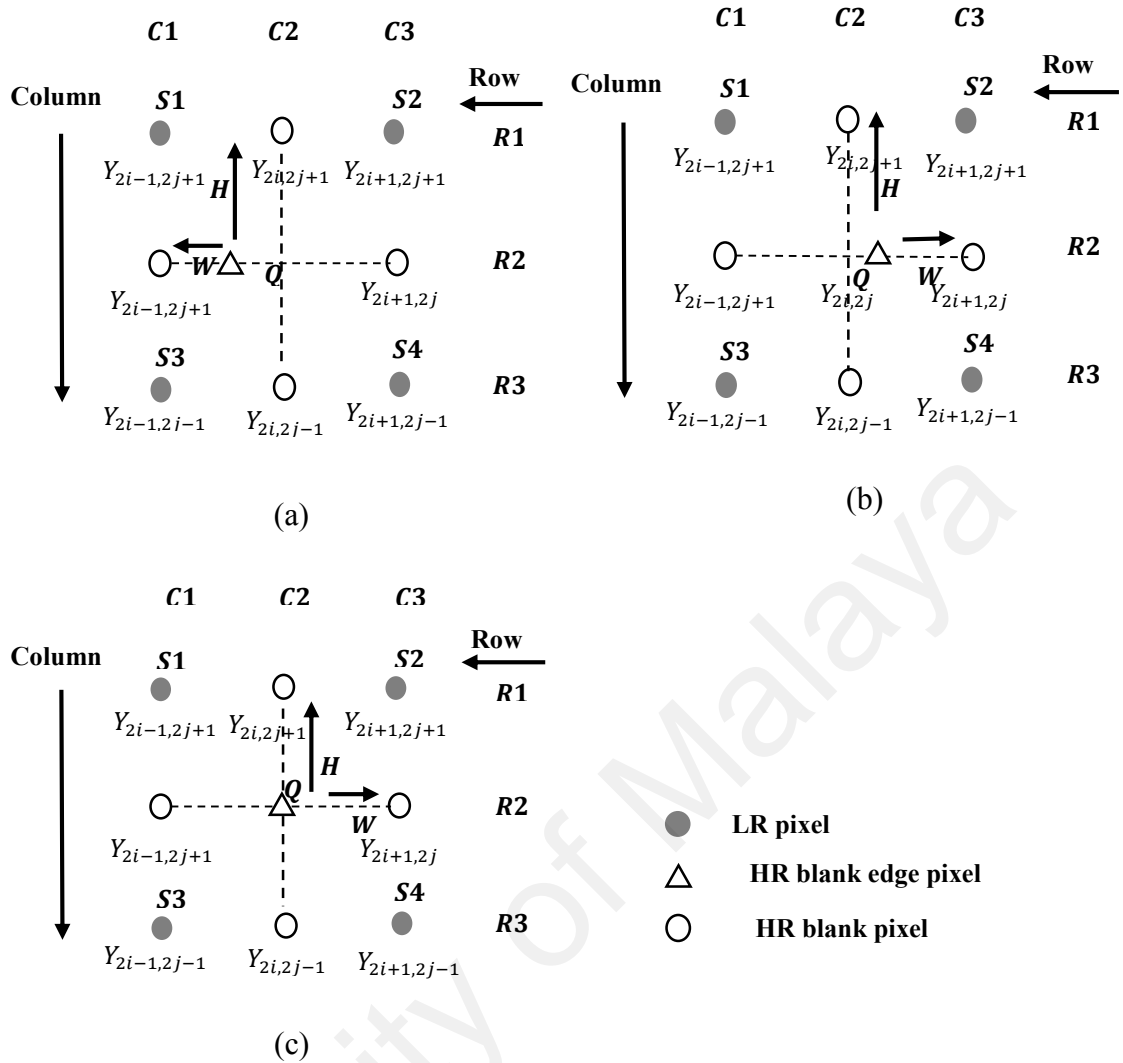


**Figure 3.9: The example of blank HR edge pixel  $Q$  and the selection of improved EDI is continued through vertical edge direction**  
 (a) When,  $W < 0.5$  ; (b) and (c)  $W \geq 0.5$

- If the condition is  $W > 0.5$ , then blank HR edge pixel position would be the right side of the middle point as presented by the bolt black dot line as shown in Figure 3.9 (b).
- If the condition is  $W = 0.5$ , then the HR edge pixel position would be the middle point as presented by the bolt black dot line as shown in Figure 3.9 (c).

For these two conditions, the  $S2$  and  $S4$  LR pixel values are used to interpolate blank HR edge pixel through vertical HR edge direction.

The HR edge pixel value  $Q$  is calculated as follow:

$$Q = (1 - H)S2 + HS4 \quad (3.27)$$

Where,  $H$  is defined as the unit distance and known as the vertical component.

### 3.5.2.2 Improved Edge-Directed Interpolation On Horizontal Direction

After determined the horizontal HR edge direction with the minimum intensity difference method, the three possible position of HR edge pixel is considered as shown in Figure 3.10. The appropriate pair of LR pixels are selected for improved EDI method according to the three condition as follows (Kao et al., 2015):

- If the condition is  $H < 0.5$ , then blank HR edge pixel  $Q$  position would be upside of the middle point as presented by the bolt black dot line as shown in Figure 3.10 (a). So,  $S1$  and  $S2$  LR pixel values are used to interpolate blank HR edge pixel through horizontal HR edge direction. The HR edge pixel value  $Q$  is calculated as follow:

$$Q = (1 - W)S1 + HS2 \quad (3.28)$$

Where,  $H$  is defined as the unit distance and known as the vertical component;

$W$  is defined as the unit distance and known as the horizontal component.

- If the condition is  $H > 0.5$ , then blank HR edge pixel position would be the bottom side of the middle point as presented by the bolt black dot line as shown in Figure 3.10 (b).
- If the condition is  $H = 0.5$ , then the HR edge pixel position would be the middle point as presented by the bolt black dot line as shown in Figure 3.10 (c).

For these two conditions, the  $S3$  and  $S4$  LR pixel values are used to interpolate blank HR edge pixel through horizontal HR edge direction.

The HR edge pixel value  $Q$  is calculated as follow:

$$Q = (1 - W)S3 + HS4 \quad (3.29)$$

Where,  $H$  is defined as the unit distance and known as the vertical component;  $W$  is defined as the unit distance and known as the horizontal component.

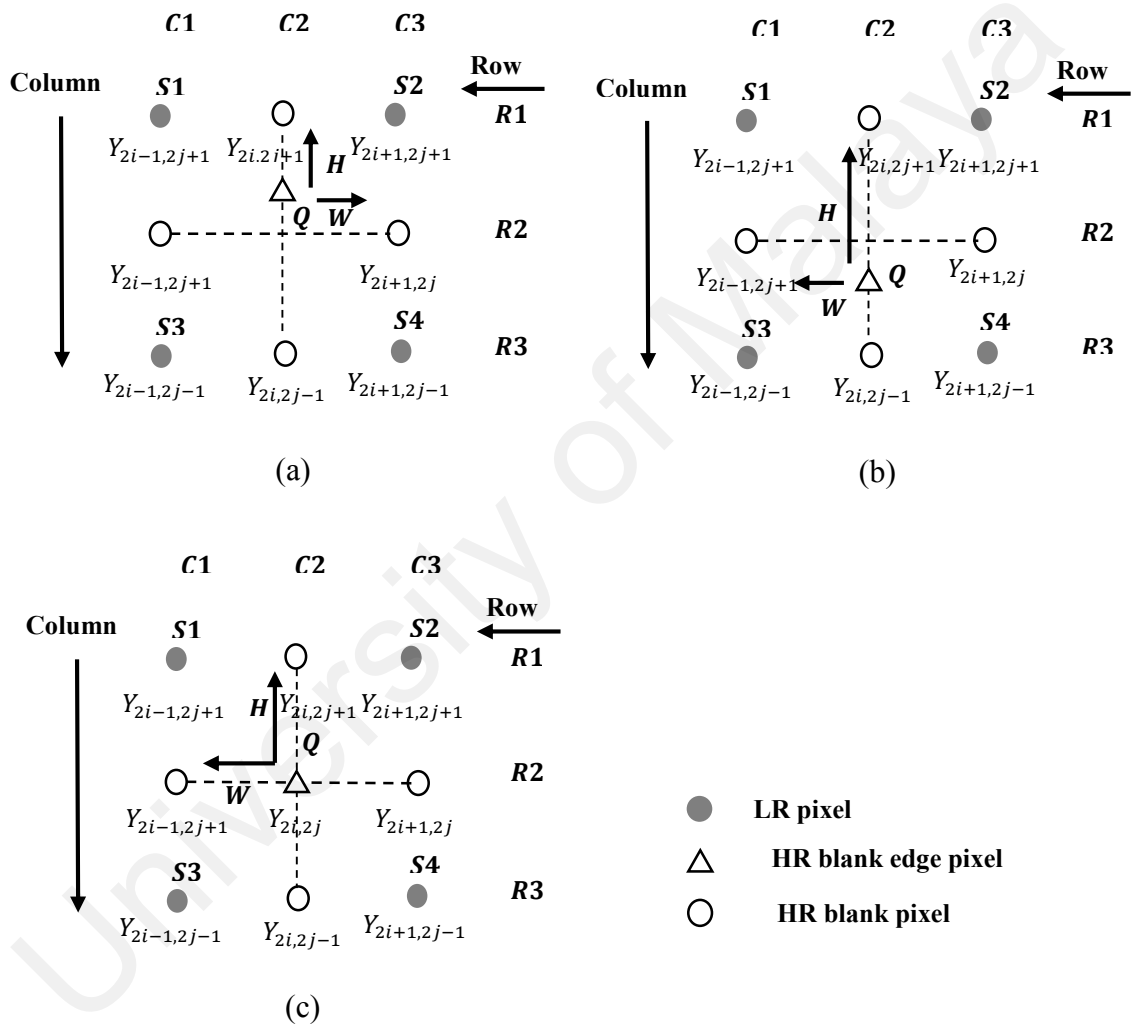


**Figure 3.10: The example of blank HR edge pixel  $Q$  and the selection of improved EDI is continued through horizontal HR edge direction**

(a) When,  $H < 0.5$ ; (b) and (c)  $H \geq 0.5$

### 3.5.2.3 Improved Edge-Directed Interpolation On 45° angle Direction

After determined the 45° angle HR edge direction with the minimum intensity difference method, the three possible position of HR edge pixel is considered as shown in Figure 3.11. The appropriate pair of LR pixels are selected for improved EDI method according to the three condition as follows (Kao et al., 2015):

- If the conditions are  $H < 0.5$  and  $W < 0.5$ , then blank HR edge pixel  $Q$  position would be upside of the middle point as presented by the bolt black dot line as shown in Figure 3.11 (a).
- If the conditions are  $H > 0.5$  and  $W > 0.5$ , then blank HR edge pixel position would be the bottom side of the middle point as presented by the bolt black dot line as shown in Figure 3.11 (b).
- If the conditions are  $H = 0.5$  and  $W = 0.5$ , then the HR edge pixel position would be the middle point as presented by the bolt black dot line as shown in Figure 3.11(c).

For these three conditions, the  $S2$  and  $S3$  LR pixel values are used to interpolate blank HR edge pixel through 45° angle HR edge direction. The HR edge pixel value  $Q$  is calculated as follow:

$$Q = 0.5[WS2 + (1 - W)S3] + 0.5[(1 - H)S2 + HS3] \quad (3.30)$$

Where,  $H$  is defined as the unit distance and known as the vertical component;  $W$  is defined as the unit distance and known as the horizontal component.

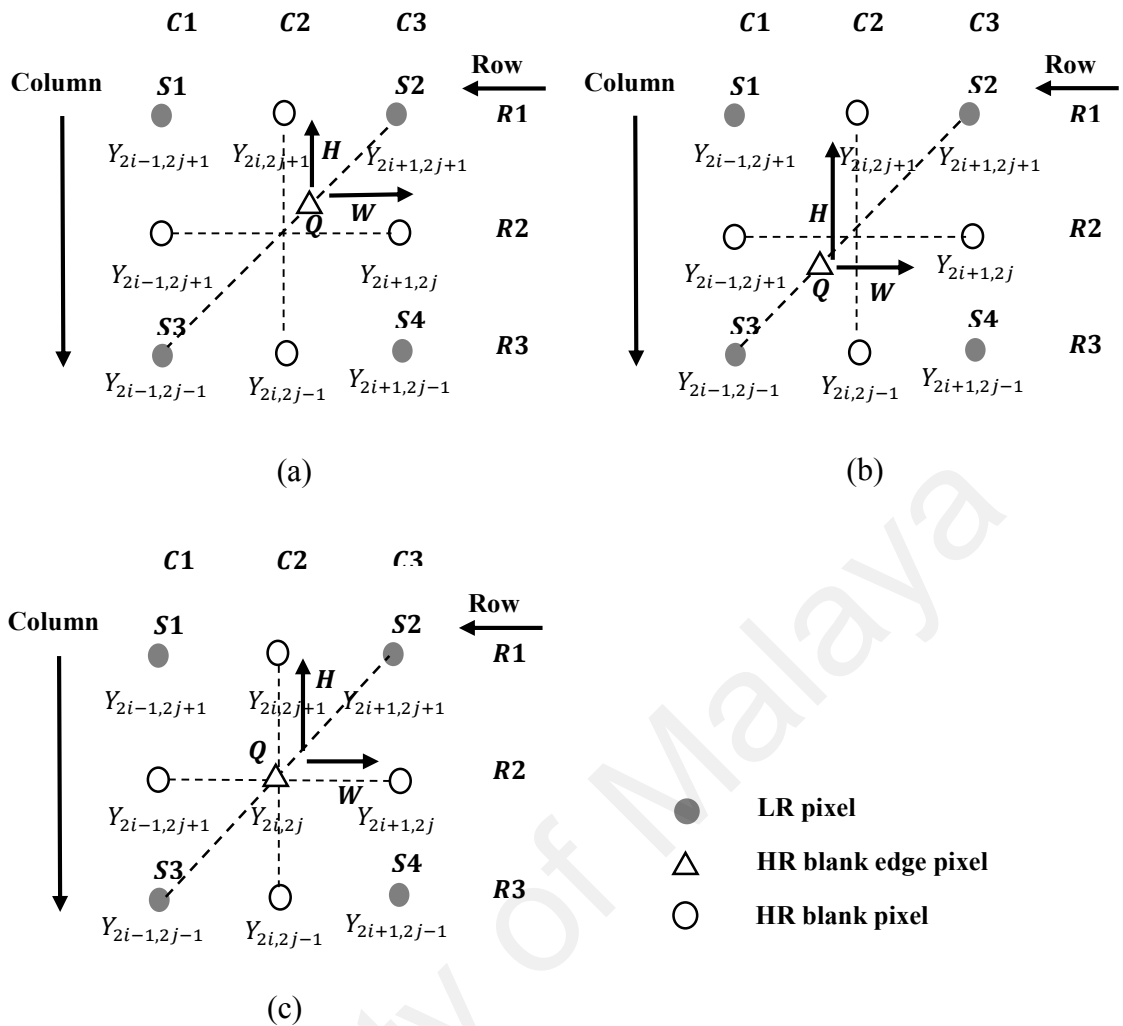


**Figure 3.11: The example of blank HR edge pixel  $Q$  and the selection of improved EDI is continued through  $45^\circ$  angle edge direction**  
 (a) When,  $H < 0.5$  and  $W < 0.5$  ; (b) and (c)  $H \geq 0.5$  and  $W \geq 0.5$

### 3.5.2.4 Improved Edge-Directed Interpolation On $135^\circ$ angle Direction

After determined the  $135^\circ$  angle HR edge direction with the minimum intensity difference method, the three possible position of HR edge pixel is considered as shown in Figure 3.12. The appropriate pair of LR pixels are selected for improved EDI method according to the three condition as follows (Kao et al., 2015):

- If the conditions are  $H < 0.5$  and  $W < 0.5$ , then blank HR edge pixel  $Q$  position would be upside of the middle point as presented by the bolt black dot line as shown in Figure 3.12 (a).

- If the conditions are  $H > 0.5$  and  $W > 0.5$ , then blank HR edge pixel position would be the bottom side of the middle point as presented by the bolt black dot line as shown in Figure 3.12 (b).
- If the conditions are  $H = 0.5$  and  $W = 0.5$ , then the HR edge pixel position would be the middle point as presented by the bolt black dot line as shown in Figure 3.12(c).

For these three conditions, the  $S1$  and  $S4$  LR pixel values are used to interpolate blank HR edge pixel through  $135^\circ$  angle HR edge direction.

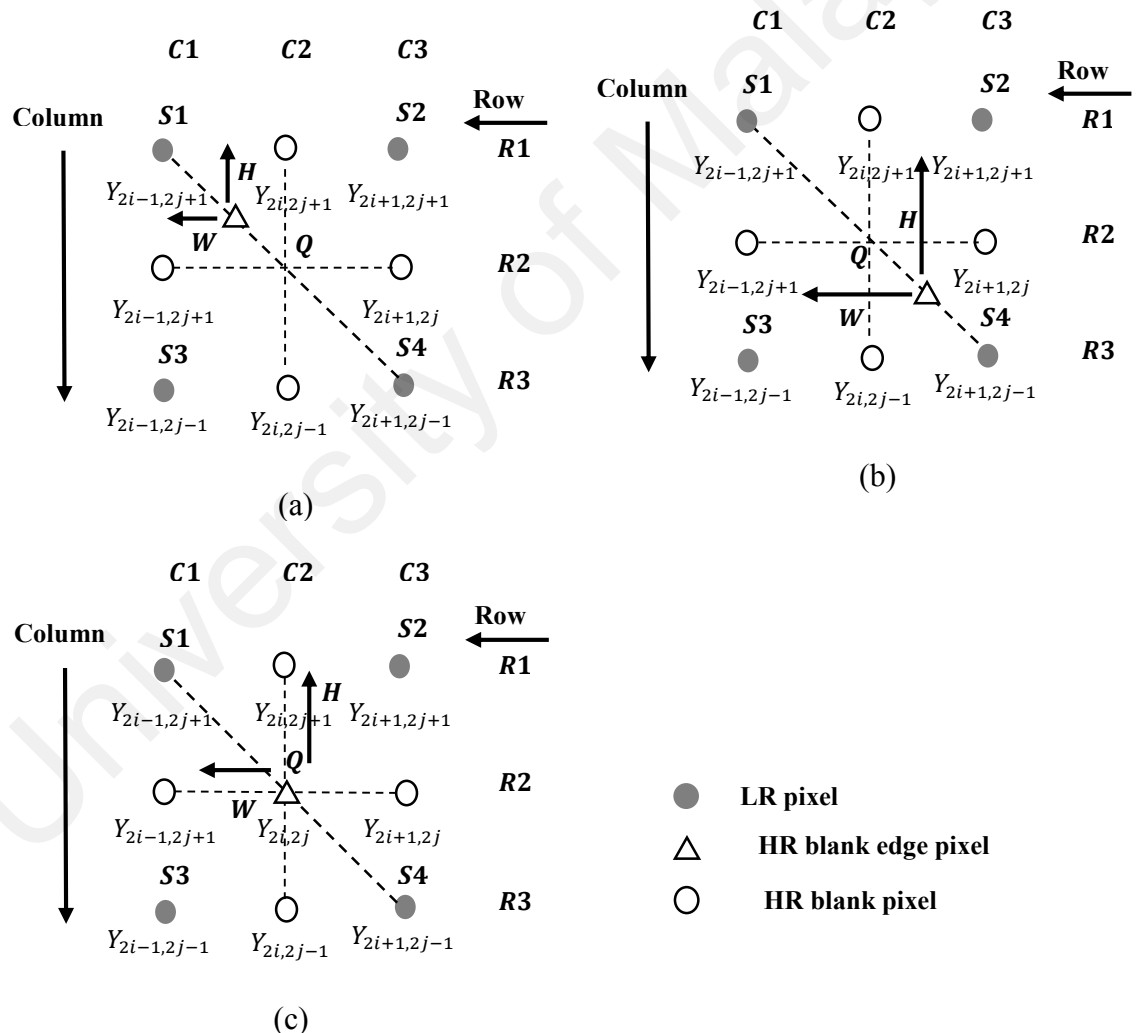


**Figure 3.12: The example of blank HR edge pixel  $Q$  and the selection of improved**

**EDI is continued through  $135^\circ$  angle edge direction**

(a) When,  $H < 0.5$  and  $W < 0.5$  ; (b) and (c)  $H \geq 0.5$  and  $W \geq 0.5$

The HR edge pixel value  $Q$  is calculated as follow:

$$Q = 0.5[WS4 + (1 - W)S1] + 0.5[(1 - H)S1 + HS4] \quad (3.31)$$

Where,  $H$  is defined as the unit distance and known as the vertical component;  $W$  is defined as the unit distance and known as the horizontal component.

### 3.6 Summary

The proposed improved EDI method for image resolution enhancement is covered in this chapter. The details about modified canny edge detection technique are highlighted and the classification process of HR non-edge pixel and HR edge pixel is explained. After that, the nearest neighbor LR pixel pairs around the HR edge pixel are analyzed and the directions of the HR edge pixel based on the minimum intensity difference are discussed. Next, the proposed improved EDI method along the four edge directions: horizontal, vertical and  $45^\circ$  angle direction and  $135^\circ$  angle direction are briefly described. Finally, the different positions of the HR edge pixels are analyzed according to the different conditions and the appropriate interpolation equation for each position is pointed out. The details of the experimental results of the proposed improved EDI method are presented in the following chapter.

## CHAPTER 4: EXPERIMENTAL RESULTS

### 4.1 Introduction

In this chapter, the information about the standard test images is provided. The software and platform which are required for the testing purpose are described. The pre-processing of the experimental images before applying the improved edge directed interpolation (EDI) method is explained. After that, the proposed improved EDI method and different interpolation methods are applied to the test images and different assessments results are presented.

### 4.2 Software and Platform

All interpolation and the proposed algorithm codes are implemented on the MATLAB-2017a platforms and run on the PC with Intel (R) Core (TM) i7-6700 CPU @ 3.40 GHz-3.41GHz, (RAM) 8.00 GB and Operating system 64-bit, Windows 10 Home Edition. The cache memory of the system - L2 is 1MB and L3 is 8MB.

### 4.3 Experimental Images

The natural image in different conditions and features are used for the experimental purpose. A group of standard images is taken which contain five images from the website of University of Wisconsin-Medison, Madison, WI 53706, USA. provided by Fabien A. P. Petitcolas (Engineering, 10 Aug 2008) as shown in Figure 4.1. All images are RGB and size  $512 \times 512$  pixel. Another set of the image which is contained 300 images are taken for extra evaluation of the proposed method. This image set is available on the Berkeley website (Martin, Fowlkes, Tal, & Malik, 2001). These five images represent the image set to understand the performance of proposed method clearly.



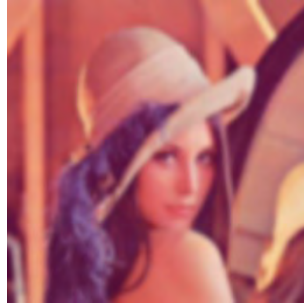
Barber



Bicycle



Butterfly



Lena



Peppers

**Figure 4.1: The sample of test images**

In the test images, the content is significantly different and the huge variations are existed in the texture regions as well as edge regions as shown in Figure 4.1. These variations are able to draw proper experimental results and evaluation of the proposed improved EDI method. In the different papers, all the test images are used to evaluate the interpolation algorithm (Martin et al., 2001).

#### **4.4 Experiment Design**

The experiment is started from the natural images. In the proposed method, the grey scale image is used for image enlargement. All color images are converted to greyscale image where the image intensity range from 0 to 255. Only just interpolation in one color channel. This method is able to apply on the color images. In the color image, three color channel is used to represent all colors. They are Red (R), Green (G) and Blue (B). Each color range is from 0 to 255. It is possible to enlarge the color image in the

same technique by repeating the processes individually along each color channel. After that, all the test images are converted to 8-bit grey scale image using the Matlab built-in function. Then downsample the image from  $512 \times 512$  pixels to  $256 \times 256$  pixels then rescale to  $512 \times 512$  pixels with the proposed improved EDI method.

In the proposed improved EDI method, we use the Canny edge detector for classifying the HR non-edge and HR edge pixel regions. In the Canny edge, detector parameter  $\alpha$  is set for detecting the edge regions. The value of  $\alpha = 2,4,8$  is taken for the proposed method. In this condition, the low and high threshold value is automatically selected which is defined as the strong and weak edges. Among the lots of images, few example images are selected for evaluation which would be easier for comparison.

#### **4.5 Existing Methods**

The source code of different existing methods such as Bi-cubic interpolation (BCI) (Pan et al., 2016), Nearest Neighbour interpolation (NNI) (R.-G. Zhou, Tan, & Fan, 2017), Iterative Curvature Based interpolation (ICBI) (Haris, Widyanto, & Nobuhara, 2017), Directional Cubic Convolution (DCC) interpolation (Baghaie & Yu, 2015) are implemented in Matlab platform according to the description of the cited paper for the experimental purpose to evaluate this study. The basic Bilinear Matlab function is used for Bilinear interpolation and Improved New Edge Directed interpolation (iNEDI) (Wu et al., 2017) is collected from the respective author.

#### **4.6 Experiment Results**

The  $512 \times 512$  pixels size image is taken as the input image and downsampled the image into  $256 \times 256$  pixels size. The weighted vector is created for each edge pixel. After that, the LR image is up-sampled by the improved EDI method to enhance the

image resolution. The sample image butterfly is selected. The proposed edge directed interpolation is applied to sample image.

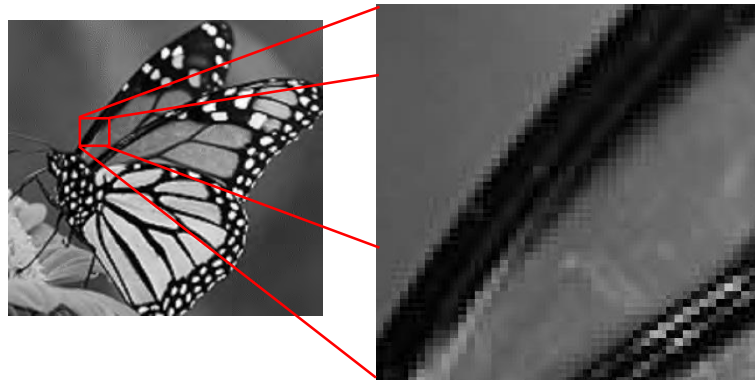


**Figure 4.2: The example of cross section of image before applied the edge directed interpolation method**

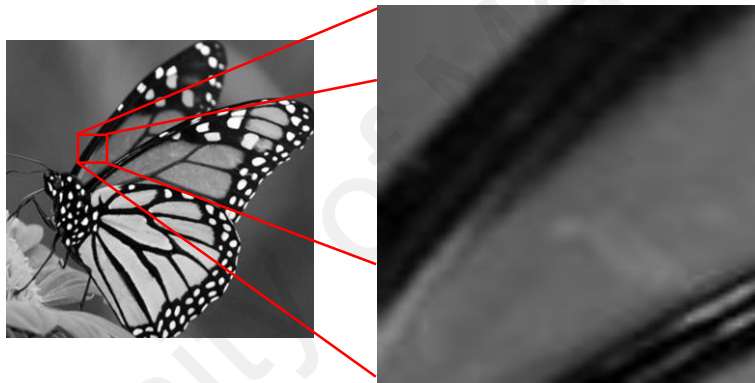


**Figure 4.3: The example of cross section of image after applied the proposed improved edge directed interpolation method**

The comparison is as shown in Figure 4.2 and 4.3. All the artifacts, aliasing and blocky problem are removed by the proposed method. The proposed method is tested on 300 images with a different value of  $\alpha$  and the results are stable. It is proved that the SSIM and PSNR results are efficient when  $\alpha = 4$  as shown in Figure 4.3.

The number of testing is done by changing the input images to investigate the efficiency of the proposed method. The quality of output HR image is compared with the other different methods where the same factors and parameters are used and proposed improved EDI method provides excellent results.

## 4.7 Quantitative Test

After applying the proposed improved EDI method, the quantitative tests are performed to evaluate the proposed method. Bi-cubic interpolation, Nearest Neighbour interpolation, Iterative Curvature-based interpolation (ICBI), Directional Cubic Convolution interpolation (DCCI), Bilinear interpolation and Improved New Edge Directed interpolation (iNEDI) existing methods are selected the quantitative comparison purpose. All methods are applied to tested images.

On the other hand, Means Square Error (MSE), Root Means Square Error (RMSE), Signal to Noise Ratio (SNR), Peak Signal to Noise Ratio (PSNR), Structural Similarity Index Measurement (SSIM) and computational complexity measurements are carefully chosen for the performance assessment. The MSE, RMSE, SNR, and PSNR are an error based model and widely used to measure the distortion of the image. The similarity information at the features and pixel level is provided by the SSIM. The average of all output results is calculated and compared with the proposed method.

### 4.7.1 Means Square Error

Means square error (MSE) is the basic standard assessment for evaluation of the proposed method. The MSE can be described as if the two grey scale images are  $L$  and  $Y$  and each image size is  $H \times W$ . Therefore, the MSE is defined as how much noise is existed in an image with respect to the other image. The less error is indicated by the lower value of MSE that means image quality is good. The equation of MSE is given as follow (X. Wang et al., 2012):

$$MSE = \frac{1}{2H \times 2W} \sum_{i=0}^{2H-1} \sum_{j=0}^{2W-1} Z_{i,j}^2, \quad Z_{i,j} = |L_{i,j} - Y_{i,j}| \quad (4.1)$$

Where,  $H$  is the number of rows and  $W$  is the number of columns of the image.

$L_{i,j}$  are the pixels of the original image and  $(i, j)$  defines the location of the interpolated image. The average MSE results corresponding to the different methods are as shown in Table 4.1.

**Table 4.1: MSE results of the selected images**

Method Image	Nearest Neighbour	Bilinear	Bi-cubic	DCCI	ICBI	iNEDI	Proposed Method
Barber	172.064	143.393	136.044	141.299	98.808	133.806	105.207
Bicycle	913.555	751.414	576.666	586.995	404.959	654.224	402.075
Butterfly	395.695	159.619	196.215	238.347	104.888	224.990	106.884
Lena	146.352	125.343	73.666	186.450	32.737	65.980	37.914
Peppers	49.182	31.327	23.527	29.799	14.757	21.097	12.145
Average	335.369	242.219	201.223	236.578	134.429	220.019	132.845

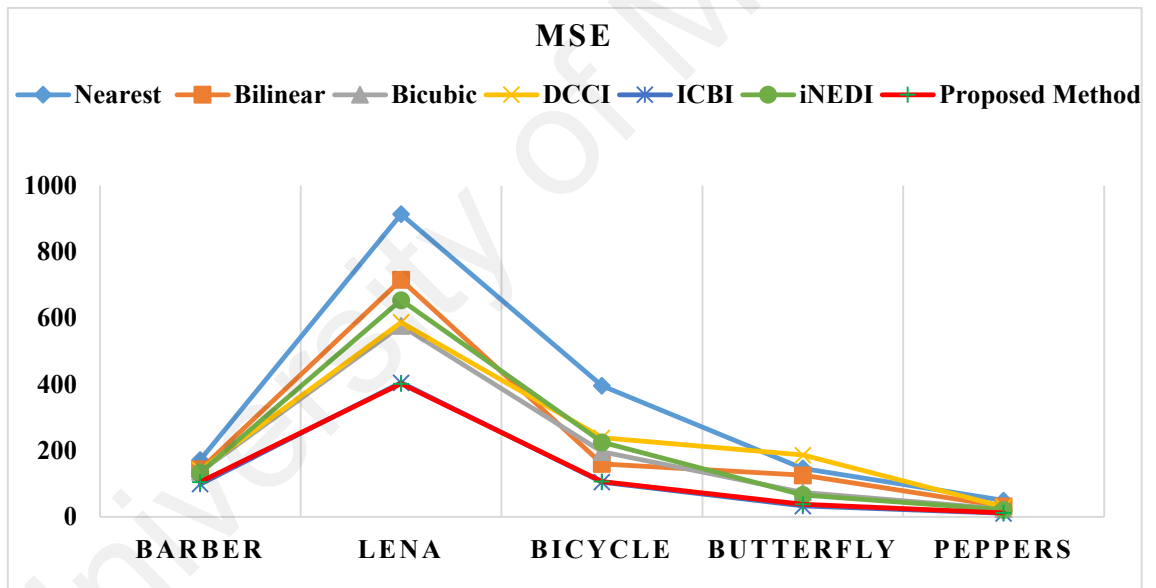


**Figure 4.4: The graph line of the MSE results**

The MSE results are presented by graph line with different symbols and colors as shown in Figure 4.4. The proposed method is represented by the red line. According to the average MSE statistical results, the minimum error is measured by the proposed method.

#### 4.7.2 Root Means Square Error

Root Means Square Error (RMSE) is derived from the MSE and the good quality of HR image is provided by the lower value of RMSE. The equation of the MSER is given as follow (L. Wang et al., 2013):

$$RMSE = \sqrt{MSE} \quad (4.2)$$

The average RMSE information is as shown in Table 4.2 to compared with other methods straightforwardly. The RMSE results are presented by graph line with different symbols and colors as shown in Figure 4.5.

**Table 4.2: RMSE results of the selected images**

Method Image	Nearest Neighbour	Bilinear	Bi-cubic	DCCI	ICBI	iNEDI	Proposed Method
Barber	13.117	11.974	11.663	11.886	9.940	11.567	10.257
Bicycle	30.225	26.747	24.013	24.227	20.123	25.577	20.051
Butterfly	19.892	12.634	14.007	15.438	10.241	14.999	10.338
Lena	12.097	11.195	8.582	13.654	5.721	8.122	6.157
Peppers	7.013	5.597	4.850	5.458	4.279	4.593	3.485
Average	16.468	13.629	12.623	14.132	10.860	12.971	10.057

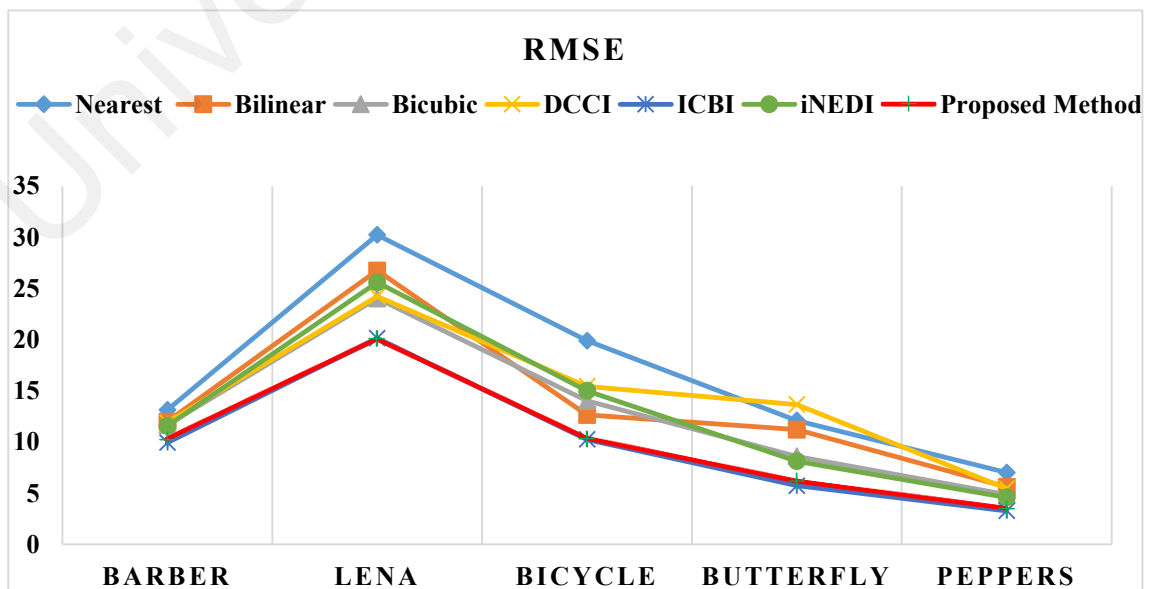


**Figure 4.5: The graph line of the RMSE results**

The proposed method is represented by the red line. Similarly, the RMSE value of the proposed method is closed to the ICBI method. However, the top result is generated by the proposed method.

### 4.7.3 Signal to Noise Ratio

Signal to Noise Ratio (SNR) is the physical measurement and represents in terms of the signal power and noise power. It measures, how the original image quality affected with added noise. The SNR measuring rule is given as follow:

$$SNR = 10 \log_{10} \left( \frac{I}{\sqrt{MSE}} \right) dB \quad (4.3)$$

**Table 4.3: SNR *dB* results of the selected images**

Method Image	Nearest Neighbour	Bilinear	Bi-cubic	DCCI	ICBI	iNEDI	Proposed Method
Barber	19.242	19.995	20.264	11.562	21.655	20.327	21.385
Bicycle	16.052	17.049	18.039	11.294	19.587	17.494	19.609
Butterfly	15.277	19.127	18.316	8.716	21.020	17.702	20.976
Lena	20.844	21.482	23.834	9.441	27.363	24.303	26.723
Peppers	22.564	24.503	25.766	7.987	29.183	26.241	28.649
Average	18.795	20.431	21.243	9.8	23.761	21.213	23.468

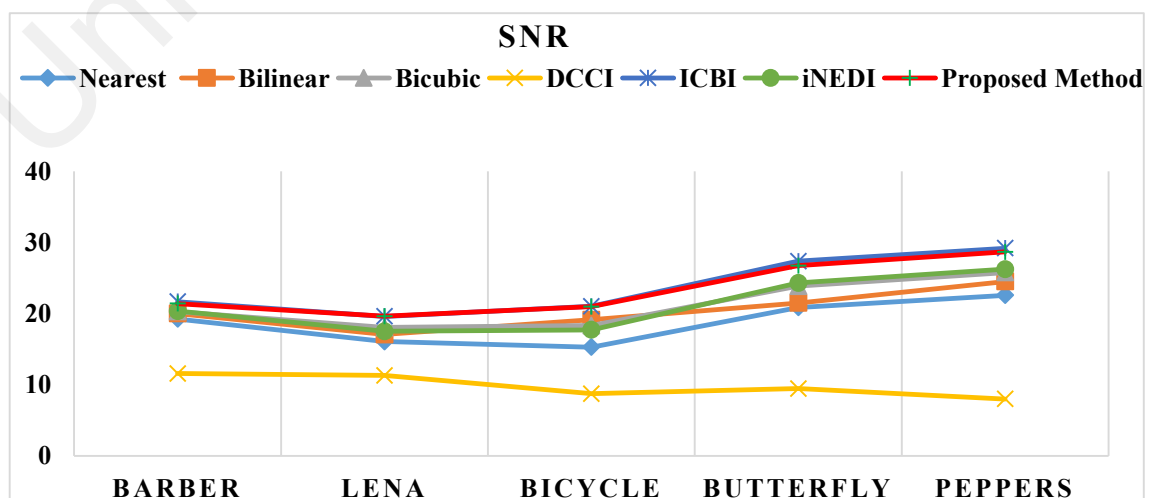


**Figure 4.6: The graph line of the SNR results**

Where,  $I$  is the intensity value of the image pixel. So the higher value of SNR is good because it means that the ratio of signal to noise is higher (Yu, Zhu, et al., 2013). The average SNR results of different methods are presented in Table 4.3. The SNR results are presented by graph line with different symbols and colors as shown in Figure 4.6. The proposed method is represented by the red line. According to the SNR Table information, the SNR result of the proposed method is relatively higher than the others methods but slightly lower than the ICBI method.

#### 4.7.4 Peak Signal to Noise Ratio

Peak Signal to Noise Ratio (PSNR) is the primary and the common measurement for evaluating the image quality in terms of quantitative analysis. The PSNR always consider the image edges and the characteristics of the errors around the edges. It is unable to reflect the visual quality of the image.

PSNR is an engineering word and defined as the ratio of the overall power of the signal and the power of detecting noise that affects the image representation. Most of the signal is in a wide range. The logarithmic scale is used by the PSNR to define the dynamic wide range of the signal.

The PSNR is calculated as follow (Park & Jeong, 2017):

$$PSNR = 20 \log_{10} \left( \frac{MAX_I^2}{\sqrt{MSE}} \right) dB \quad (4.4)$$

Where,  $MAX_I$  is the maximum intensity value of the image pixel. Therefore, PSNR is measured from MSE where the peak error of MSE is considered. As a result, the inverse relation is existed between the error and signal. The higher image quality, lower distortion and less error are indicated by the higher PSNR value. So, the higher value of PSNR is better because it means that the ratio of the signal to noise is higher. The

higher noise is indicated by the lower value of PSNR. The average statistical values of the PSNR are displayed in Table 4.4.

The PSNR results are presented by graph line with different symbols and colors as shown in Figure 4.7.

**Table 4.4: PSNR (dB) results of the selected images**

Method Image	Nearest Neighbour	Bilinear	Bi-cubic	DCCI	ICBI	iNEDI	Proposed Method
Barber	25.773	26.565	26.794	16.629	28.182	26.866	27.910
Bicycle	18.523	19.585	20.521	13.552	22.056	19.973	22.087
Butterfly	22.157	26.099	25.203	14.358	27.923	24.609	27.841
Lena	26.476	27.149	29.458	12.259	32.980	29.936	32.342
Peppers	31.212	33.171	34.415	13.388	37.818	34.888	37.286
Average	24.828	26.513	27.278	14.037	29.791	27.254	29.493

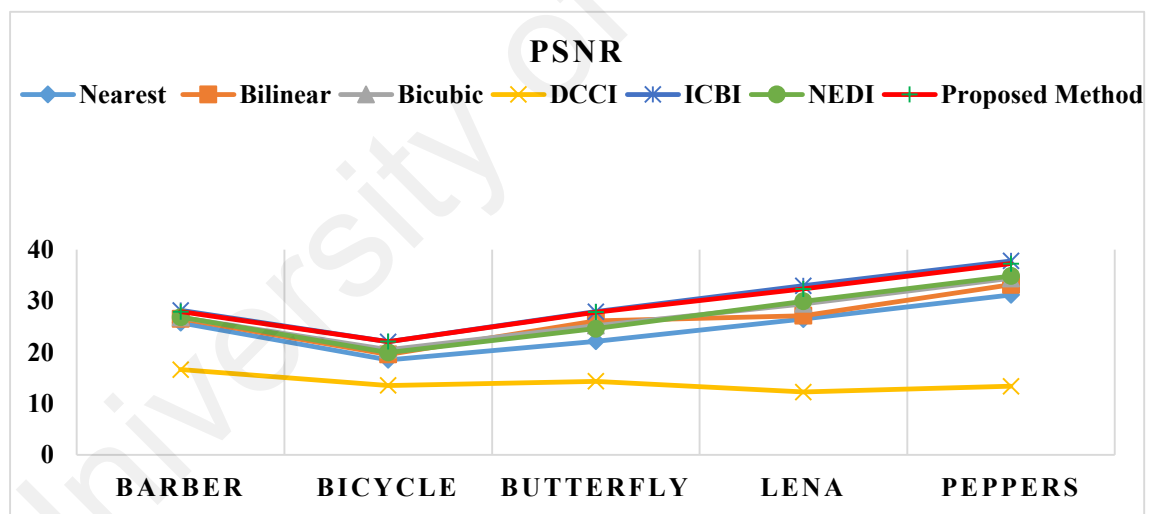


**Figure 4.7: The graph line of the PSNR results**

The proposed method is represented by the red line. The highest PSNR value of the proposed method for the 'Peppers' image is 37.28 dB corresponding to the other methods. Compared with the iNEDI method the PSNR value is raised 2.239 dB in the proposed method. So the proposed method is superior among the current methods. The PSNR is not only the best parameter to indicate the good image. For example, in the

ICBI method, the PSNR value is improved by adding extra weight but the computational complexity and artifacts are increased.

#### 4.7.5 Structural Similarity Index Measurement

Structural Similarity Index Measurement (SSIM) is a method for measuring the similarity between two images based on luminance, contrast, and structure. The good quality of HR image is depended on the larger value SSIM. The mean of SSIM results which are applied on selected images is shown in Table 4.5. The SSIM results are presented by graph line with different symbols and colors as shown in Figure 4.8.

**Table 4.5: SSIM results of the selected images**

Method Image	Nearest Neighbour	Bilinear	Bi-cubic	DCCI	ICBI	iNEDI	Proposed Method
Barber	0.765	0.813	0.805	0.749	0.837	0.797	0.836
Bicycle	0.691	0.771	0.767	0.650	0.814	0.751	0.820
Butterfly	0.838	0.896	0.879	0.743	0.921	0.889	0.921
Lena	0.840	0.895	0.869	0.698	0.919	0.891	0.916
Peppers	0.918	0.949	0.946	0.725	0.967	0.957	0.966
Average	0.810	0.864	0.853	0.713	0.891	0.857	0.8918

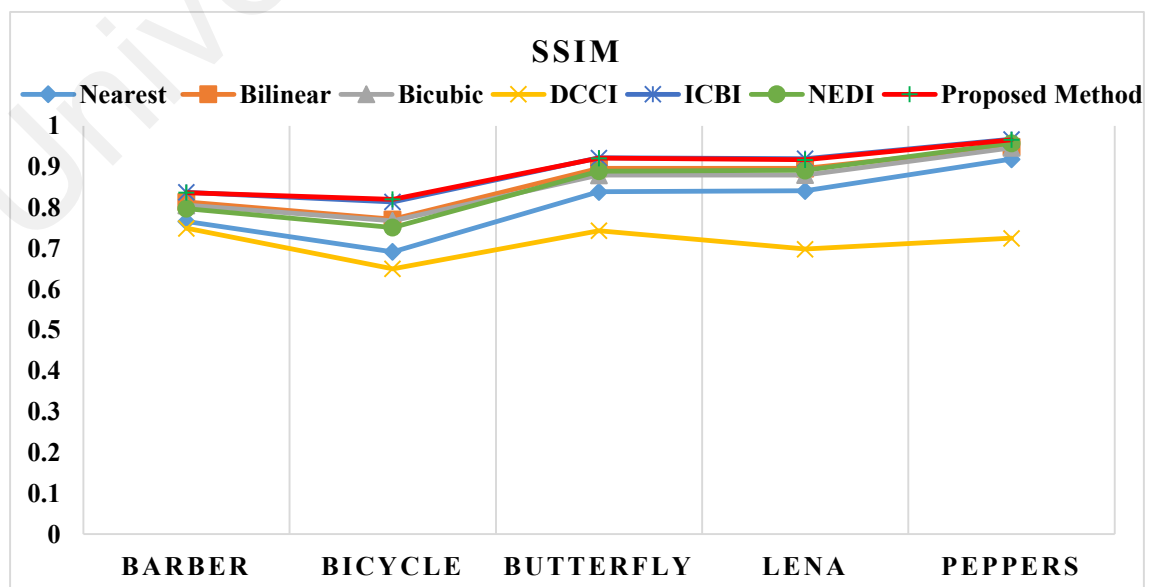


**Figure 4.8: The graph line of the SSIM results**

The proposed method is represented by the red line. According to the SSIM statistical data, the performance of the proposed method is excellent. The interpolated image is similar to the original image. SSIM measurement is related to the human visual observation. After applying the proposed method and the different standing interpolation methods, the visual quality of the output image is easily observed if the interpolated HR image is viewed within a normal distance (Yu, Zhu, et al., 2013).

#### **4.7.6 Computational Complexity**

The proposed method is the best method in terms of computational time and cost. The computational complexity of the proposed method is depended on the input image and the amount of edge pixels which are required to process. The switching from Bilinear interpolation to improved edge directed interpolation is also measured. The processing time of proposed and different EDI methods are recorded, which is used as computational complexity as shown in Table 4.6. The computational complexity results are presented by graph line with different symbols and colors as shown in Figure 4.9. The proposed method is represented by the red line.

The computationally is depended on software platform and the system specification where interpolation code is run. The computational complexity is not dependent on the average interpolation time for only edge pixel rather than the average interpolation time for all pixels of the image. Better results are found by the nearest neighbor, Bilinear and Bi-cubic methods among the all methods but computational complexity is high. But based on the visual quality, the proposed method better than these methods because of image edge are not considered by these methods. On the other hand, the proposed improved EDI method consumed less execution time than the other edge directed methods such as DCCI, ICBI, and iNEDI. As a result, the image resolution enhancement is faster than the other methods.

**Table 4.6: Processing time of the proposed and other interpolation methods (s)**

Method Image	Nearest Neighbour	Bilinear	Bi-cubic	DCCI	ICBI	iNEDI	Proposed Method
Barber	0.023	0.025	0.042	2.612	8.125	6.352	2.660
Bicycle	0.022	0.027	0.036	3.420	10.540	7.388	2.534
Butterfly	0.018	0.022	0.032	3.376	8.612	5.510	2.497
Lena	0.026	0.028	0.033	2.845	9.860	6.264	2.393
Peppers	0.021	0.023	0.037	4.120	7.918	5.421	2.219
Average	0.022	0.025	0.036	3.274	9.011	6.187	2.460

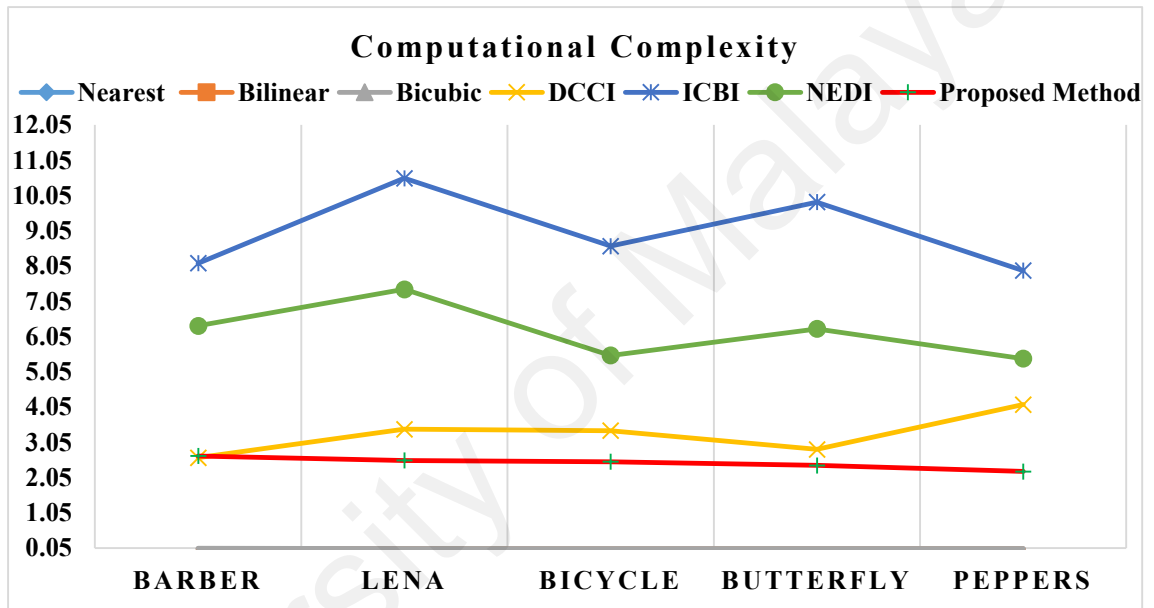


**Figure 4.9: The graph line of the computational complexity results**

#### 4.8 Qualitative Assessment

The quantitative evaluation of the proposed method is not completely assessed the proposed method. The visual masking effects, distortion, and artifacts are noticed around the edges regions when LR image resolution is enhanced by the different interpolation methods. Generally, these effects are not counted by the image quantitative assessments. Only these assessments are not able to estimate the accurate evaluation of the HR interpolated images. For the qualitative evaluation, the visual appearance of interpolated images with different interpolation methods is required. The

ten students of the image processing lab are selected for the qualitative evaluation. The five interpolated images with existing and proposed interpolation methods are displayed on computer screen side by side to find the maximum visual quality image. The slices of the output images are presented. The visual change among different interpolation methods is small and it is difficult to inspect visually. The smooth edges and better visual quality are preserved by the proposed improved EDI method. Sharpness of the image are preferred rather than the removal of artifacts. (Giachetti & Asuni, 2011).

#### 4.8.1 Comparison with Nearest Neighbour Interpolation

The visual analysis of the proposed and Nearest Neighbour interpolation method is as shown in Figure 5.1.

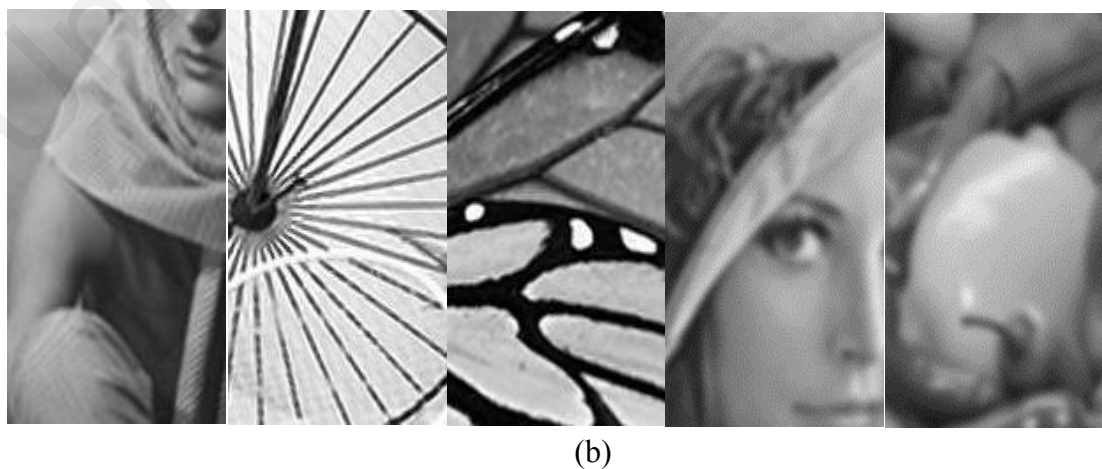
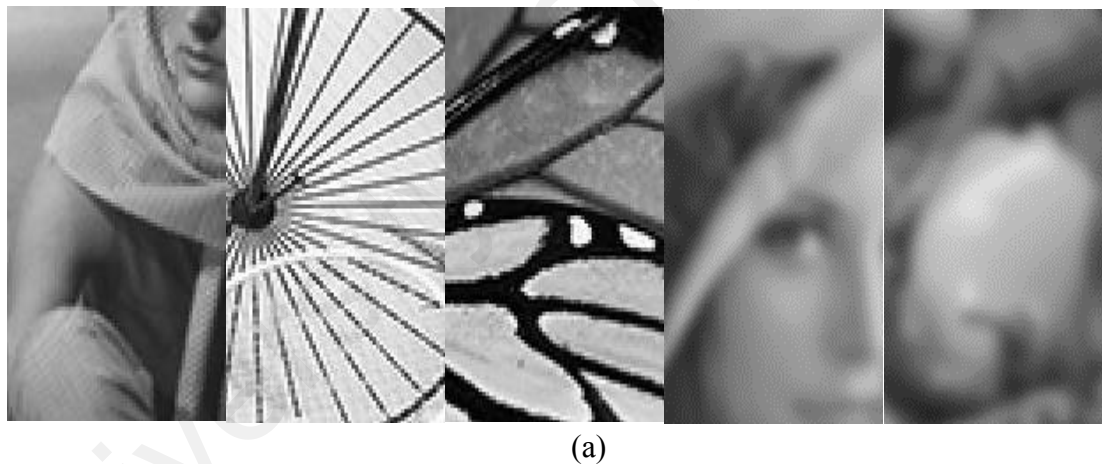


**Figure 4.10: The visual comparison between Nearest Neighbor interpolation and proposed improved EDI method**

(a) Nearest Neighbor interpolation; (b) Proposed improved EDI method

In this method, the structural information of the interpolated image is lost because of the non-edge preserving process. The jugged and staircase problem is seen in the contours area. These problems are happened because of the HR pixel is not interpolated properly based on LR pixel position. The false textures and edges are introduced because of over-fitting problem. However, all the difficulties of this method are recovered by the proposed method (R.-G. Zhou et al., 2017).

#### 4.8.2 Comparison with Bilinear Interpolation

The visual analysis of the proposed and Bilinear interpolation method is as shown in Figure 5.2. The sever blurring and blocking problems are raised by Bilinear

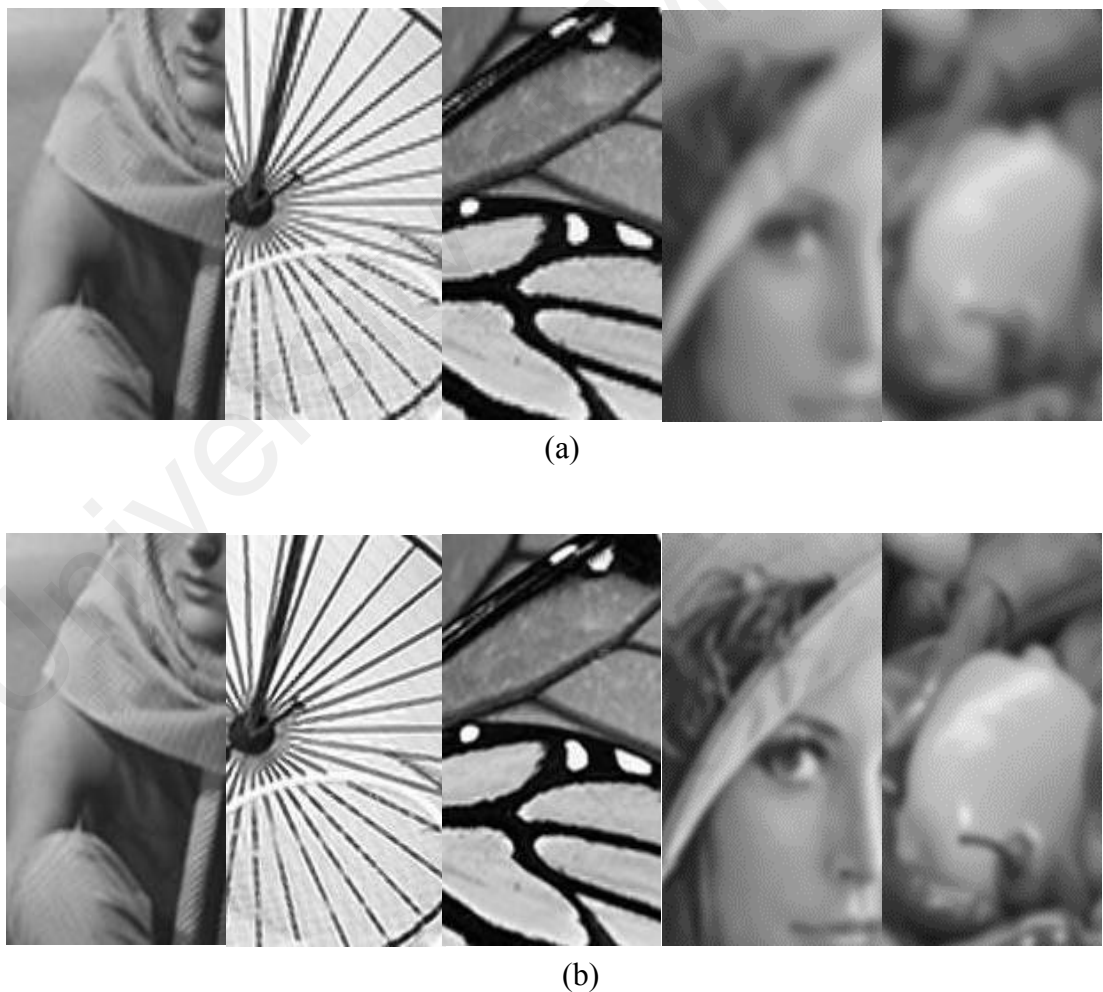


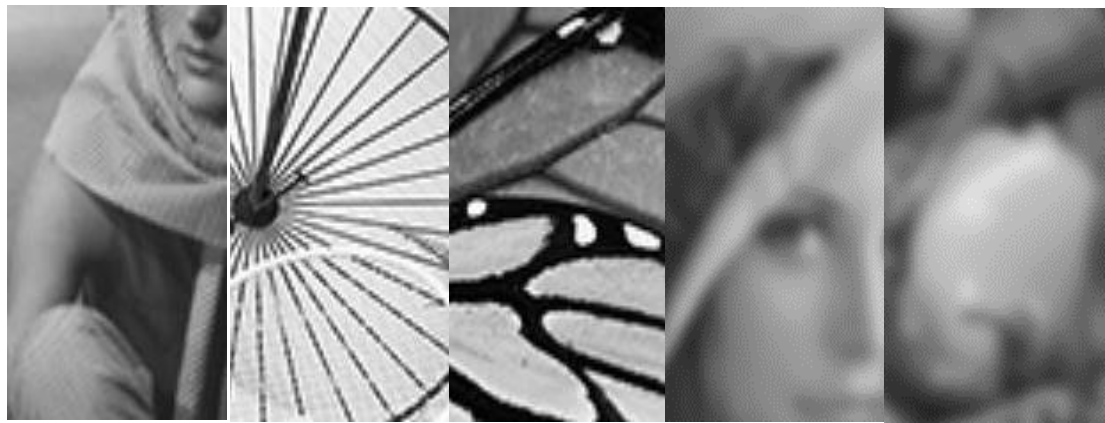
**Figure 4.11: The visual comparison between Bilinear interpolation and proposed EDI method**

(a) Bilinear interpolation; (b) Proposed improved EDI method

interpolation method. As a result, relevant artifacts problem is visible. The Bilinear interpolation is not able to provide the better result in the edge regions. Therefore, the edges become unnatural and reconstruction error is increased. The unnatural whirlpool is introduced by this method because of unable to estimate the orientation of the unknown HR edge pixels. Also, the jaggies are visible in the Barber and Lena images. In this case, the jaggies are removed and the better visual result is provided by the proposed method. However, this method is not reliable for image resolution enhancement (Kao et al., 2015).

#### **4.8.3 Comparison with Bi-cubic Interpolation**

The visual analysis of the proposed and Bi-cubic interpolation method is as shown in Figure 5.3. According to the output results, this method can produce a sharp image but the jaggies are visible at the sharp edge regions. The noticeable artifacts are visible on the sharp intensity transition area around the edge regions. The brightness of the image is discontinuous through the edge direction. As a result, the ringing effects and blurry image are introduced by this method. These problems degraded the visual quality of the edge as well as the enhanced HR image. However, the artificial details of this method are removed by the proposed improved EDI method (Pan et al., 2016).



(a)



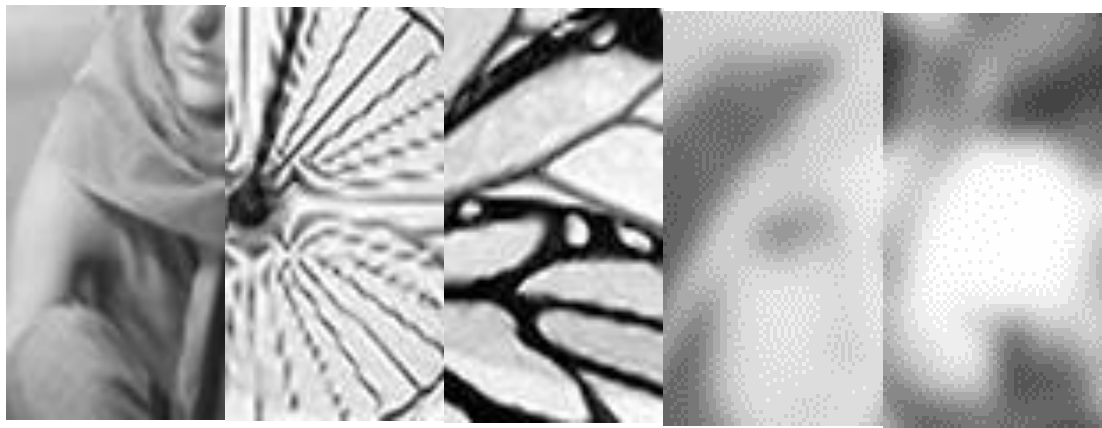
(b)

**Figure 4.12: The visual comparison between Bi-cubic interpolation and proposed EDI method**

(a) B-cubic interpolation; (b) Proposed improved EDI method

#### 4.8.4 Comparison with DCCI

The visual analysis of the proposed and DCCI method is as shown in Figure 5.4. In the DCCI method, artifacts are reduced by the segmentation of image edges. The unpleasant visual quality is seen in the edge area as well as the textures regions. The one more important problem with this method is that the pixel intensity of the interpolated image is totally changed from the original image because of the interpolation of HR pixel is not accurate. On the other hand, the interpolation value of the HR pixel is more accurate whatever the pixel position is. Also, the edge structure is recovered and improved (Baghaie & Yu, 2015).



(a)



(b)

**Figure 4.13: The visual comparison between DCCI interpolation and proposed EDI method**

(a) DCCI interpolation; (b) Proposed improved EDI

#### 4.8.5 Comparison with ICBI

The visual analysis of the proposed and ICBI method is as shown in the Figure 5.5. The much more better result is produced by the edge directed interpolation method rather than the conventional interpolation methods. In the ICBI method, the edges are relatively continuous and the large edges are preserved. The edge detection is more accurate than the other methods but still ringing effects is existed. Thin edge is produced by this method which is unable to generate more detail information about the HR edges. So, the visible artifacts are produced. The more problems are produced by this method when multiple edges are intersected and image features have curvatures. Therefore, in the texture regions the performance of this method is worse than the

proposed method. The perceptually sharper and continuous edges are provided by the proposed method because of improved edge directed interpolation method and the ringing effects are also reduced. (Haris et al., 2017).

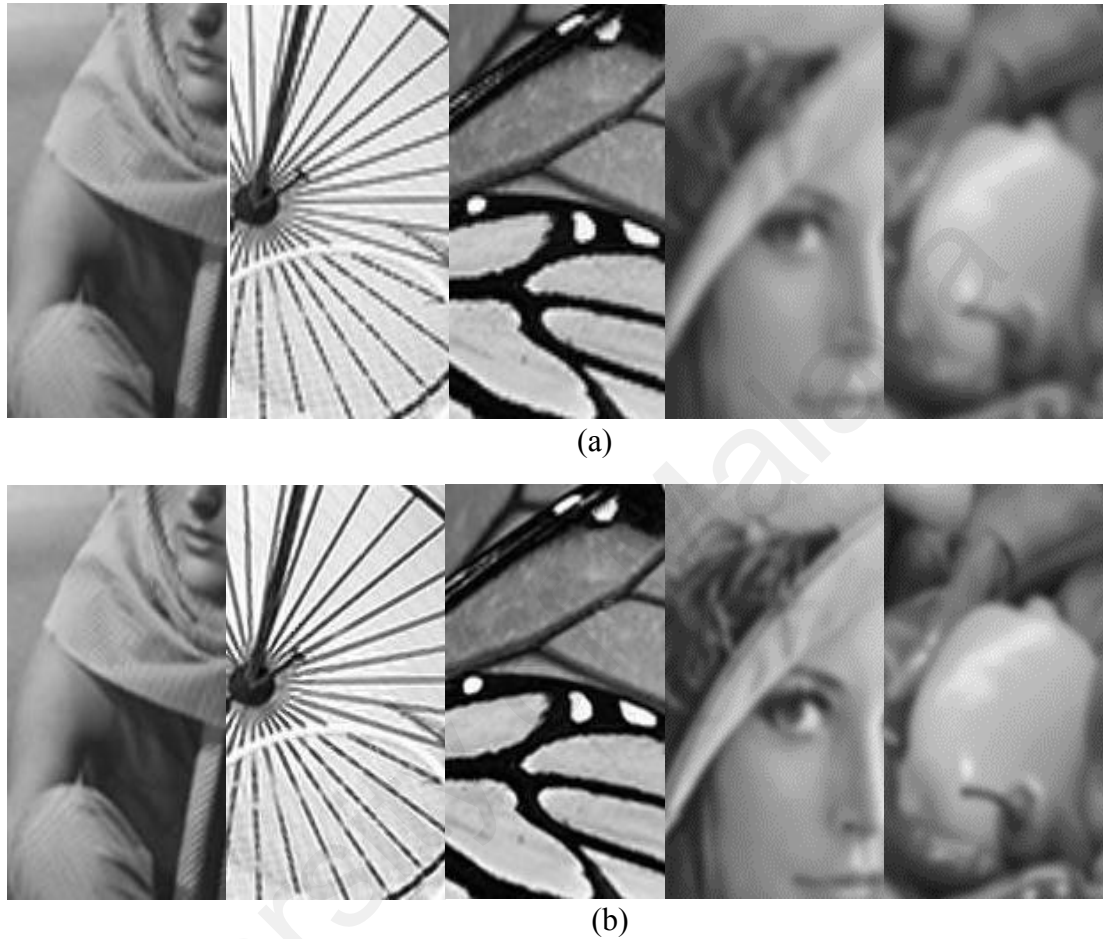


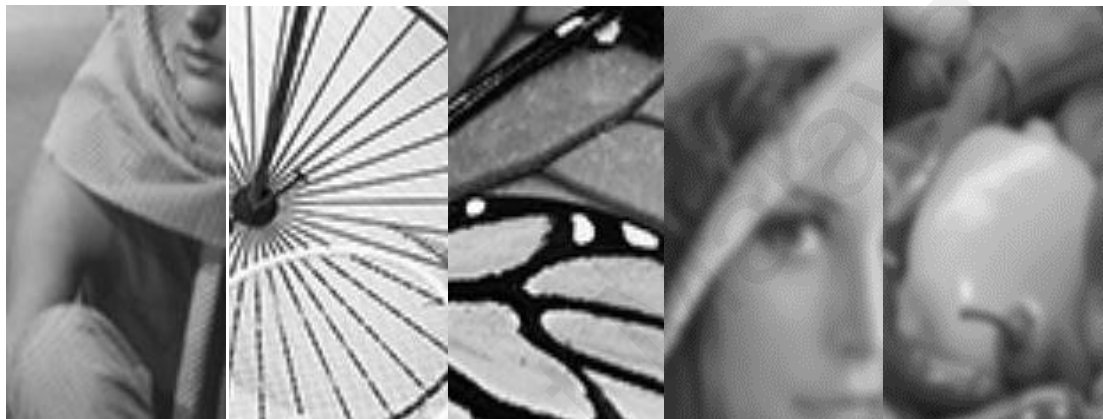
**Figure 4.14: The visual comparison between ICBI interpolation and proposed EDI method**

(a) ICBI interpolation; (b) Proposed improved EDI

#### 4.8.6 Comparison with iNEDI

The visual analysis of the proposed and iNEDI method is as shown in Figure 5.6. This method is the middle of the ICBI and the proposed improved EDI method. The strong continuity of the edge directed interpolation along the long edges are produced by the iNEDI method and this is the major attribute of this method. But unnatural intensity transitions of the HR edge pixels are provided with this method. As a result, the ringing effects are produced. In the iNEDI method, all the neighbor pixels inside the local

regions are treated as equally without considering the edge pixel or not. Therefore, the artifacts are produced along the thin edges regions and the noise level is increased. The sharp edges are preserved by this method but sometimes the qualitative comparison is worse than the proposed method. However, the larger, as well as the smaller edge, are handled by the proposed method and the prediction error of the iNEDI method is reduced. (Wu et al., 2017).



(a)



(b)

**Figure 4.15: The visual comparison between iNEDI interpolation and proposed EDI method**

(a) iNEDI interpolation; (b) Proposed improved EDI method

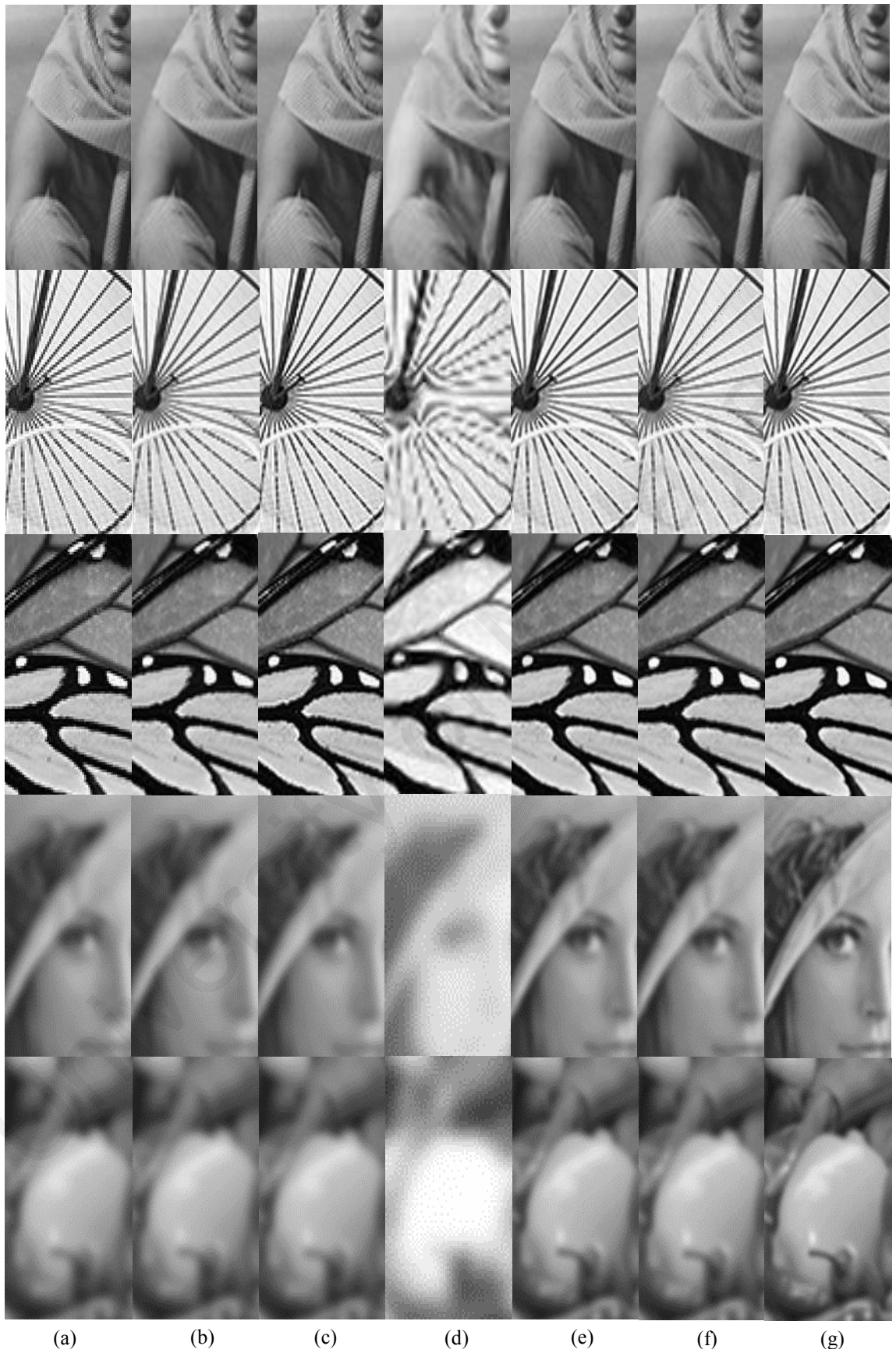


**Figure 4.16: The example of overall visual comparison**  
 (a) Nearest Neighbour; (b) Bilinear; (c) Bi-cubic; (d) DCCI; (e) ICBI; (f) iNEDI; (g)  
 Proposed improved EDI method

Finally, all the slices of output HR images are graphically as shown in Figure 5.7 for comparison. According to the qualitative and quantitative analysis, the proposed method is close to the ICBI method based on the quantitative measurements where the qualitative analysis is lower. On the other hand, the visual quality of the proposed method is similar to the iNEDI method but the quantitative assessments are relatively poor.

#### **4.9 Summary**

The summary of the proposed method is that, it provides the highest qualitative and quantitative results than the others state of arts methods. Even the blur image also provides better results with the improved EDI method. The graphical output is presented after applied the proposed improved EDI method and compared with the other EDI methods. The different quantitative assessments such as MSE, RMSE, SNR, PSNR, SSIM and computational complexity are mentioned for comparative analysis where the highest average PSNR value is 29.493 which is obtained for the proposed improved EDI method. On the other hand, the average SSIM value is 0.8918 which is the maximum value among the other EDI methods. However, the conventional interpolation methods are faster than the EDI methods but the qualitative result is worse than EDI methods. The average processing speed of the proposed is 2.460 which is faster than other EDI methods. Though, processing speed depends on the machine platform. Here, all algorithms are run on the same environment and platform. All the output images of different methods and proposed EDI method are sliced. Finally, the portion of the images are displayed together for better qualitative analysis.

## CHAPTER 5: CONCLUSION AND FUTURE WORK

### 5.1 Introduction

In this chapter, the fulfillment of the research objectives is described and the potential outcomes of the proposed method are presented. The important contributions and applications are discussed. The further works of this research are pointed out to enhance the proposed improved EDI method at the end of this chapter.

### 5.2 Fulfilment of the Research Objectives

The interpolation from LR image to HR image is challenging. The maximum information of the image is carried by the edge regions and most of the image interpolation methods are failed to preserve the edge regions. Therefore, to preserve the edge regions, the edge directed interpolation method is the primary focus for image resolution enhancement. An improved edge directed image resolution enhancement method is developed and tested. In the proposed method, the input image is converted to downsample LR image and then proposed EDI method is applied for rescaling the LR image to HR image of the same size of the input image. The HR edge pixels and HR non-edge pixels are separated by the Canny edge detection method. Then Bi-cubic interpolation is applied for HR non-edge pixels and the proposed improved EDI method is applied for HR edge pixels. In the proposed method, the HR edge pixels are interpolated based on the pixel position and the interpolation is continued along the edge direction. As a result, computational complexity is comparatively less and visual quality is higher than the other methods. The sharpening edge is another advantage of the proposed method, which is able to make a proper balance between edge regions and the non-edge regions.

The proposed method is able to interpolate the HR edge pixels in any position. So the interpolation value is more accurate than the other methods.

The experimental results show that proposed method outperforms the conventional edge directed interpolation in terms of qualitative and quantitative image analysis. The proposed method is able to preserve the high quality of sharp HR edge as well as the clear image and the quality of the texture regions are improved. Artifacts, aliasing, blurring and blocky problems are suppressed by the proposed method and ensured that the edge pixel is interpolated properly with neighboring pixels no matter where the edge pixel position is. On the other hand, the proposed method is locally adaptive and free from the losing fidelity problem.

### **5.3 Contribution**

The potential applications of the proposed method are video streaming, interpolation from LR textures to HR textures, high-resolution printing, and image distribution etc. The proposed method can be used to enhancing the internet image as well as the image repository to assist the user. This method can be applied in many image processing applications where the fast image processing, computational complexity, and visual quality are important such as real-time HR video enhancement. The proposed method can be integrated with the industrial application such as different types of image enlargement applications and able to run in the small size memory such as camera and mobile phone. The natural color CCD demosaicing, the HDTV video and SDTV video can be combined with the proposed method.

### **5.4 Future Work**

The extension of this work can be the interpolation on super-resolution edge pixels no matter where the position of edge pixel is. In the proposed method most of the time is

spent for estimating weights and classify the pixels. The parallel interpolation procedure can improve the computational time of the proposed method. The pixels which are not shared by the neighbor pixels can be processed at the same time. This procedure can alleviate the burden of the computational complexity of the proposed method.

In future, the computational time can be reduced by modifying the proper hardware and programming source code and can be feasible for the real-time use. Also, it is essential to find a way of measuring the accurate value of the parameters.

## **5.5 Summary**

The outcomes of the proposed method are briefly described according to the research objective. The overview of the proposed improved EDI method is given and all the potentiality of the proposed method are presented. The contributions and the possible industrial applications are pointed out. The result of the proposed method is not only outperformed than the mentioned interpolation methods but also better than the recently published methods according to the objective and subjective results. Finally, the conclusion is drawn by explaining the future work.

## REFERENCES

- Allebach, J., & Wong, P. W. (1996). *Edge-directed interpolation*. Paper presented at the Image Processing, 1996. Proceedings., International Conference on.
- Asuni, N., & Giachetti, A. (2008). Accuracy Improvements and Artifacts Removal in Edge Based Image Interpolation. *VISAPP (1)*, 8, 58-65.
- Baghaie, A., & Yu, Z. (2015). Structure tensor based image interpolation method. *AEU-international Journal of Electronics and Communications*, 69(2), 515-522.
- Bo Wang, D. Z., Dawei Yang. (2013). Improved Fast Color Image Edge-Directed Interpolation With Statistical Feature. *Journal of Image and Graphics*, 6(2), 105-109.
- Chen, M.-J., Huang, C.-H., & Lee, W.-L. (2005). A fast edge-oriented algorithm for image interpolation. *Image and Vision Computing*, 23(9), 791-798.
- Engineering, C. i. t. C. o. (10 Aug 2008). Public-Domain Test Images for Homeworks and Projects. Retrieved from <https://homepages.cae.wisc.edu/~ece533/images/>
- Freedman, G., & Fattal, R. (2011). Image and video upscaling from local self-examples. *ACM Transactions on Graphics (TOG)*, 30(2), 12.
- Gao, X., Zhang, K., Tao, D., & Li, X. (2012). Image super-resolution with sparse neighbor embedding. *IEEE transactions on Image Processing*, 21(7), 3194-3205.
- Giachetti, A., & Asuni, N. (2008). *Fast Artifacts-Free Image Interpolation*. Paper presented at the BMVC.
- Giachetti, A., & Asuni, N. (2011). Real-time artifact-free image upscaling. *IEEE transactions on Image Processing*, 20(10), 2760-2768.
- Haris, M., Widyanto, M. R., & Nobuhara, H. (2017). First-order derivative-based super-resolution. *Signal, Image and Video Processing*, 11(1), 1-8.
- He, H., & Siu, W.-C. (2011). *Single image super-resolution using Gaussian process regression*. Paper presented at the Computer Vision and Pattern Recognition (CVPR), 2011 IEEE Conference on.

- Hosogai, E., & Tanaka, Y. (2014). *Iterative edge-directed image upscaling with high directionality*. Paper presented at the Signal and Information Processing Association Annual Summit and Conference (APSIPA), 2014 Asia-Pacific.
- Jagadeesh, P., & Pragaswari, J. (2011). *Image resolution enhancement based on edge directed interpolation using dual tree—Complex wavelet transform*. Paper presented at the Recent Trends in Information Technology (ICRTIT), 2011 International Conference on.
- Jana, B. (2018). Reversible data hiding scheme using sub-sampled image exploiting Lagrange's interpolating polynomial. *Multimedia Tools and Applications*, 77(7), 8805-8821.
- Kao, C.-C., Lai, Y.-T., & Tseng, C.-F. (2015). Improved edge-directed super resolution. *International Journal of Computers and Applications*, 37(3-4), 160-167.
- Kim, K., & Kwon, Y. (2008). Example-based learning for singleimage SR and JPEG artifact removal. *MPI-TR*, (173), 8.
- Li, M., & Nguyen, T. Q. (2008). Markov random field model-based edge-directed image interpolation. *IEEE transactions on Image Processing*, 17(7), 1121-1128.
- Li, X., & Orchard, M. T. (2001). New edge-directed interpolation. *IEEE transactions on Image Processing*, 10(10), 1521-1527.
- Lin, Z., & Shum, H.-Y. (2004). Fundamental limits of reconstruction-based superresolution algorithms under local translation. *IEEE Transactions on Pattern Analysis and Machine Intelligence*, 26(1), 83-97.
- Liu, L., Liang, F., Zheng, J., He, D., & Huang, J. (2018). Ship infrared image edge detection based on an improved adaptive Canny algorithm. *International Journal of Distributed Sensor Networks*, 14(3), 1550147718764639.
- Liu, T.-S., Liu, R.-X., & Pan, S.-W. (2014). Improved Canny Algorithm for Edge Detection of Core Image. *The Open Automation and Control Systems Journal*, 6(1).
- Mareboyana, M., & Le Moigne, J. (2018). *Super-resolution of remote sensing images using edge-directed radial basis functions*. Paper presented at the Signal Processing, Sensor/Information Fusion, and Target Recognition XXVII.
- Martin, D., Fowlkes, C., Tal, D., & Malik, J. (2001). *A database of human segmented natural images and its application to evaluating segmentation algorithms and measuring ecological statistics*. Paper presented at the Computer Vision, 2001. ICCV 2001. Proceedings. Eighth IEEE International Conference on.

- Meijering, E., & Unser, M. (2003). A note on cubic convolution interpolation. *IEEE transactions on Image Processing*, 12(4), 477-479.
- Meng, Y., Zhang, Z., Yin, H., & Ma, T. (2017). Automatic Detection of Particle Size Distribution by Image Analysis Based on Local Adaptive Canny Edge Detection and Modified Circular Hough Transform. *Micron*.
- Ousguine, S., Essannouni, F., Essannouni, L., & Aboutajdine, D. (2014). A new image interpolation using gradient-orientation and cubic spline interpolation. *International Journal of Innovation and Applied Studies*, 5(3), 215.
- Pan, Z., Chen, W., Jiang, Z., Tang, L., Liu, Y., & Liu, Z. (2016). Performance of global look-up table strategy in digital image correlation with cubic B-spline interpolation and bicubic interpolation. *Theoretical and Applied Mechanics Letters*, 6(3), 126-130.
- Park, D., & Jeong, J. (2017). Adaptive Edge-Directed Interpolation Using Edge Map Analysis. *International Journal of Communications*, 2, 86-91.
- Shan, Q., Li, Z., Jia, J., & Tang, C.-K. (2008). Fast image/video upsampling. *ACM Transactions on Graphics (TOG)*, 27(5), 153.
- Stosic, Z., & Rutesic, P. (2018). An Improved Canny Edge Detection Algorithm for Detecting Brain Tumors in MRI Images. *International Journal of Signal Processing*, 3.
- Sun, J., Xu, Z., & Shum, H.-Y. (2011). Gradient profile prior and its applications in image super-resolution and enhancement. *IEEE transactions on Image Processing*, 20(6), 1529-1542.
- Sun, J., Zhu, J., & Tappen, M. F. (2010). *Context-constrained hallucination for image super-resolution*. Paper presented at the Computer Vision and Pattern Recognition (CVPR), 2010 IEEE Conference on.
- Tai, Y.-W., Liu, S., Brown, M. S., & Lin, S. (2010). *Super resolution using edge prior and single image detail synthesis*. Paper presented at the Computer Vision and Pattern Recognition (CVPR), 2010 IEEE Conference on.
- Tam, W.-S., Kok, C.-W., & Siu, W.-C. (2010). Modified edge-directed interpolation for images. *Journal of Electronic imaging*, 19(1), 013011.
- Tian, Q., Wen, H., Zhou, C., & Chen, W. (2012). *A fast edge-directed interpolation algorithm*. Paper presented at the International Conference on Neural Information Processing.

- Vairavaraja, M., & Gunasekaran, M. (2013). Iterative Curvature Based Interpolation for Image Upscaling.
- Van Ouwerkerk, J. (2006). Image super-resolution survey. *Image and Vision Computing*, 24(10), 1039-1052.
- Wang, L., Xiang, S., Meng, G., Wu, H., & Pan, C. (2013). Edge-directed single-image super-resolution via adaptive gradient magnitude self-interpolation. *IEEE Transactions on Circuits and Systems for Video Technology*, 23(8), 1289-1299.
- Wang, Q., & Ward, R. (2001). *A new edge-directed image expansion scheme*. Paper presented at the Image Processing, 2001. Proceedings. 2001 International Conference on.
- Wang, X., Chen, Z., & Bao, X. (2012). An improved edge-directed image interpolation algorithm. *International Journal of Image and Graphics*, 12(04), 1250023.
- Warbhe, S., & Gomes, J. (2016). Interpolation Technique using Non Linear Partial Differential Equation with Edge Directed Bicubic. *International Journal of Image Processing (IJIP)*, 10(4), 205.
- Wee, S., Park, D., & Jeong, J. (2017). Modified New Edge-Directed Interpolation Using Window Extension. *International Journal of Mathematical and Computational Methods*, 2.
- Wong, C.-S., & Siu, W.-C. (2010a). *Adaptive directional window selection for edge-directed interpolation*. Paper presented at the Computer Communications and Networks (ICCCN), 2010 Proceedings of 19th International Conference on.
- Wong, C.-S., & Siu, W.-C. (2010b). *Further improved edge-directed interpolation and fast EDI for SDTV to HDTV conversion*. Paper presented at the Signal Processing Conference, 2010 18th European.
- Wu, J., Li, W., & Jeon, G. (2017). From coarse-to fine-grained implementation of edge-directed interpolation using a GPU. *Information Sciences*, 385, 457-474.
- Xiong, Z., Sun, X., & Wu, F. (2009). *Image hallucination with feature enhancement*. Paper presented at the Computer Vision and Pattern Recognition, 2009. CVPR 2009. IEEE Conference on.
- Yu, S., Zhang, R., Wu, S., Hu, J., & Xie, Y. (2013). An edge-directed interpolation method for fetal spine MR images. *Biomedical engineering online*, 12(1), 102.

- Yu, S., Zhu, Q., Wu, S., & Xie, Y. (2013). Performance evaluation of edge-directed interpolation methods for images. *arXiv preprint arXiv:1303.6455*.
- Yun, Y., Bae, J., & Kim, J. (2011). *Adaptive multidirectional edge directed interpolation for selected edge regions*. Paper presented at the TENCON 2011-2011 IEEE Region 10 Conference.
- Zhang, X., Ma, S., Zhang, Y., Zhang, L., & Gao, W. (2009). Nonlocal edge-directed interpolation. *Advances in Multimedia Information Processing-PCM 2009*, 1197-1207.
- Zhou, D., Shen, X., & Dong, W. (2012). Image zooming using directional cubic convolution interpolation. *IET image processing*, 6(6), 627-634.
- Zhou, H., Yan, L., Zhang, L., Zheng, R., & Yu, F. (2016). *Improved single image super-resolution based on edge directed interpolation*. Paper presented at the 8th International Symposium on Advanced Optical Manufacturing and Testing Technologies: Optoelectronic Materials and Devices.
- Zhou, Q., Chen, S., Liu, J., & Tang, X. (2011). *Edge-preserving single image super-resolution*. Paper presented at the Proceedings of the 19th ACM international conference on Multimedia.
- Zhou, R.-G., Tan, C., & Fan, P. (2017). Quantum multidimensional color image scaling using nearest-neighbor interpolation based on the extension of FRQI. *Modern Physics Letters B*, 31(17), 1750184.